2019

THE DEVELOPMENT OF NOVEL PROTEASOME INHIBITORS FOR THE TREATMENT OF MULTIPLE MYELOMA AND ALZHEIMER'S DISEASE

Min Jae Lee

University of Kentucky, minjaelee87@gmail.com
Digital Object Identifier: https://doi.org/10.13023/etd.2019.169

Recommended Citation

THE DEVELOPMENT OF NOVEL PROTEASOME INHIBITORS FOR THE TREATMENT
OF MULTIPLE MYELOMA AND ALZHEIMER'S DISEASE

_____

DISSERTATION

_____

A dissertation submitted in partial fulfillment of the
requirements for the degree of Doctor of Philosophy in the
College of Pharmacy
at the University of Kentucky

By
Min Jae Lee
Lexington, Kentucky

Director: Dr. Kyung Bo Kim, Associate Professor of Pharmaceutical Sciences

Lexington, Kentucky

2019

ABSTRACT OF DISSERTATION

THE DEVELOPMENT OF NOVEL PROTEASOME INHIBITORS FOR THE TREATMENT
OF MULTIPLE MYELOMA AND ALZHEIMER'S DISEASE

Over a decade, proteasome inhibitors (PIs), bortezomib, carfilzomib (Cfz) and ixazomib, have contributed to a significant improvement in the overall survival for multiple myeloma (MM) patients. However, the response rate of PI was fairly low, leaving a huge gap in MM patient care. Given this, mechanistic understanding of PI resistance is crucial towards developing new therapeutic strategies for refractory/relapsed MM patients.

In this dissertation work, we found H727 human bronchial carcinoid cells are inherently resistant to Cfz, yet susceptible to other PIs and inhibitors targeting upstream components of the ubiquitin-proteasome system (UPS). It indicated H727 cells may serve as a cell line model for *de novo* Cfz resistance and remains UPS dependent for survival. To examine the potential link between proteasome catalytic subunit composition and cellular response to Cfz, we altered the composition of proteasome catalytic subunits via interferon-γ treatment or siRNA knockdown in H727 cells. Our results showed alteration in composition of proteasome catalytic subunits results in sensitization of H727 cells to Cfz. It supported that proteasome inhibition by alternative PIs may still be a valid therapeutic strategy for patients with relapsed MM after having received treatment with Cfz. With this in mind, we designed and synthesized a small library of epoxyketone-based PIs by structural modifications at the P1' site. We observed that a Cfz analog, harboring a hydroxyl substituent at its P1' position was cytotoxic against cancer cell lines with *de novo* or acquired resistance to Cfz. These results suggested that peptide epoxyketones incorporating P1'-targeting moieties may have the potential to overcome Cfz resistance mechanisms in cells.

The immunoproteasome (IP), an inducible proteasome variant which is harboring distinct catalytic subunits, LMP2, MECL1 and LMP7 of the proteasome typically expressed in cells of hematopoietic origin, plays a role in immune response and is closely linked to inflammatory diseases. It has been reported that the IP is upregulated in reactive glial cells surrounding amyloid β (Aβ) deposits in brains of Alzheimer's disease (AD) patients and AD animal models.

To investigate whether the IP is involved in the pathogenesis of AD, we examined the impact of IP inhibition on cognitive function in AD mouse models. We observed that YU102, an epoxyketone peptide targeting the IP catalytic subunit LMP2, improved cognitive dysfunction in AD mice without clearance of Aβ deposition or tau aggregation. Our cell line model study also showed a potential mode of action of YU102 which is suppressing pro-inflammatory cytokine production in microglial cells. It suggested that LMP2 contributes to microglia-mediated inflammatory response. These findings supported that LMP2 may offers a valuable therapeutic target for treatment of Alzheimer's disease, expanding the therapeutic potential of the LMP2-targeting strategy.

Min Jae Lee

04/22/2019

THE DEVELOPMENT OF NOVEL PROTEASOME INHIBITORS FOR THE TREATMENT
OF MULTIPLE MYELOMA AND ALZHEIMER'S DISEASE

By

Min Jae Lee

Dr. Kyung Bo Kim

_____
Director of Dissertation

Dr. David Feola

_____
Director of Graduate Studies

04/22/2019

_____
Date

To my family, who taught me the importance of education

Thank you for your endless love, support and encouragement.

ACKNOWLEDGEMENTS

environment during my PhD. I am grateful to Catina Rossoll, Ned Smith, Chris Porter, Todd Sizemore, Kristi Moore, and Janice Butner for their support over the years.

Last but not the least, I specially thank my family for their patient, support, and encouragement. I would not be where I am today without their sacrifices and unconditional love. Many thanks to my fiancé, Seon Gu Kim. You have always been a great support through the hard journey. Thank you for being the first audience of my practice presentations. Thanks to my grandparents for their love and patient throughout the years. They also taught me the value of education. Finally, my heartfelt thanks to my Mom, Dad, and Sister who taught me to always work hard and never give up. Your countless sacrifices and support led me to pursue my dream becoming a scientist. Thank you all for everything that each of you have done for me. I could not have done any of this without you.

TABLE OF CONTENTS

LIST OF TABLES

CHAPTER 1. INTRODUCTION

1.1   The Ubiquitin-Proteasome System (UPS)

The highly regulated degradation of cellular proteins is significantly crucial for cells to proliferate and differentiate. Before the discovery of the ubiquitin-proteasome system (UPS), cellular protein degradation was thought to highly rely on lysosomes which were discovered by Christian de Duve in 1949 [1]. In 1977, Alfred Goldberg suggested the presence of another intracellular degradation mechanism in cells and Goldknopf and Busch identified an ubiquitin, a small protein with 76 amino acids, but the function was not defined [2]. In the same period, the 1970's and 1980's, Aaron Chiechanover, Avram Hershko, and Irwin Rose also worked on how cells degrade or destroy the proteins that are not useful anymore, which finally resulted in discovery and characterization of the ATP-dependent, ubiquitin-mediated protein degradation system [3-5]. The fundamental importance of the UPS in protein degradation mechanisms was highlighted when Rose, Hershko, and Ciechanover were awarded the 2004 Nobel Prize in Chemistry for their contributions in that field, the discovery of both ubiquitin and the proteasome [6].

The UPS, they found, is responsible for the degradation of ~80% of intracellular proteins [7]. Protein degradation by the UPS is mediated by the covalent conjugation of ubiquitin [8]. Protein substrates, destined to be degraded by the UPS, are labeled with multiple copies of ubiquitin, which are recognized by the proteasome and initiates their degradation [9] (Figure 1.1). Polyubiquitinated protein is processed in a stepwise fashion involving a series of three enzymes: Ubiquitin ligase E1, the ubiquitin activation enzyme, uses ATP hydrolysis to catalyze a thioester bond between E1 and the glycine residue of ubiquitin. After activation, the ubiquitin is transferred to the ubiquitin-conjugating enzyme E2. Next, E3 ubiquitin ligase proteins bind to the protein substrate. Finally, the polyubiquitinated protein is then

recognized by the proteasome and degraded [10, 11]. The removal of ubiquitin monomers or polyubiquitin chains from the substrate protein is catalyzed by deubiquitinating enzymes (DUBs); these enzymes counter the function of E3 ubiquitin ligases [12]. Over 70 DUBs encoded in the human genome play roles in recycling of ubiquitin from the substrate proteins, protection from protein degradation by removing the ubiquitin tags, and also regulation of non-proteasomal functions such as DNA damage repair [13, 14].
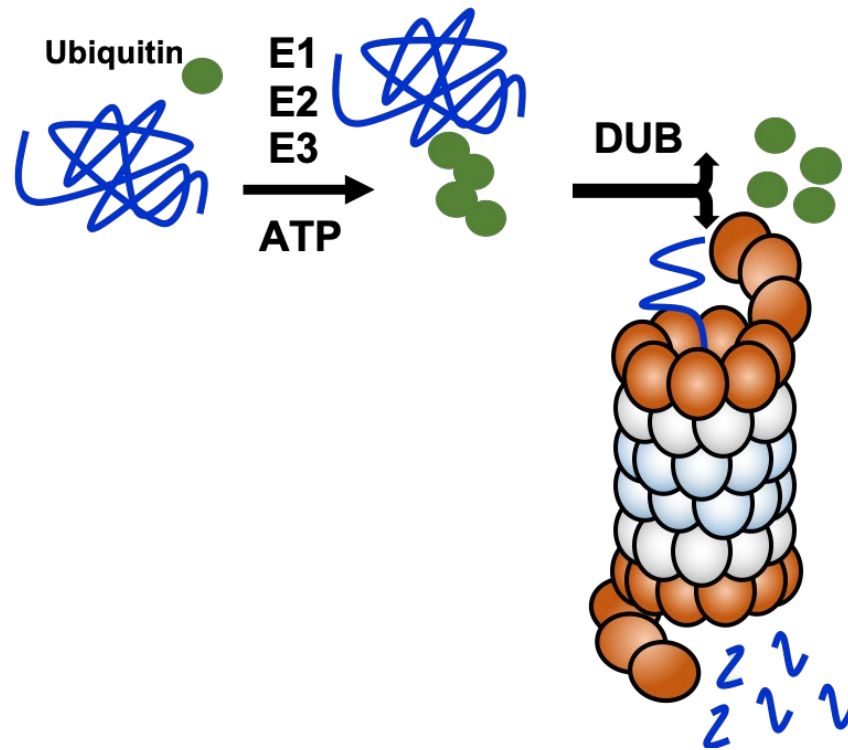
Figure 1.1 Ubiquitin Proteasome System

A polyubiquitin chain is covalently linked to a protein substrate through a series of three enzymes: an E1, an E2, and an E3. This polyubiquitin chain is recognized by the proteasome, which degrades the protein to short peptides and releases free ubiquitin.

1.2   Proteasome Structure and Subtype

1.2.1   Proteasome Structure

As the final executioner of the UPS, the proteasome is responsible for the controlled degradation of substrate proteins modified with a polyubiquitin chain. The proteasome is large protein complex, approximately 2.4 MDa, and consisted of two main components, the 20S core proteasome particle and a 19S regulatory complex. The 19S regulatory complex harbors 18 subunits containing the components to remove the polyubiquitin chain for recycling of ubiquitin, unfold the protein, and control the access of substrate proteins to the proteolytic 20S core [15-19]. The 20S core itself has a molecular weight of approximately 700 kDa and is formed from four heptameric rings: two outer α-rings and two inner β-rings (Figure 1.2).

The α-rings made from the α1-α7 subunits play an important role in regulating substrate entry into the 20S core for proteolysis. The inner two rings are also each made up of the β1-β7 subunits. The 20S proteasome has three types of catalytically active subunits, the β1, β2, and β5 subunits located in the two inner beta rings [20]. These catalytically-active subunits utilize an N-terminal threonine residue for their catalytic activity, placing them in the N-terminal nucleophile hydrolase family. Each catalytic subunit is initially made with propeptides that protect the N-terminal threonine residue from acetylation and prevent premature proteolysis [21]. Removal of these propeptides occurs through an autocatalytic mechanism with the fully assembled proteasome, indicating that these subunits cannot degrade proteins prior to their proteasome incorporation [22-26]. When a substrate protein enters the core 20S core particle, the active sites start cleaving the peptide bonds, generating peptide fragments ~3-22 amino acids in length [27,28]. Most of the products produced by the proteasome are then hydrolyzed by peptidases to single amino acids [29]. The

catalytically-active β1, β2, and β5 subunits also possess distinct substrate specificities. Structural and mutational studies revealed that the β5-subunit is responsible for chymotrypsin-like (CT-L) activity and cleaves peptide bonds preferentially after hydrophobic residues. The β1-subunit has caspase-like (C-L) activity cleaving the peptide bonds after acidic residues; and β2 cleaves after basic residues, consistent with trypsin-like (T-L) activity [30-34]. Together, these subunits cleave proteins into small peptides of unique and diverse sequences, which are especially important for antigen presentation and immune response [35].
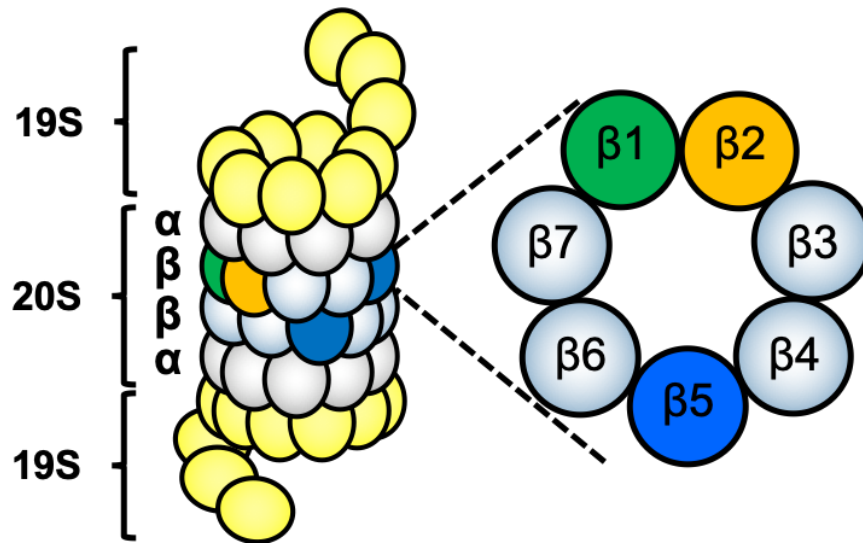
Figure 1.2. Structure of the 26S proteasome and the view of subunits of a β-ring

26S proteasome consists of a 20S core particle with two 19S regulatory particles at either end. The 20S core particle is formed with four heptameric rings, two α-rings and two β-rings. Each β-ring contains three catalytically-active β-subunits (β1, β2, and β5).

1.2.2   The Immunoproteasome and Thymoproteasome

Apart from the standard or also termed constitutive proteasome, there are subtypes of proteasomes having different structures: the immune proteasome and the thymoproteasome. A decade after the constitutive proteasome was discovered, another major subtype of the proteasome, the immunoproteasome was identified [36]. The immunoproteasome is predominant in immune cells such as monocytes and lymphocytes and is dramatically induced in non-immune tissues by proinflammatory cytokines such as interferon-γ (IFN-γ) and tumor necrosis factor-α (TNF-α) or viral infection [37]. Whereas the most common subtype of the proteasome, constitutive proteasome, comprises the catalytic subunits $\beta1$(Y, PSMB6), $\beta2$(Z, PSMB7), and $\beta5$(X, PSMB5), immunoproteasome differs mainly in incorporation of a distinct set of additional catalytic subunits in the 20S proteasome. The three catalytic immune subunits, $\beta1i$ (LMP2, lower molecular weight protein 2, PSMB9), $\beta2i$ (MECL-1, multicatalytic endopeptidase complex-like-1, PSMB10) and $\beta5i$ (LMP7, PSMB8) subunits, are the homologues of the $\beta1$, $\beta2$, and $\beta5$ subunits, respectively, with 59-71% amino acid sequence identity to respective constitutive homologues [38]. The $\beta1i$, $\beta2i$, and $\beta5i$ catalytic subunits are incorporated to 20S proteasomes in place of the $\beta1$, $\beta2$, and $\beta5$ subunits resulting in formation of the immunoproteasomes (Figure 1.3).

The most recently discovered subtype of the proteasome is the thymoproteasome. In 2007, Murata et al. identified a previously unrecognized catalytic subunit called $\beta5t$ expressed in cortical thymic epithelial cells [39]. The $\beta5t$ subunit is the homolog of the $\beta5$ subunit with 50% amino acid sequence identity [38]. In cortical thymic epithelial cells, $\beta5t$ subunit is incorporated with $\beta1i$ and $\beta2i$ subunit forming the specific subtype of the proteasome, thymoproteasome. Thymoproteasome plays a role in the positive selection of CD8+ T cells, acting as the safeguard against mature T cells deriving autoimmune response. Indeed, $\beta5t$ - deficient mice with lacking CD8+ thymocytes were not able to survive by influenza

7

virus infection [40, 41]. However, there is little data to show the exact functions of thymoproteasome in cancer or in non-cancer disease.
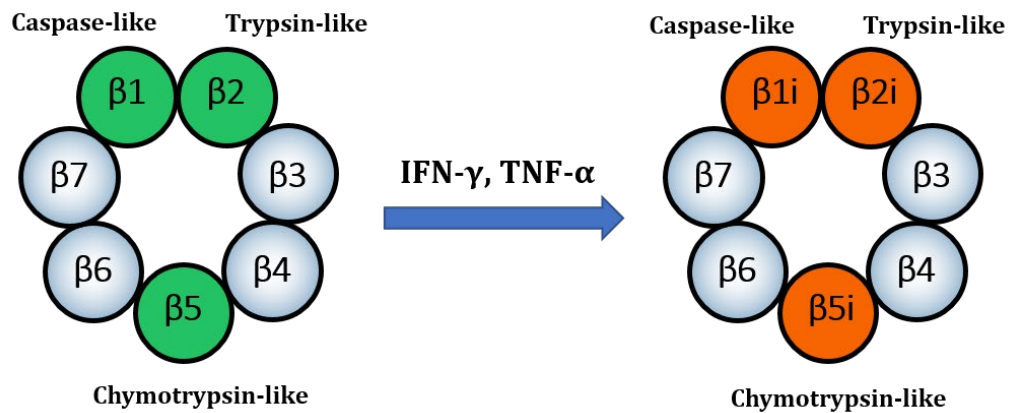
Figure 1.3. **Catalytic subunit compositions of the constitutive proteasome and the immunoproteasome**

The constitutive proteasome β-ring contains three catalytic β subunits β1, β2, and β5 as well as four catalytically inactive β-subunits. The synthesis of immunoproteasome is induced by cytokine stimulations such as IFN-γ or TNF-α. The induced immunoproteasome catalytic subunits β1i, β2i, and β5i are incorporated into the 20S proteasome to form the 20S immunoproteasome. Catalytic subunits β1/ β1i, β2/ β2i, or β5/ β5i have caspase-like, trypsin-like, or chymotrypsin-like activity, respectively.

1.3 Proteasome Function

The life cycle of all proteins starts from the synthesis at ribosomes to their degradation to peptides and further single amino acids. Protein degradation is the important step for cellular functions such as protein homeostasis, signal production, and cell proliferation. The proteasome located in the cytosol and the nucleus degrades more than 90% of cytosolic proteins by protecting cells from accumulation of harmful protein aggregates [42]. Proteasomes also play the major role in antigen presentation by production of peptides with hydrophobic C-terminal amino acids that bind with high affinity to major histocompatibility class I (MHC-I) receptors on the cell surface to control immune responses whereas another protease generates the correct N-terminus [43]. Especially, the immunoproteasome catalytic subunits are known to produce the peptides with a hydrophobic or basic C-terminal amino acid but less acidic C-termini [44].

The immunoproteasome, beyond the antigen presentation, regulates oxidative stress, and cytokine production. The role of the immunoproteasome was defined on reducing the oxidized proteins under Interferon-induced oxidative stress to maintain cellular homeostasis [45]. More interestingly, previous studies showing β1i knock out mice displayed the significantly increase levels of oxidized proteins in the brain and retinal pigmented epithelial (RPE) cells were more sensitive to oxidative stress in double knock-out mice of β2i and β5i suggested that immunoproteasome are protective against oxidative stress and damage [46, 47].

Additional studies of β1i knockout mice showed that their cognitive function was quite similar comparted to control mice, but they had a higher body weight and displayed the greater motor function [48-50]. Martin. et al. suggested that the increased motor function observed in patients with Parkinson's and Huntington's disease may relate to changes in the expression levels of proteasome subunit expression in the brains of these patients [50]. More recent study showed β5i knockout altered the levels of cytokines in whole brain and the profiles of microglial cytokine production without impacting levels of Aβ or amyloid precursor protein

(APP). Notably, the production of the proinflammation cytokines such as TNF-α, IL-6, and IL-1β in isolated microglia was significantly reduced in cells lacking β5i [51].

In addition, the immunoproteasome (specifically β5i) has been shown to modulate pro-inflammatory cytokine production in human tissues (T-cells, B-cells, neutrophils, monocytes, etc) and thus considered as a promising therapeutic target for autoimmune diseases [52-57]. β5i/LMP7-selective inhibitors (ONX-0914, KZR-616) are currently in early phase clinical development for the treatment of rheumatic diseases, such as lupus nephritis (LN). For β1i LMP2, there have been a few reports suggesting its involvement in processing of NF-κB precursors (p100/p105) and degradation of IκBα [58-60]. However, recent studies dispute the involvement of LMP2 in inflammatory responses showing using human peripheral blood mononuclear cells (PBMCs) reported no effect of LMP2 inhibition on cytokine secretion [56].

1.4   Development of Proteasome Inhibitors

To elucidate the functions of the proteasome in the cells, proteasome inhibitors were initially developed but it became evident that proteasome inhibitors may have therapeutic potential for diseases including cancer and inflammatory disease. Most of the proteasome inhibitors that have been developed are composed of a peptide sequence followed by a C-terminal warhead, pharmacophore, which interacts with the catalytic threonine residues of the proteasome's active sites. The most of proteasome inhibitors can be classified by the unique warhead pharmacophore into five main classes; the peptide aldehydes, peptide boronates, β-lactones, peptide vinyl sulfones, and peptide epoxyketones (Figure 1.4). In this section, known proteasome inhibitors classified will be discussed.

1.4.1   *Peptide Aldehyde Inhibitors*

Peptide aldehydes were the first class of synthetic proteasome inhibitors to be developed. Since the catalytic activity of the proteasome were initially thought to be similar to that of serine and cysteine protease, the first type of proteasome inhibitors were developed by using a C-terminal aldehyde, Z-LLF-CHO, Ac-LLnL-CHO, and Ac-LLM-CHO [61]. Co-crystallization of a peptide aldehyde inhibitor with the yeast proteasome showed aldehyde group of the inhibitor binds the active sites of the proteasome reversibly by producing hemiacetal adducts with the threonine residue of the catalytic site [30]. While a number of studies have used the peptide aldehyde inhibitors, further development of this class of proteasome inhibitors has been limited because of their off-target inhibition of cysteine and serine protease. forming hemiacetal adducts with their catalytic threonine residues [30, 33]. In this dissertation work, MG132 (Z-LLL-CHO, shown in Figure 1.4.) was used as a representative of peptide aldehyde inhibitor.

1.4.2   *Peptide Boronate Inhibitors*

Peptide boronates were also initially developted to inhibit serine protease. However, peptide boronates harbor the high affinity for the active site of the proteasome by interaction between a boronate hydroxyl group and the N-terminal amino group of the threonine residue of the proteasome active site. By that means, peptide boronates can achieve better potency and high selectivity to the proteasome over the serine protease. In the meantime, Adam et al. reported peptides boronates such as MG262 which is the boronate analog of MG132 with better potency and higher selectivity compared to the inhibitors with aldehyde pharmacophore in 1998 [62]. Further medicinal chemistry efforts with peptide boronates led to the development of the FDA-approved proteasome inhibitor drugs, bortezomib and ixazomib (Figure 1.4). Bortezomib and ixazomib will be discussed in detail below.

1.4.3   *β- Lactone Inhibitors*

Lactacystin was the first reported natural product of proteasome inhibitor with a non-peptide backbone (Figure 1.4). In 1995, Fenteany et al. found lactacystin bound to the threonine residue of the proteasome catalytic β5 subunit. Later, it was demonstrated lactacystin, converting to active form, *clasto*-lactacysistin β-lactone, at pH 8 from inactive itself, irreversibly inhibits CT-L activity predominantly and trpsin-like (T-L) and Caspase-like (C-L) activities at much slower rates [63]. Although lactacystin also found to be more specific to proteasome than the peptide aldehyde inhibitors, later works suggested β- Lactones also bind to some serine proteases [64, 65]. Besides this, the unstability of β- Lactones at neutral pH, and highly complex synthesis were considered as limitations of β- Lactones. Marizomib, known as salinosporamide A or NPI-0052, is a second natural product β-lactone, is currently in clinical development [66]. Notably, Di et al. observed that orally dosed marizomib significantly reduced the proteasome activity in pre-fontal cortex of healthy

cynomolgus monkeys, postulating the activity of marizomib to cross the blood-brain barrier [67].

1.4.4   *Peptide Vinyl Sulfone Inhibitors*

Peptide vinyl sulfones are another early class of proteasome inhibitors. Initially, Z-LLL-VS displayed the activity to target all three proteasome catalytic activities in purified proteasome and in cells. Bogyo et el. showed the vinyl sulfone pharmacophore binds to the hydroxyl group of the threonine residue, giving rise to irreversible-binding between proteasome inhibitors to the catalytic residue [68] (Figure 1.4). In line with this, this class of proteasome inhibitors labeled with a radioisotope, biotin, or fluorescent groups were utilized to understand the relationships between the peptide sequence of the inhibitor and its subunit binding specificities [69-71]. However, since the peptide vinyl sulfones were also initially developed as cysteine protease inhibitors, the use of vinyl sulfones is limited.

1.4.5   *Peptide Epoxyketone Inhibitors*

Another important class of natural product proteasome inhibitors, eponemycin and epoxyketone, was reported in 1999. Both eponemycin and epoxyketone are consisted of a peptide backbone with and N-acyl group and a C-terminal α′,β′-epoxyketone moiety (Figure 1.4). Eponemycin isolated from a *Streptomyces* strain was later shown to bind to β1i, β5i and β5 subunits of the proteasome whereas epoxyketone isolated from a *Actinomycete* strain was found to bind to β2, β5, β2i, and β5 by a group under Dr. Craig Crews [72, 73]. Their further studies showed epoxomicin primarily targets the CT-L acitivity of bovine proteasomes in an irreversible fashion. In 2000 Groll et al. reported the formation of a 6-membered morpholino ring between the catalytically active threoine residue and the inhibitor by X-ray crystallographic study of epoxomicin bound to the proteasome, giving rise to high specificity for the proteasome over other proteases such as serine

and cysteine proteases [74]. However, in 2016, Schrader et al. revealed a 7-membered 1,4- oxazepane ring, instead of a 6-membered morpholino ring between the threonine residue and the epoxyketone inhibitors using high-resolution X-ray structures of human 20S proteasome with three different epoxyketone inhibitors [75]. A notable peptide epoxyketone inhibitor, of special interest, Carfilzomib, is the second proteasome inhibitor to receive FDA approval for use as an anticancer agent [76].
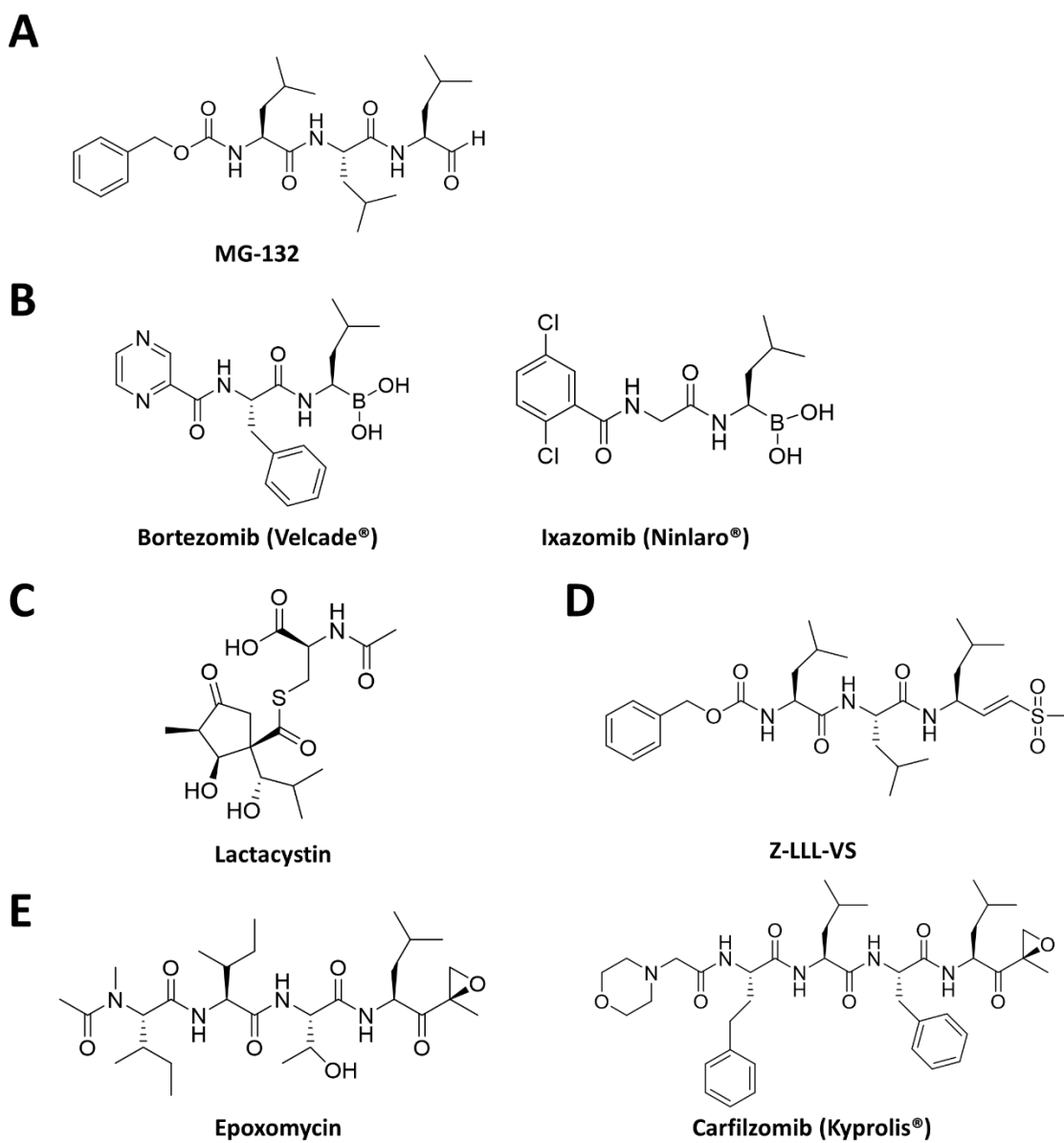
Figure 1.4. Representative members of the five major classes of proteasome inhibitors

A. Peptide aldehydes. A synthetic peptide aldehyde inhibitor MG-132 is shown. **B.** Peptide boronates. FDA-approved bortezomib and ixazomib are shown. **C.** β-lactone. The natural product lactacystin is shown. **D.** Peptide vinyl sulfone. Early proteasome inhibitor Z-LLL-VS is shown. **E.** Peptide epoxyketones. The natural product epoxomicin and FDA-approved carfilzomib are shown.

1.4.6 *Subunit-Selective Proteasome Inhibitors*

a. β5-selective inhibitors

PR-825 is the β5-seletive peptide expoxyketone inhibitor (Figure 1.5). This compound was used to distinguish the effects of selective β5-inhibition versus β5i inhibition on the production of pro-inflammatory cytokines in activated peripheral blood mononuclear cells (PBMCs) and an animal model of multiple sclerosis [52, 77].

PR-893, also known as CPSI (Constitutive proteasome selective inhibitor), was another β5-seletive peptide expoxyketone inhibitor. ProCISE assay showed this compound is highly selective for β5 over β5i (~21 fold) or β1i (~13 fold). PR-893 was utilized to examine the cellular effect of selective- β5 inhibition in cells, showing that inhibition of β5 subunit alone was not sufficient to induce cytotoxicity in hematologic cancer cells. Furthermore, selectively inhibiting β5 with PR-893 did not block production of IFN-α by bone marrow cells [78, 79].

b. β5i-selective inhibitors

The first β5i-selective inhibitor to be reported was ONX 0914, also referred as PR-957 (Figure 1.5). The tripeptide epoxyketone ONX 0914 showed a 20- and 40- fold selectivity for β5i over β1i or β5, respectively in human leukemia cell line MOLT-4 cells. Interestingly, ONX 0914 has shown to block the production of pro-inflammatory cytokines in PBMCs as well as T-cell activation and differentiation and to attenuate progression of experimental arthritis in mouse model, indicating a role of β5i during inflammation [52]. This supports the futher investigations to the potential therapeutic benefits of β5i inhibitors in treating autoimmune diseases are going [80].

The second β5i-selective epoxyketone inhibitor to be reported was IPSI (immunoproteasome-selective inhibitor), also known later as PR-924 [79] (Figure 1.5). ProCISE assay showed IPSI was highly potent for β5i (IC$_{50}$ of 22 nM against β5i) and 132-fold selectivite for β5i over β5. Later, there were a few studies reporting PR-924 inhibited cell growth and induce apoptosis in multiple myeloma cells whereas

PBMCs were not affected and further it exerted antitumor activity in mouse xenograft models [81].

c. β1i-selective inhibitors

As described above, the peptide epoxyketone natural products eponemycin and epoxomicin exerted a preference for β1i over other subunits. This gives rise for our lab to examine the the structure-activity relationship (SAR) for β1i inhibition using eponemycin analogues. Further medicinal chemistry efforts yielded the first immunosubunit-selective inhibitor, β1i-selective peptide epoxyketone inhibitor UK 101, to be reported by our group [82] (Figure 1.5). Our group reported UK101 was more cytotoxic to cancer cells highly expressing β1i than immunosubunit- deficient cells, suggesting β1i may play a role in regulating cell-growth in cancer cells abundantly expressing β1i. Later, Wehenkel et al. found that UK101 significantly reduced tumor growth in a mouse xenograft model of prostate cancer [83]. Later, UK101 was also reported to be highly selective for β1i over β1 (144-fold), but less selective for β1i over β5 (10-fold) [84].

Most recently, proteasome activity assay using subunit-selective fluorogenic peptide substrates showed the previously reported caspase-like inhibitor YU 102 (Ac-GPFL-epoxyketone) had high selectivity for β1i over β5 (> 100 fold) (submitted data by our group).

A
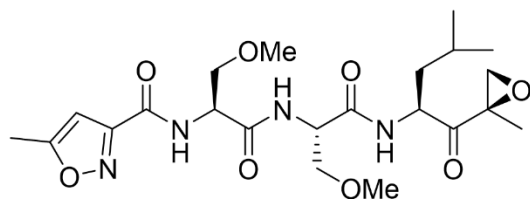
PR-825

B
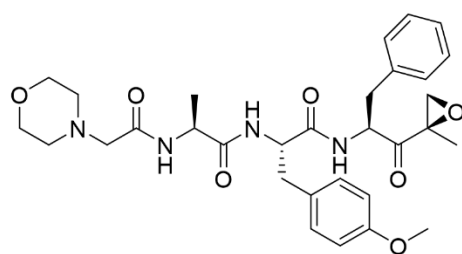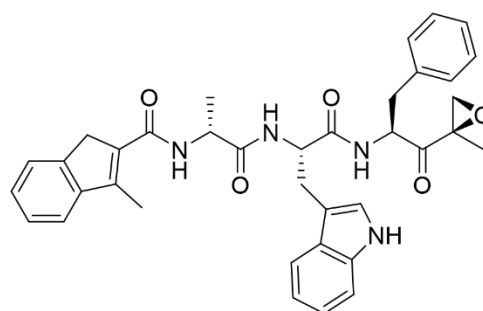
ONX0914 (PR-957)   IPSI (PR-924)

C
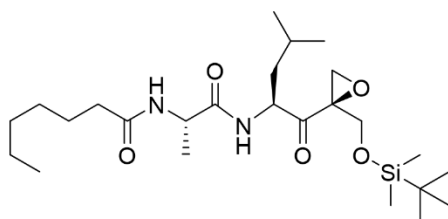
UK101

Figure 1.5. **Representative of subunit-selective proteasome inhibitors**
A. β5-selective inhibitor. The peptide epoxyketone inhibitor PR-825 is shown. **B.** β5i-selective inhibitors. The peptide epoxyketone ONX0914 (PR-957) and IPSI (PR-924) are shown. **C.** β1i-selective inhibitor. The epoxyketone inhibitor UK101 is shown.

1.5 The FDA-Approved Proteasome Inhibitors for MM

1.5.1 *Bortezomib* (Velcade®)

The first proteasome inhibitor to receive FDA approval was Bortezomib (Btz), formerly known as PS-341 and now marketed as Velcade® [85]. Structurally, bortezomib is a dipeptide boronate, mainly targets the both β5 and β5i subunits specifically and reversibly [86-88]. It has also been shown to target β1 and β1i with lower affinity [89, 90].

As previously described in chapter 2.4.1, considerable effort had been put forth to develop the peptide boronates with the improved selectivity for proteasome activity over serine proteases, leading to yield the derivatives of peptide boronates with the dramatically enhanced selectivity for the CT-L activity of the proteasome and the improved inhibitory potency. Meaningful results from collaboration work between ProScript and scientists at the National Cancer Institute (NCI) were published in 1999. The peptide boron ester PS-341 showed the most potent proteasome inhibition and significant cytotoxicity in the National Cancer Institute (NCI) panel of 60 cancer cell lines for assessing their anti-cancer activities among 13 derivatives of the peptide boronates. Following these results, PS-341 was tested against mice bearing tumor xenografts. This study showed that a single i.v. injection of 0.3 mg/kg PS-341 could significantly inhibit proteasome activity in white blood cells and in PC-3 tumor cells. Four direct injections of 1 mg/kg PS-341 into PC-3 tumors on a daily or weekly schedule significantly reduced tumor volume as compared to vehicle [62].

These significant results from preclinical trials of PS-341 led this compound into clinical trials in 2000 for further investigation of PS-341 as a potential anti-cancer reagent. Adams et al. reported in phase I trials PS-341 was well tolerated by patients in general, but with toxicities such as thrombocytopenia, fatigue, and peripheral neuropathy. Anecdotal reports of efficacy of the PS-341in non-small cell lung cancer, melanoma, and multiple myeloma were also noted in the study [91]. During its

clinical development at Millenium Pharmaceuticals, PS-341 received the nonproprietary name bortezomib and was finally marketed under the brand name Velcade®. In phase II clinical trials, bortezomib also demonstrated notable anti-cancer efficacy in newly diagnosed and relapsed/refractory multiple myeloma patients when administered in combination with other reagents including thalidomide, dexamethasone, and doxorubicin [92-94].

Based on promising clinical trial results, bortezomib was received the FDA approval in 2003 for the treatment of relapsed and refractory multiple myeloma [95]. Following the initial approval, the FDA expanded the bortezomib (Velcade) label to allow for previously untreated patients with multiple myeloma and mantle cell lymphoma [96, 97].

1.5.2 *Carfilzomib* (Kyprolis®)

Carfilzomib, formerly called PR-171 and now marketed as Kyprolis®, is the second proteasome inhibitor to be FDA-approved in 2012 for treating relapsed or refractory multiple myeloma. In a 2007 publication by Demo et al., carfilzomib inhibited the CT-L activity of the proteasome more selectively compared to bortezomib also slightly targeting $\beta 1$ [86, 98]. Another remarkable difference between carfilzomib and bortezomib is the proteasome specificity derived from the unique interaction of the epoxyketone pharmacophore and the N-terminal Threonine residues of the catalytic subunits of the proteasome. The proteasome specificity led to lower in vivo toxicity of carfilzomib relative to that of bortezomib and lower peripheral neuropathy, which is an off-target side effects of bortezomib, in carfilzomib-treated patients than bortezomib-treated patients [86, 99-103]. Furthermore, in comparison with bortezomib, the irreversible binding mechanism of the carfilzomib also facilitates a more sustained proteasome inhibition following a single exposure [86], suggesting carfilzomib exerts enhanced anticancer efficacy over bortezomib.

21

As previously described in chapter 2.4.5, the design of carfilzomib was begun from the natural product epoxomicin which was found to have proteasome inhibition in cells [73]. Traditional medicinal chemistry efforts from the Crews lab to optimize epoxomicin for anticancer activity led to development of potent YU101 derivatives. Following the successful clinical trials of bortezomib, Proteolix Inc. was established to develop YU101 as an anticancer therapeutic based on the great potency of YU101. Further medicinal chemistry efforts at Proteolix resulted in optimization of YU101 to improve poor water solubility (< 1 µg/mL) of YU101, yielding the lead compound PR-171, with the modified to the N-cap moiety of YU101 [86]. The potent anti-cancer efficacy of PR-171 was further verified in mouse xenograft models. Notably, PR-171 exerted its activity in multiple myeloma cell lines and tumor cells derived from patients who did not respond to bortezomib and cells resistant to conventional chemotherapeutics.

Based on these promising results of PR-171, Proteolix began phase I clinical trials of PR-171 with the generic name carfilzomib. Two phases I dose-escalation trials of single-agent carfilzomib were conducted in patients with relapsed or refractory hematologic malignancies to determine its safety and efficacy in patients with hematologic malignancies. Results from these studies established a dosing schedule of carfilzomib i.v. infusions, a consecutive-day, twice weekly at dose up to 27 mg/m^3 [101]. During the two trials, carfilzomib was well tolerated by patients and the objective response rate (ORR) was 16.7% and the median duration of response was 7.2 months for the ORR population [100, 101], giving rise to additional phase 2 trials to evaluate the activity of single-agent carfilzomib i.v. infusions at 20 or 27 mg/m^3 in patients with relapsed or refractory multiple myeloma patients who did not respond to prior therapies such as bortezomib and a single immunomodulatory agent (e.g. thalidomide and lenalidomide). In 2010, Siegel at al. reported the ORR was 24% and the median duration of response was 7.4 months [104]. In 2009, Onyx Pharmaceuticals acquired Proteolix for clinical development of carfilzomib and presented additional safety data from a total of 768 patients treated in phase I and II studies. Together, carfilzomib was granted accelerated FDA approval on July 20th,

2012 [76]. From the phase III trial to further confirm the drug's efficacy and safety, the clinical benefits of carfilzomib were examined in combination with the immunomodulatory agent lenalidomide and high-dose dexamethasone in patients with relapsed and refractory multiple myeloma. Results showed combination treatment of carfilzomib with the lenalidomide and dexamethasone had superior activity in comparison to only lenalidomide and dexamethasone, without carfilzomib [105]. More recently, ENDEAVOR the phase III trial study to compare combination of carfilzomib and dexamethasone versus that of bortezomib and dexamethasone in relapsed or refractory multiple myeloma patients, supporting the safety of higher doses of carfilzomib and better efficacy in those patients: the median progression free survival (PFS) in the carfilzomib group was 18.7 months, the bortezomib groups median PFS of 9.4 months [106].

1.5.3 *Ixazomib (Ninlaro®)*

Ixazomib, previously known as MLN9708 and now marketed as Ninlaro®, is the third proteasome inhibitor to be received the FDA approval in 2015 for the treatment of relapse multiple myeloma patients. Ixazomib is the first orally administered proteasome inhibitor. Structurally, Ixazomib is a N-capped dipeptide boronate and the boronate pharmacophore. Ixazomib can be formed from the hydrolized prodrug ixazomib citrate in aqueous solution or plasma, giving rise to the improved oral bioavailability compared to bortezomib and carfilzomib [107]. Ixazomib has a similar selectivity profile of the proteasome subunit to that of bortezomib, preferentially inhibiting $\beta 5$ reversibly, and to a lesser extent, $\beta 1$ catalytic subunit [107]. Chauhan et al. also reported that ixazomib inhibited the CT-L activity more strongly and displayed anticancer activity in multiple myeloma cells, even in bortezomib resistant multiple myeloma cells. Moreover, ixazomib exerted greater antitumor efficacy in xenograft mouse models of multiple myeloma, lymphoma, and solid cancers, supporting ixazomib's superior anti-cancer activity compared to bortezomib [107, 108].

In clinical trials, the median time of progression free survival of patients with relapsed or refractory myeloma in combination therapy of ixazomib with dexamethasone and lenalidomide was significantly prolonged (20.6 months in ixazomib-treated group versus 14.7% in the control group) [109, 110]. Notably, ixazomib had the improved toxicity profile despite the same pharmacophore as bortezomib [111]. Taken together, FDA approval was granted to ixazomib in 2015 for use in combination with dexamethasone and lenalidomide in treating multiple myeloma in patients who have received at least one prior therapy [112].

1.6 Resistance to Proteasome Inhibitors

As previously discussed, the FDA approvals of proteasome inhibitors, bortezomib, carfilzomib, and ixazomib in 2003, 2012, and 2015, respectively, have transformed treatment paradigm for patients with newly diagnosed and refractory multiple myeloma. However, multiple myeloma remains incurable with an expected median survival of 7-8 years [113, 114]. The biggest challenge of the use in treatment of multiple myeloma patients is drug resistance. Although the response rates of bortezomib and carfilzomib were increased up to ~70-90% when combined with other drugs including lenalidomide, all patients eventually develop resistance to therapy and have a dismal prognosis once resistance emerges [115]. In order to understand the mechanisms of proteasome inhibitor resistance in patients, extensive preclinical efforts have been undertaken. Although the exact resistance mechanisms of clinical proteasome inhibitors are still unknown, several preclinical studies reported the candidate resistant mechanisms to proteasome inhibitors.

1.6.1 *Bortezomib resistance*

Over the last decade many potential mechanisms, including proteasome-dependent and proteasome-independent mechanisms, have been studied for

bortezomib resistance. Mainly reported mechanisms for bortezomib resistance were mutations in the PSMB5 gene and upregulation of constitutive catalytic subunits.

Using the established bortezomib resistant lurkat cell line model developed by adapting cells to increasing concentration of bortezomib, Lu et el. and Oerlemans et al. reported the mechanisms responsible for bortezomib resistance in cancer cells. The bortezomib resistant- lurkat cell line or -THP-1 cell line containing overexpressed *PSMB5* gene encoding the β5 catalytic subunit of the proteasome. Moreover, CT-L activity and the expression levels of β5 catalytic subunit were increased in these cell lines, supporting the β5 catalytic subunit is the key component for bortezomib resistance [116, 117]. Indeed, siRNA-mediated silencing of the *PSMB5* gene resulted in sensitization of bortezomib-resistant THP-1 cells to bortezomib. In such models, point mutations (Met45, Ala49Thr, and Cys52) in the *PSMB5* gene affecting the proteasomal inhibitory activity of bortezomib were also identified. Since the location of those point mutations was highly conserved S1 binding pocket of β5, it was postulated that mutations in the *PSMB5* gene interfered the binding of bortezomib to β5, thus affecting the cytotoxic effects of bortezomib in cells. Although these preclinical findings suggested the potential bortezomib-resistant mechanism in several cell line models, only one case study has identified *PSMB5* gene mutations in a patient who had treated with bortezomib [118-120].

Recent study has focused on the potential role of the unfolded protein response (URP) in resistance to proteasome inhibitors. The UPR is a stress response pathway and causes cell apoptosis when it is activated. One of main transcription factors involved in the UPR signaling, X-box binding protein 1 (Xbp-1), is known to be highly expressed in myelomas compared other cancer types, suggesting Xbp-1 is indispensable for multiple myeloma pathogenesis such as development of plasma cells [121, 122]. While it has been reported that proteasome inhibitors can both induce the UPR and inhibit Xbp-1, the roles of the UPR and Xbp-1 in proteasome inhibitor resistance was not explored in detail until early 2000's [123]. In 2012 Ling et al. reported response of myeloma to bortezomib is correlated to the Xbp-1 and the study showed the downregulated Xbp-1 expression in bortezomib resistant multiple

myeloma cells, suggesting low Xbp-1 expression is associated with lower bortezomib sensitivity [124]. In 2016, Nikesitch also found the significant role of Xbp-1 in determination of the sensitivity to bortezomib in hematological cell lines and primary multiple myeloma samples [125]. In contrast to 2012 Ling et al.'s study, Leung-Hagesteijn et al. found that Xbp-1 silenced mediated bortezomib resistance in multiple myeloma cell lines and identified two Xbp-1 mutations Xbp-1 L178I and P326R in bortezomib-resistant multiple myeloma. Multiple myeloma cell lines with Xbp-1-silenced or Xbp-1 mutations with lower protein load and the UPR activation may exhibit a survival advantage against proteasome inhibition induced cytotoxicity [126]. In line with this, high Xbp-1 expression can be a prognostic marker of clinical outcome in multiple myeloma patients who treated with bortezomib [127]. While Xbp-1 may play a key role in the sensitivity to multiple myeloma to bortezomib, it is still unknown whether resistance of other cancer types to PIs are also related to the function of Xbp-1.

1.6.2 *Carfilzomib resistance*

The studies conducted to date have mainly focused on elucidating bortezomib resistant mechanism, and there are only a few have explored resistant mechanisms against carfilzomib in cancers.

P-glycoprotein (P-gp), also termed as MDR1, is a transporter that extrudes a wide range of substrates out of the cells in an ATP-dependent manner and it is well documented that it can mediate cancer resistance to other anti-myeloma agents such as doxorubicin, paclitaxel, and vincristine [128-131]. Verbrugge et al. found the several drug efflux transporters have involved in the sensitivities to proteasome inhibitors such as bortezomib, carfilzomib, ONX 0912, ONX 0914 in carfilzomib/ONX 0914 cross-resistant cancer cells [132]. In this study, overexpression of P-gp was observed in carfilzomib resistant cells compared to in the its parental cells. Moreover, the use of reversin 121, a P-gp inhibitor, restored the sensitivity to proteasome inhibitors in both CEM/VLB cells and peripheral blood mononuclear cells, suggesting

P-gp plays a significant portion of resistance mechanism in cancers against epoxyketone proteasome inhibitors. Consistent with these findings, our group also found that the expression levels of P-gp was upregulated in carfilzomib resistant H23 lung and DLD-1 colon cancer cells and P-gp inhibition by verapamil altered carfilzomib sensitivity to near that of the parental cell lines [133]. More interestingly, a 2016 publication showed the induced gene expression of P-gp in primary cells derived from multiple myeloma patients who did not respond to carfilzomib therapy [134]. Using multiple myeloma cells isolated from patients during carilzomib therapy, Besse et al. also showed that ABCB1 gene expression was increased and gene deletion resulted in sensitization of carfilzomib resistant AMO cells to carfilzomib [135]. Since only these two studies showed the clinical evidence of P-gp mediated resistance to proteasome inhibitors, further validations of this mechanism are important to confirm their relevance in the clinic and to develop the therapeutic strategies overcoming proteasome inhibitors resistance in cancers.

1.7 Alzheimer's Disease

Alzheimer's disease (AD) is the most common form of dementia in the elderly, accounting for around 60% of all dementia cases [136]. An estimated 5.7 million Americans of all ages are living with AD in 2018, and the proportion of elderly people in the population has been increasing steadily, thus the burden of the disease is expected to become greater over years. AD is a neurodegenerative disorder with a mean duration of around 8.5 years between clinical symptoms and death.

Alzheimer's disease was first described by Alois Alzheimer. In 1906, a psychiatrist and neuropathologist Alois Alzheimer first reported "A severe disease process of the cerebral cortex" to the 37th Meeting of South-West German Psychiatrists in Tubingen, Germany. At the meeting, Alzheimer described an unusual case, a 50-year-old woman Auguste D. with memory impairment, psychosocial incompetence and disorientation until her death 5 years later. While the unfamiliar

notion that a "mental" disorder like presenile dementia could be due to "physical" aberrations was not easily accepted at the time, nevertheless, the disorder would be named in 1910 after Alois Alzheimer by his mentor, Emil Kraepelin. Alois Alzheimer also presented the observation of the neuropathological lesions, neurofibrillary tangles in the brain of her at autopsy in 1911 [137, 138]. Until the late 1960's, Alzheimer's disease itself was not considered as a disease separated from dementia. Kay et al. identified AD was different from normal aging symptoms in 1964 and it was reported there was a relationship between cognitive dysfunction and the hallmarks of the disease such as neurofibrillary tangles and neuropathological lesions in a 1968 publication by Blessed et al. [139, 140]. In 1981, Heston et al. first reported that relatives of 125 subjects who had autopsy-confirmed AD exhibited a significant excess of dementing illness consistent with genetic transmission [141]. Later study also identified mutations involved in hereditary forms of AD in 1996 [142]. These findings supported AD may be no longer considered as aging but should be diagnosed differently from other forms of dementia.

According to most sources, AD is defined to consist of irreversible memory loss, and deterioration of language, judgement, confusion with time or place, and trouble understanding visual images, progressing over 10 to 15 years. Brain regions, particularly the neocortex and hippocampus, are associated with higher mental functions, are most affected by the characteristic pathology of Alzheimer's disease. Pathologically, AD is characterized by the accumulation of extracellular amyloid plaques in senile plaques made by the amyloid-beta protein and intracellular formation of neurofibrillary tangles which are aggregates of hyperphosphorylated tau protein, and the loss of neuronal synapses and pyramidal neurons. These changes develop the typical symptomology of Alzheimer's disease [143, 144].

Amyloid precursor protein (APP) is cleaved by three types of proteases, α-, β- and γ-secretases. Amyloid-beta (Aβ) is generated when the APP is cleaved by β secretase and then by γ secretase complex. β secretase cleaves APP at the bond between Met671 and Asp672 (β-site) and γ secretase cleaves at the site between 711-713 amino acid, resulting in A$\beta_{1\text{-}40}$ or A$\beta_{1\text{-}42}$. A$\beta_{1\text{-}42}$ is mainly found in the amyloid

plaques, a hallmark of AD, while $A\beta_{1-40}$ also found in the plaque is predominantly involved in the brain vessels which is known as cerebral amyloid angiopathy. Since α secretase cleaves within the $A\beta$ sequence of APP, cleavage of APP by combination of α secretase and γ secretase does not generate $A\beta$ [145].

Neurofibrillary tangles (NFTs), are aggregates of tau. Tau protein found in cytosol, axons, and neurons is the member of microtubule-associated proteins family. Blennow et al. suggested tau proteins might be synthesized in glial cells, mostly in pathological situations [146]. Microtubule-associated proteins regulates the stability of axon microtubules by promoting polymerization and binding with tubulin, resulting in suppression of their dephosphorylation. Phosphorylation of tau can occur at 30 different sites and hyper-phosphorylation of tau causes self-assemble into tangles and then accumulation of tau aggregates, thereby, leading the loss of axonal or dendritic transport in diseases [147-149].

1.8 Causal Theories of Alzheimer's Disease

Over the past two decades, a considerable research effort has been directed towards discovering the cause of Alzheimer's disease. To develop safe and effective pharmacological treatments, it is important to acknowledge that multiple causal theories for AD have been proposed. A few of these hypotheses are discussed briefly in this section.

1.8.1 *Cholinergic theory*

Martorana et al. reported a theory pertaining to the cause of AD, cholinergic hypothesis based on data showing AD brains expressed lower levels of a neurotransmitter acetylcholine in the brain compared to non-demented elderly [150].

Extensive efforts in discovering and characterizing the most important neurotransmitters and their receptors in the brain underlay specific nervous connections with brain functions, giving rise to establish the idea that altered function of neurotransmitter systems was associated with neuropathology. In a 1976 publication, a specific cholinergic deficit was consistently identified from a forebrain to hippocampus and the cortex from AD patients [151]. Moreover, the activity of choline acetyltransferase, the enzyme for the synthesis of acetylcholine, was reduced in pathological samples from the hippocampus and cortex of the patients with AD. Based on these significant observations, Bartus et al. first stated the cholinergic hypothesis of age-related cognitive dysfunctions and dementia [152]. In addition, the 1986 Nobel prize was awarded to Rita Levi Montalcini and Stanley Cohen for the discovery of nerve growth factor, leading the interest of neuronal survival factors in Alzeheimer's disease. Taken all together, several drugs targeting cholinergic transmission were introduced for treatment of AD patients [153]. Four cholinesterase inhibitors, tacrine, donepezil, rivastigmine and galantamine, have received approval by FDA and have been widely used for years in many countries, in particular for patients who were diagnosed with mild and intermediate forms of AD. Reduction of cholinesterase resulted in retaining acetylcholine in the brain. Though the therapeutic options available on the market target the cholinergic system, the strategies have been failed to delay disease progression.

1.8.2 *Amyloid theory*

Amyloid hypothesis is the most heavily investigated theory for the cause of AD over 25 years [154-156]. The importance of amyloid was not the prevailed idea in a field of AD and Alzheimer's researchers were considering the cholinergic hypothesis in the 1980s and assumed that a decline in the neurotransmitter acetylcholine is a cause of the disease at that time. Dennis Selkoe who is now a major proponent of amyloid hypothesis was not interested in acetylcholine at the time. After he met George Glenner who initially identified and biochemically characterized Aβ, Selkoe

moved his research to amyloid field from studying tau protein and built multiple findings from genetic, molecular, biochemical, and neuropathological studies of amyloid. Kang et al. reported the discovery of genetic mutations of APP in AD [157]. These mutations in APP/Presenilin are closely linked to the Aβ production process, providing a rational for the idea that Aβ production and Aβ amyloid fibril formation represent the central pathogenic cause of AD. In 1992, it was hypothesized by Seiko et al. that Aβ aggregation was the initiating factor in AD progression since the genetic links to AD all led to an increase in Aβ protein rather than tangles [158].

While Aβs excised from APP by β- and γ-secretase are released outside the cell and then are degraded in normal subject, degradation of Aβ is decreased and Aβ peptides are accumulated in the aged subject. In the brain of normal subject, the concentration of the Aβ peptide is regulated by following mechanisms: the Aβ peptide generation from APP, influx into the brain across the blood-brain barrier (BBB), clearance from the brain, and enzymatic degradation within brain [159-161]. Thereby, impairment of these regulatory mechanisms could result in the accumulation and deposition of excessive amounts of the Aβ peptide in the brain of AD patients. This amyloid hypothesis states that an increase in Aβ aggregation either from decreased clearance or increased production, leads to microglial and astrocytic activation, altered neuronal ionic homeostasis, altered kinase and phosphatase activity which increases phosphorylation of tau leading to tangle formation, leading to neuronal cell death and neurodegeneration. Thus, drugs that remove the amyloid should slow the progression of AD. Yet all drugs targeting amyloid, including solanezumab, bapineuzumab, and gantenerumab, have failed to reduce cognitive dysfunctions in phase III clinical trials and another antibody, ponezumab also failed after phase II [162-165]. These results have led scientists to become increasingly skeptical of the amyloid hypothesis and explore other potential pathogeneses of AD.

1.8.3   *Tau theory*

As discussed before, the discovery of neurofibrillary tangles (NFTs) by Alois Alzheimer in the brains of patients with the neurodegenerative disorder named after him (Alzeimer's disease) provided the basis for many studies to elucidate the molecular, cellular and genetic features of this disease more than a century ago. However, the discovery that the protein components of NFTs and the paired helical filaments (PHFs) were hyperphosphorylated forms of tau was achieved only during the 1980s. In 1986, Kosik et al. discovered that the NFTs in the brains of AD patients are composed of phosphorylated tau proteins [166]. Microtubule-Associated Protein Tau (MAPT) stabilizes microtubules and can undergo post-translational modifications such as phosphorylation. When tau is hyperphosphorylated, it dissociates from microtubules and aggregates into paired helical filaments (PHFs) and NFTs. The tau hypothesis speculates that tau tangle pathology precedes Aβ plaque formation and that tau phosphorylation and aggregation is the primary cause of neurodegeneration in AD. Tau phosphorylation reduces its ability to promote assembly of microtubule, giving rise to neurodegeneration through synaptic disruptions and neuronal loss [167, 168]. Furthermore, the NFT can cause neuronal impairment and death.

While the amyloid hypothesis suggests that tau aggregation occurs downstream of Aβ aggregation, tau tangles can be detected in the brains of patients with very mild dementia and no Aβ pathology [169]. Tau pathology also correlates more closely with AD progression and severity than Aβ plaque load does [167, 170]. Tau hypothesis-based strategies have shown some promising results and there are currently seven anti-tau therapies in phase II trials [171]. However, anti-tau therapies have also failed in phase III clinical trials. Tau phosphorylation was facilitated by a protein kinase, glycogen synthase kinase 3 beta (GSK-3β), which is an attractive target for anti-tau therapies. GSK-3β inhibitors are arguably in the most advanced stages of clinical development for AD. Among the various drugs that are currently being investigated, tideglusib, an irreversible inhibitor of GSK3-β, has recently

completed phase II trials yet did not show significant clinical improvement in a phase II trial [172].

1.8.4 *Neuroinflammation theory*

Since the late 1980s, several studies have shown that the chronic inflammation, seen in many diseases of the elderly, was found in the brain of AD patients and may even to initiate the recognized pathology. In 1990, McGeer et al. reported that exposure to anti-inflammatory drugs, known as non-steroidal anti-inflammatory drugs (NSAIDs), lowered the risk of AD. In addition, it was reported that NSAID delayed the progress of cognitive dysfunctions in 1995, suggesting that inflammation plays some roles in the disease and targeting inflammation may be used for treatment of degenerative brain disorder [173, 174]. Furthermore, new hypothesis suggesting amyloid peptide is involved in immunity also supports the contribution of inflammation in AD [175, 176]. Additionally, a common risk factor for the disease is brain injury, suggesting that chronic inflammation could initiate or at least partake in the course of AD [177].

It has long been thought that the brain was immunologically privileged with no resident or infiltrating immune cells; however, it is now considered that the cells of the brain are contributing to neuroinflammatory responses. The glial cells of the brain (astrocytes, microglia, oligodendrocytes, and pericytes) are involved an inflammatory response, but the main regulator of inflammation in the brain is the microglia cell [178]. Microglial cells make up ~12% of brain cells and are generally in a resting state (termed inactive or less active state). It is now thought that yolk-sac derived fetal macrophages are the precursors for microglia while originally thought to be derived from the macrophage cell line. Tumor necrosis factor alpha (TNF-α) or interferon gamma (IFN-γ) stimulates macrophages to release several pro-inflammatory cytokines and to produce reactive oxygen species [179-181]. This proinflammatory state, has high microbicidal activity and is an important defense

mechanism for the body. However, it also can cause damage to the tissues and it has been implicated in the development of autoimmune disorders.

While inflammation was typically considered a downstream event to the amyloid hypothesis, Aβ causes microglia activation, neuroinflammation may worsen the course of disease. When fully activated, microglial cells produce pro-inflammatory cytokines including TNF-α, interleukin-6 (1L-6), and interleukin-1β (IL-1β) [182]. These pro-inflammatory cytokines and activated complement factors has led to the idea that neuroinflammation is involved in the pathology of Alzheimer's disease. Indeed, the activated microglial cells were increased in AD progression, suggesting that Aβ deposition stimulates microglial activation. Several studies have shown that microglia can surrounds Aβ plaques and can phagocytose Aβ [183-185]. Microglia can be stimulated by a variety of substances to yield an inflammatory phenotype in the brain. Induction of a proinflammatory phenotype by LPS or TNF-α cause Aβ clearance [186, 187]. On the other hand, anti-inflammatory cytokines induction exacerbated Aβ deposition [188]. In a 2015 publication, a long-term induction of anti-inflammatory cytokine IL-10 showed a significant increase in Aβ deposition and led to cognitive behavior in APP transgenic mice model [189]. Thus, we postulate high levels of these markers can represent progression of AD. Several clinical anti-inflammatory drugs targeting COX or TNF-α have been investigated for their effects on AD via population-based studies or randomized controlled clinical trials, yet have yielded no clinical AD therapies so far [190]. On the other hand, several compounds that suppress neuroinflammatory responses have been identified from screening campaigns but not yet translated into effective AD drugs [191, 192].

1.9 Treatment of Alzheimer's Disease

To date, the Food and Drug Administration (FDA) and the European Medicines Agency (EMA) have approved only medications for alleviating symptoms for AD patients.

These medications include acetylcholinesterase (AChE) inhibitors such as donepezil, galantamine, rivastigmine, and a NMDA receptor antagonist, memantine. AChE inhibitors are used to induce the level of acetylcholine at synapses restraining the loss of neurotransmission found in AD. On the other hand, a NMDA receptor antagonist regulates glutamate-induced toxicity.

Donepezil hydrochloride (brand name Aricept) approved in 1996 for treatment of all stages of AD by preventing the breakdown of acetylcholine in the brain is a highly selective and reversible antagonist for AChE. In a 1998 publication, Rogers et al. reported the effect of donepezil hydrochloride on 468 participants who had mild to moderate AD. In this study, 32% of the 5mg treatment group and 38% of the 10 mg treatment group showed clinical improvement on various psychiatric scales, indicating donepezil is effective in cognition and global function decline in AD [193]. So far, donepezil is the only AchE inhibitor approved for treatment of severe AD.

Rivastigmine tartrate (brand name Exelon) approved in 2000 is less frequently used than other AChE inhibitors for treatment of mild to moderate AD patients. Lanctot et al reported the effect of rivastigmine at different dosages and various treatment intervals. The patients administered at high dose (6-12mg/day) showed dramatic improvement in cognitive function at all intervals (12, 18, and 26 weeks), proving treatment of rivastigmine at 6-12mg daily over a long time periods may be an effective strategy [194].

Galantamine hydrobromide (brand name Razadyne) approved in 2001 for treatment of mild to moderate AD by inhibiting the hydrolysis and increasing the concentration of acetylcholine. Galantamine is a specific, competitive, and reversible AChE inhibitor. As described in a 2006 review article by Loy and Schneider et al.,

treatment of galantamine (18-32 mg/day) showed significant improvement on cognitive symptoms at 3 months and 6 months intervals [195].

Memantine (brand name Namenda) was approved by FDA in 2003 for treatment of moderate to severe AD [196]. Memantine is a noncompetitive NMDA receptor antagonist, blocking glutamatergic receptors and regulates the action of glutamate. Under physiological conditions, magnesium ions are capable of blocking NMDA receptor which is a glutamate receptor and ion channel protein found in nerve cells. Glutamate signaling enhances depolarization of the post-synaptic membrane and unblock NMDA allowing calcium ions to flow into the postsynaptic neuron. In AD, however, constantly stimulated glutamate and over-activated NMDA receptor could be observed, causing cognitive impairment. Thus, memantine is considered as a neuroprotective agent by preventing excess glutamate-related excitotoxicity [197]. In a 2003 publication, Reisberg et al. showed memantine regulated NMDA receptors, leading to alleviation of AD symptoms. Among 345 elderly participants with moderate to severe AD, 29% of the memantine treated group showed the improvement of cognitive dysfunctions [198]. Although memantine has shown to positive results to reduce the rate of cognitive decline, it is not also capable of preventing the neuronal damage detected in AD.

1.10 Efforts to Develop Alzheimer's Disease Therapeutics

As we discussed previously, evidence supporting the amyloid theory led to development of AD therapeutics either disrupting aggregation, or promoting removal of Aβ. Based on the amyloid theory, Inhibitors targeting Aβ aggregation have been developed, including glycosaminoglycan 3-amino-1-propaneosulfonic acid (3APS), colostrinin, scyllo-inositol and Zinc/Copper chelators. Among these compounds, only 3APS designed to interfere with endogenous glycosaminoglycans, which were shown to promote aggregation of Aβ, has reached to phase III clinical trials, however, results of the clinical trials were disappointing [199].

Immunotherapy has been one of the most attractive approaches for AD drug development. It has been reported that both vaccination and monoclonal antibodies approaches have been developed to be successful. At the first time, using an active vaccine (AN1792) with $A\beta_{1-42}$ showed the promising results only in preclinical studies, but not in clinical trials with side effect such as encephalitis [200]. Since encephalitis was found in one patient treated with AN1792 in a Phase I clinical trial who died approximately one year after her last injection, vaccines have been developed to improve the safety issue. However, the various types of antibody responses were found in elderly and it led to further investigation of passive immunization using monoclonal antibodies.

Bapineuzumab (Janssen/Pfizer) and Solanezumab (Eli Lilly) are monoclonal antibodies designed to increase the clearance of Aβ and have been heavily investigated. Bapineuzumab is a humanized, N-terminal specific anti-Aβ monoclonal antibody, binding to neurotoxic amyloid proteins in the brain. Several preclinical studies have shown that passive immunotherapy with monoclonal antibodies led to a significant clearance of Aβ protein levels in the brain and improved the memory loss in transgenic mouse models with excessive Aβ proteins [201-205]. Additionally, phase II clinical trials have shown that bapineuzumab can reduce deposition of amyloid proteins and the concentration of phosphorylated tau proteins in the cerebrospinal fluid [206, 207]. Based on ongoing Phase II study, Elan/Wyeth announced the start of the Phase III clinical trials for bapineuzumab on May 2007. However, bapineuzumab was failed in phase III clinical trials [208]. Solanezumab developed by Lilly, on the other hand, is a monoclonal antibody that recognizes an epitope in the core of the amyloid peptide, binding to soluble Aβ and with low affinity for the fibrillar Aβ form. Solanezumab has also been tested in two phase III clinical trials (Expedition 1 and 2) in a population of patients with mild to moderate AD similar to that in trials with bapineuzumab. Unfortunately, it was recently found that solanezumab also could not meet its clinical endpoints for efficacy in patients with mild AD [209]. The human monoclonal antibody Aducanumab (Biogen) is another attractive passive immunization strategy for treatment of AD and has been fast-

tracked to phase III clinical trials. Aducanumab is currently being evaluated in two global Phase 3 studies (ENGAGE and EMERGE) designed to evaluate its safety and efficacy in slowing cognitive impairment in people with very early AD or mild AD. This study is set to end in April 2022.

Considerable efforts to prevent Aβ production have focused on inhibiting β-secretase, which are responsible for production of Aβ since the proteolytic processing of APP by β-secretase (beta-site APP cleaving enzyme 1, BACE1) is the rate-limiting step in the production of Aβ. Thus, BACE1 is thought to be a major therapeutic target and BACE1 inhibitors have the potential to be disease-modifying drugs for AD treatment. Due to the location of BACE1 in the brain BACE1 inhibitors need to cross the BBB to access the target and it is quite challenging [210]. Furthermore, BACE1 displays the large catalytic pocket, suggesting BACE1 inhibitor needs to be large enough to interact with the active site though the inhibitors also should be small enough to have drug-like physiochemical properties [211]. Vassar also reported that several BACE1 inhibitors during the clinical trials showed off-target toxicity, indicating the inhibitors are also required to be selective over other aspartic proteases to prevent toxic effects by cross inhibition. With efforts to search for effective and selective BACE1 inhibitors, some compounds have shown promising results in preclinical studies and six drugs, JNJ-54861911, CNP520, LY3202626, elenbecestat, lanabecestat, and verubecestat, are currently being evaluated in clinical trials in patients with mild to moderate AD [212, 213]. Especially, verubecestat was the first BACE1 inhibitor to reach to phase III clinical trials. However, Merck has discontinued its pivotal trial in patients with mild to moderate AD due to low efficacy in cognitive decline reduction [214]. Consequently, these disappointing results remain questions regarding the potential use of BACE1 inhibitors as AD drugs. Nevertheless, recent results from an animal model to mimic BACE1 inhibition in patients with AD by deletion of BACE1 support that BACE1 inhibition can completely reduce amyloid pathology and inhibiting BACE1 may have a potential for treatment of AD [215].

The large body of results showing tau protein aggregates accumulated in the brain of AD patients highly led to investigation of therapeutic strategy targeting tau to treat AD patients. Preclinical studies from the transgenic mouse models using various anti-tau antibodies have shown that antibodies against tau prevented extracellular trans-synaptic transmission of misfolded tau between cells. Following toxicology studies, the compound C2N-8E12, now known as ABBV-8E12 (AbbVie & C2N Diagnostics), was reached to initiation of clinical trials in 2015. In a phase I clinical study safety, tolerability and pharmacokinetics of ABBV-BE12 were tested on 32 patients. As a result, ABBV-BE12 was found to be safe and tolerable when single injected into the blood [216-218]. Positive results from a phase I trial led to phase II clinical trials of ABBV-BE12 and the study is set to end in May 2019. Another anti-tau monoclonal antibody BIIB029 (Biogen) was also moved to phase II clinical trials with the patients with early AD and the estimated study completion date is July 2021 [219, 220].

Azeliragon (vTv Therapeutics Inc), also known as TTP488, is an orally bioavailable small molecule that inhibits the receptor for advanced glycation end products (RAGE) that is thought to be involved in the development of Alzheimer's disease. RAGE found in the brain and the periphery is an immunoglobulin family member and is expressed in endothelial cells and microglia cells and is upregulated in AD [221-224]. In a 2012 publication, Li et al. suggested that RAGE may contribute to AD pathology by promoting influx of peripheral Aβ into brain and regulating Aβ induced oxidative stress, mediating AGE induced hyperphosphorylation of tau [225]. RAGE is also thought to interfere with inflammation and transfer Aβ into the brain. A number of preclinical studies and positive results of phase I/II clinical trials led to phase III clinical trials of azeliragon to evaluate the efficacy and safety of this compound in patients with mild Alzheimer's disease. The company vTv Therapeutics, conducting a phase III trials of the drug in mild AD, announced preliminary results in early 2018. Unfortunately, the study was terminated due to a lack of efficacy at the 5 mg azeliragon dose [226].

Lumateperone (Intra-Cellular Therapies Inc), known as ITI-007, is a first-in-class molecule designed to selectively and simultaneously modulate certain neuronal pathways. This molecule acts on serotonin, dopamine, and glutamate receptors. It is an investigational therapy being developed to treat agitation in dementia, including Alzheimer's disease and mental illness as well as schizophrenia. In 2014, Intra-Cellular announced the phase I/II clinical trials results that lumateperone was safe and well-tolerated and showed improved cognitive function and thereby the phase III clinical trials were initiated in 2016 to evaluate the efficacy and safety of lumateperone in about 360 people diagnosed with probable Alzheimer's disease [227,228]. Lumateperone, however, was not likely to meet its primary endpoint upon completion and therefore the study was stopped for futility in Dec 2018 [229].

1.11 Proteasome in Alzheimer's Disease

While years of debate have not provided a conclusive answer to the question of events related to the proteasome causing to AD pathology, there is growing evidence showing changes in the UPS have been associated with AD [230-232]. In the early phase of AD, proteasome activity was decreased, and ubiquitin accumulation found in plaques and tangles was also associated in late AD [231, 233-236]. Interestingly, it was reported alterations in the UPS affect the degradation of Aβ in neurons and astrocytes. In addition, Aβ oligomers downregulated *in vitro* proteasome activity and lower proteasome activity was also observed in the several brain areas of AD patients [237-239]. However, these studies were limited to assess the proteasome activity in whole brain homogenates or in cell line models, not examining activity and the expression levels of immunoproteasome in glial cells. While the role of immunoproteasome in neuroinflammation is not clearly understood, researchers also observed whether expression and activity of immunoproteasome are involved in microglial activation in AD patients and in a mouse model of brain injury [240-243].

In a 2006 publication, Mishto reported that β1i expression was elevated with age, and in the brain of AD patients [244]. In line with this, Orre et al. showed that activities of immunoproteasome subunits were increased along with promoted plaque in AD mice and patients, suggesting the tight correlation between upregulation of immunoproteasome and reactive astrocytes and microglial cells derived from patients with AD [240]. Importantly, most recent study has shown that LMP7/β5i knockout altered microglial cytokine production profiles and improved cognitive dysfunctions in a mouse model of Aβ deposition, indicating a potential role of immunoproteasome in Aβ-induced neuroinflammation [51]. While it becomes clear that immunoproteasome activity is enhanced in microglia of AD, suggesting the involvement of immunoproteasome in neuroinflammatory responses and therapeutic potential for AD treatment, it is still unknown whether immunoproteasome selective inhibitors display pharmacological inhibition on AD pathology.

CHAPTER 2. HYPOTHESIS AND SPECIFIC AIMS

The overall goal of this research is to develop novel, effective proteasome inhibitors for treating multiple myeloma patients who do not respond to PI therapies and Alzheimer's disease patients.

In order to design new and effective therapeutic strategies to bypass resistance, it is important to better understand the mechanisms of proteasome inhibitors resistance. Recently, several studies have shown that UPS-targeting inhibitors retain anticancer activity in Btz-resistant MM cells, indicating that the UPS remains essential in these cells [245, 246]. Furthermore, PIs other than Btz remained cytotoxic to Btz-resistant MM cells [247], suggesting that alternative PIs can overcome Btz resistance. However, information on the ability of UPS-targeting inhibitors to overcome Cfz resistance is currently limited. Additionally, it is currently unclear whether the proteasome is still a valid target in Cfz-resistant cancer cells. To date, investigations of Cfz resistance have largely focused on acquired resistance due to the Cfz-adapted cancer cell line models and the availability of clinical samples derived from patients who have developed resistance after prolonged Cfz therapy. On the other hand, mechanistic investigations of *de novo* Cfz resistance have been scarce, due to the lack of appropriate cell line models and patient samples. We hypothesized that proteasome function remains vital to the survival of *de novo* Cfz-resistant cancer cells, and that targeting the proteasome using alternative proteasome inhibitors is a good strategy to overcome Cfz resistance.

As described previously, the immunoproteasome known to be involved in regulation of inflammatory immune responses, is currently investigated as a potential therapeutic target for autoimmune diseases [51, 248]. Likewise, the immunoproteasome is also reported to be upregulated in in reactive astrocytes and microglia isolated from AD patients and AD mouse models [240, 241, 244, 249, 250]. However, the physiological role of immunoproteasome in these AD brains, is still

completely unknown. Recent study showed LMP7 knockout altered microglial cytokine production profiles and improved cognitive deficits in a mouse model of Aβ deposition, indicating a potential role of immunoproteasome in Aβ-induced neuroinflammation [51]. Interestingly, moderate up-regulation of LMP2 expression in AD patients was also reported. Despite these data suggesting the involvement of immunoproteasome in neuroinflammatory responses and therapeutic potential for AD treatment, the pharmacological inhibition of LMP2 has never been tested for the impact on AD pathology. With this in mind, we also hypothesize whether LMP2 inhibitors could offer a novel strategy in AD progression via regulation of inflammation. Our overall study had the following aims:

Aim 1. Determine whether alterations in proteasome catalytic subunit composition are causally linked with changes in the sensitivity of cancer cells to Cfz. I initially identified the first *de novo* Cfz-resistant cancer cell line model. Proteasome activity and immunoblotting analyses were used to detect changes in proteasome catalytic subunits. I altered proteasome catalytic subunit compositions in cancer cell lines using genetic (overexpression & knockdown) and biochemical (INF-γ) tools and investigated whether those alterations led to changes in proteasome inhibitor sensitivity in Cfz-resistant cancer cells.

Aim 2. Optimize small molecules that inhibit the growth of Cfz-resistant cancer cells. I performed cell-based screens of in-house proteasome inhibitor libraries containing proteasome catalytic subunit-specific inhibitors to identify compounds that are effective against Cfz-resistant cancer cells. Using selected lead compounds, I tested their efficacy against primary multiple myeloma cells derived from patients who are proteasome inhibitor-resistant. To improve the potency of the lead compound, we utilized a previously reported docking model of the compound to its targets. Traditional medicinal chemistry was performed to design and synthesize analogues of the most promising hit compound. Compound analogues were assayed for *in vitro* proteasome inhibitory activity and later for their cytotoxic activity in Cfz-resistant cancer cells.

Aim 3. Investigate whether LMP2 inhibitor has anti-AD activity via regulation of inflammation: We assessed animal behavior tests using LPS-induced inflammatory and transgenic AD mouse models to examine the effects of proteasome inhibitors on cognitive impairments. ELISA assay, Thioflavin staining of amyloid-beta, and HEK293-tau-BiFC cells were utilized to investigate the effect of the proteasome inhibitors on amyloid-beta or tau aggregation, respectively. Membrane cytokine array and ELISA assay were used to evaluate the effect of the compound on pro-inflammatory cytokines in microglial cells.

CHAPTER 3. H727 CELLS ARE INTRINSICALLY RESISTANT TO THE PROTEASOME INHIBITOR CARFILZOMIB, YET REMAIN DEPENDENT ON THE PROTEASOME FOR CELL SURVIVAL AND GROWTH

The work in this chapter was published in *Scientific Reports* **2019,** 9, 4089 [333].

3.1   Introduction

The proteasome controls numerous cellular processes via the regulated degradation of proteins. Despite its essential functions, it is now understood that agents which inhibit the proteasome have therapeutic selectivity for cancer cells as compared to normal cells. This selectivity likely occurs because rapidly proliferating cells have greater protein degradation requirements and due to the proteasome's role in regulating a variety of critical signaling pathways. In general, 20S proteasomes were thought to exist in two main types, the constitutive proteasome (cP) and the immunoproteasome (iP). More recently, various subtypes of proteasomes containing a non-standard mixture of catalytic subunits have been identified in cancer cell lines. These so-called intermediate proteasomes differ from both constitutive and immunoproteasomes, which contain mixed assortments of cP and iP catalytic subunits, such as β1i-β2-β5i [251-255]. It was further reported that these intermediate proteasomes may confer differing sensitivities to proteasome inhibitors (PIs) as compared to cPs or iPs [253, 254, 256]. However, whether intermediate proteasome subtypes contribute to the resistance of cancer cells to proteasome inhibitors is currently unknown and the clinical implications of intermediate proteasomes have yet to be defined.

The clinical and commercial successes of bortezomib (Btz, Velcade®), carfilzomib (Cfz, Kyprolis®), and ixazomib (Ixz, Ninlaro®) have validated the proteasome as a valuable target in the treatment of cancer. While the first-in-class

proteasome inhibitor (PI) drug Btz and the first oral PI Ixz utilize boronic acid pharmacophores, the second-generation PI Cfz harbors an epoxyketone that irreversibly inactivates the proteasome with high mechanistic selectivity [257, 258]. This selectivity affords Cfz a reduction in off-target interactions yielding an improved safety profile over Btz, most notably a reduced incidence of severe peripheral neuropathy[259]. With positive results from recent phase III clinical trials [260-265], Cfz is now firmly placed as a mainstay of refractory MM therapy. Nevertheless, a considerable portion of MM patients are refractory to Cfz or develop resistance after prolonged Cfz treatment. A meta-analysis of 14 clinical trials found that 44% of patients could not achieve a minimal response or better [266]. As a monotherapy in patients with relapsed MM, for example, the response rates for Cfz were in the ranges of 25-40% [267]. When used in combination with other drugs (often with dexamethasone and/or lenalidomide), response rates substantially improved, but a significant subset of non-responders persisted [105,106, 265, 268, 269]. Even for those who initially respond to Cfz-based therapy, disease eventually relapses with a median progression-free-survival (PFS) of ~17-26 months [105, 106]. To date, extensive efforts have been yielding the development of new therapeutics for these Cfz resistant patients. However, clinical effects of the new therapeutics are disappointing likely due to a lack of understanding of the biological mechanisms underlying Cfz resistance.

Mechanistic investigations of Cfz resistance have so far utilized cancer cell lines adapted to gradually increasing concentrations of Cfz, revealing that the overexpression of P-glycoprotein (P-gp) and mutations or amplification/overexpression of proteasome catalytic subunits are largely responsible for acquired Cfz resistance observed in established cell lines [132, 133]. To date, cell-based models of de novo Cfz resistance are unavailable. Here, we report for the first time that H727 cells (derived from a human bronchial carcinoid tumor) are inherently resistant to Cfz, yet remain dependent on the proteasome for their survival and growth. Our current results suggest that de novo Cfz resistance observed

in H727 cells may be mediated at the 20S proteasome level, providing previously unknown insights into the mechanisms of de novo PI resistance.

3.2   Material and Methods

3.2.1   *Cell lines and chemicals*

Hep3B, Huh7, LCSC, HepG2, and PLC/PRF/5 hepatic cancer cells were a kind gift of Dr. Roberto Gedaly (College of Medicine, University of Kentucky). MDA-MB-231, HCC1143, and HCC1937 breast cancer cells were purchased from the Korean Cell Line Bank (Seoul, Korea). All other established cell lines were obtained from the American Type Culture Collection (ATCC, Rockville, MD). All cells were cultured according to the manufacturer's protocol in 5% CO_2 in medium. Cultured cell lines were tested for Mycoplasma contamination routinely every 6 months. Specifically, H23 and H727 cells were tested three times in the course of performing the experiments described within this dissertation work. Inhibitors of UPS pathways used in this study were purchased from commercial vendors: carfilzomib (LC Laboratories, Woburn, MA), bortezomib (ChemieTek, Indianapolis, IN), MG-132 (EMD Millipore, San Diego, CA), PYR-41 (ApexBio, Houston, TX), and P5091 (ApexBio, Houston, TX). The following proteasome fluorogenic substrates were used: Suc-LLVY-AMC (Bachem, Torrance, CA; I-1395), Ac-WLA-AMC (Boston Biochem, Cambridge, MA; S-330), Ac-nLPnLD-AMC (Bachem; I-1850), Ac-RLR-AMC (Boston Biochem; S-290), Ac-ANW-AMC (Boston Biochem; S-320), and Ac-PAL-AMC (Boston Biochem; S-310). Human recombinant Interferon-γ was purchased from eBioscience (San Diego, CA).

3.2.2 *Cell viability assay*

Cell viability was determined by CellTiter 96 AQueous One Solution Cell Proliferation assay (Promega, Madison, WI) according to the manufacturer's protocol. Briefly, cells were seeded at a density of 5,000-10,000 per well in 96-well plates and allowed 24 hours to attach. After cells were treated with the indicated concentrations of compounds for 72 hours, cell viability was measured using the reagent provided in the assay kit. Absorbance at 490 nm was measured using a SpectraMax M5 microplate reader (Molecular Devices, Sunnyvale, CA). Results were analyzed using GraphPad Prism (La Jolla, CA).

3.2.3 *Immunoblotting*

Total cell lysates containing equivalent protein content were separated by 12% SDS-PAGE and transferred to polyvinylidene difluoride membranes (Millipore, Billerica, MA) via a semi-dry apparatus. Membranes were then blocked in 5% non-fat dry milk (Bio-Rad, Hercules, CA) in Tris-buffered saline with 0.05% Tween-20 (TBST) for 1 h at room temperature, followed by incubation with 3% BSA in TBST containing the respective primary antibodies overnight at 4°C: β1 (Enzo Life Sciences; PW8140), β2 (Enzo Life Sciences; PW8145), β5 (Thermo Scientific; PA1-977), β1i (Abcam; ab3328), β5i (Abcam; ab3329), β-actin (Novus Biologicals; NB600-501), and β2i (Santa Cruz; sc-133236; 3% milk-TBST used for dilution). Membranes were then washed five times with TBST and incubated with HRP (Horse radish peroxidase)-conjugated secondary antibodies for 1 hour at room temperature. Immunoreactive bands were visualized using SuperSignal West Femto Chemiluminescent Substrate (Thermo Scientific, Rockford, IL) and X-ray film (Thermo Scientific or GeneMate).

3.2.4 *Proteasome Activity Assay*

Subunit-selective fluorogenic peptide substrates were used to measure the catalytic activities of individual catalytic subunits by monitoring the rate of substrate hydrolysis over time. Briefly, protein lysates were prepared using passive lysis buffer (Promega, Madison, WI) and diluted in 20S proteasome assay buffer (20 mM Tris-HCl, 0.5 mM EDTA, 0.035% SDS, pH 8.0). Enzyme reactions were initiated by the addition of proteasome substrates. Substrates and concentrations were used as following: Suc-LLVY-AMC (β5/5i, 100 μM), Ac-WLA-AMC (β5, 20 μM), Ac-nLPnLD-AMC (β1,100 μM), Ac-RLR-AMC (β2/2i, 20 μM), Ac-ANW-AMC (β5i, 100 μM), and Ac-PAL-AMC (β1i activity, 100 μM). Fluorescence signals were measured over 1 hour at one reading per one minute using a SpectraMax M5 microplate reader at the excitation and emission wavelengths of 360 and 460 nm, respectively.

3.2.5 *Interferon-γ treatment*

H727 and H23 cells were treated with 150 U·ml^{-1} of IFN-γ or vehicle for 24 h. At the end of IFN-γ treatment, the cells were washed with PBS three times and then cultured for an additional 24 hours. Afterwards the cells were sub-cultured into a 96-well plate, and cell viability assays was performed using CellTiter 96 AQueous One Solution Cell Proliferation assay (Promega, Madison, WI) as described above. The remaining cells were then used for immunoblotting analysis and proteasome activity assays.

3.2.6 *Knockdown of proteasome catalytic subunits*

Cells were transfected with ON-TARGET Plus Smart Pool siRNAs (Dharmacon, Lafayette, CO) using Lipofectamine 2000 transfection reagent (Invitrogen, Carlsbad, CA), according to the manufacturer's instructions. H727 cells were plated in a 6-well

plate at a density of 5x105 cells per well and allowed at least 24 h to attach. Cells were then transfected with 100 nmole of siRNAs and Lipofectamine 2000. At 4 h post-transfection, serum-free Opti-MEM medium (Invitrogen, Carlsbad, CA) was replaced with complete medium and the cells were incubated for 48 h. The following siRNA pools were used: PSMB5 (L-004522-00-0020), PSMB7 (L-006021-00-0020), PSMB8 (L-006022-00-0020), PSMB9 (L-006023-00-0005), and PSMB10 (L-006019-00-0020). For the negative control, human non-targeting scrambled siRNA (D-001810-10) was used.

3.2.7 *Preparation of primary MM samples*

Cryopreserved MM primary cells isolated from the bone marrow or peripheral blood of patients with no reported history of PI treatment were purchased from Conversant Biologics (Huntsville, AL) and AllCells (Alameda, CA). CD138-positive cells were isolated from patient samples immediately after thawing using human CD138 microbeads (Miltenyi Biotec), whole blood column kit (Miltenyi Biotec), MidiMACS magnetic separator (Miltenyi Biotec), and 30 μm MACS SmartStrainers (Miltenyi Biotec). Purified cells were plated on white 96-well cell culture plates at 40,000 cells per well in RPMI 1640 media supplemented with 10% FBS. Cells were treated with proteasome inhibitors for 48 hours before viability assessment via CellTiter-Glo Luminescent Cell Viability Assay (Bio-Rad).

3.2.8 *Statistics analysis*

Results are expressed as means ± S.D. Statistical significance of the observed differences was determined using Student's t-test (with the Holm-Sidak method when appropriate). All statistical analyses were carried out using GraphPad Prism 7.04 (GraphPad Software).

3.3   Results

3.3.1   *H727 cells are intrinsically resistant to Cfz*

To identify Cfz-resistant cell lines, we first measured the cytotoxic effects of Cfz in 21 cancer cell lines derived from various types of cancer. These cell lines displayed an array of Cfz sensitivities (IC_{50} values ranged from 9 to 610.2 nM). We were especially intrigued by the marked lack of response to Cfz in the H727 human non-small cell lung cancer (NSCLC) cell line; the Cfz I IC_{50} value for this cell line (610.2 nM) was approximately 33-fold higher than that for the Cfz-sensitive NSCLC cell line H23 (18.3 nM) (Figure 3.1A). Even in the presence of 250 nM of Cfz which usually induces >95% loss of viability in most of other cancer cell lines including H23 cells, H727 cells survived and grew normally (Figure 3.1B). Thus, we selected the H727 cell line as our cell line model of intrinsic resistance to Cfz in which to test our hypothesis.

A. Cell viability (IC$_{50}$ values) for a panel of established cancer cell lines as measured by MTS assay following incubation with carfilzomib (Cfz) for 72 h. H727 cells are most resistant to Cfz among 21 tested cell lines. **B.** Representative images of H23 and H727 cells growing in the presence of Cfz (100 or 250 nM, respectively) assessed via light microscopy for 3 days.
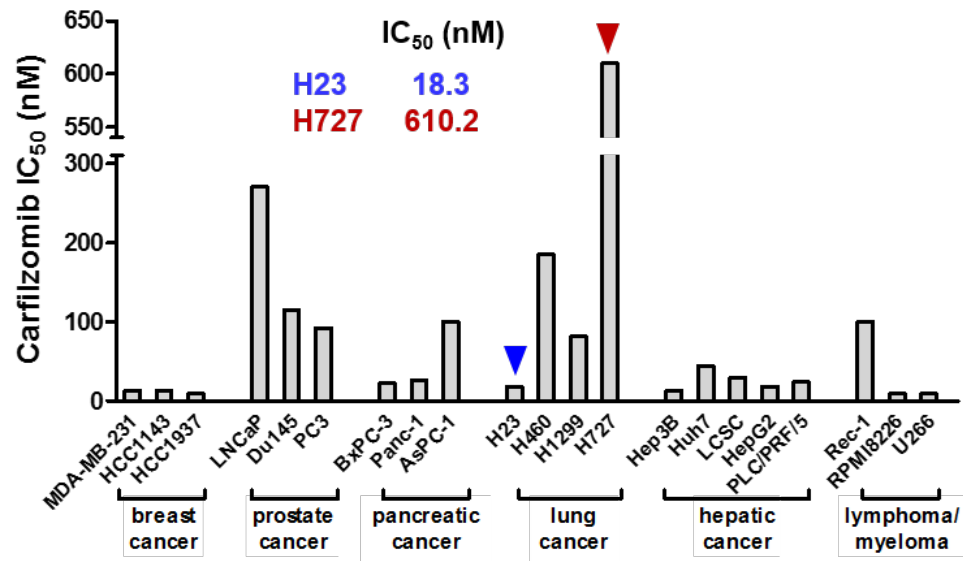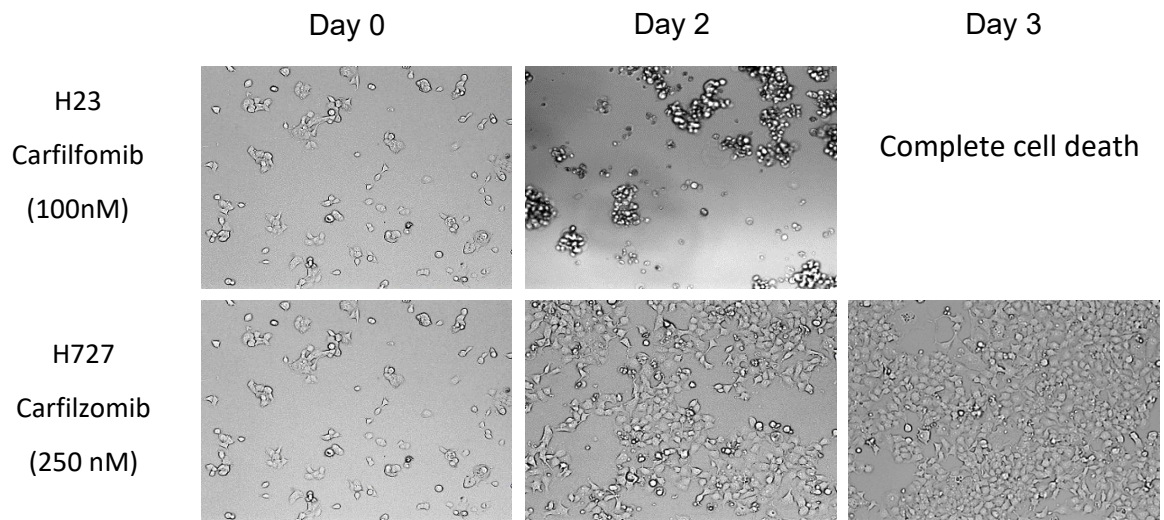
Figure 3.1 Sensitivity of H23 and H727 cells to Cfz

3.3.2 *Previously reported mechanisms do not explain de novo resistance of H727 cells*

While the mechanisms of intrinsic resistance to Cfz has not been reported to date, several studies have shown that P-gp can contribute to acquired resistance to Cfz observed in cancer cell line models and clinical samples from patients with prior Cfz therapy [132-135]. To test whether P-gp plays a role in the de novo Cfz resistance of H727 cells, we performed immunoblotting analysis but found no detectable P-gp expression (Figure 3.2A). Furthermore, treatment of H727 cells with reversin 121, a dipeptide P-gp inhibitor, did not significantly impact the IC_{50} value of Cfz (Figure 3.2B), confirming a P-gp-independent mechanism of resistance. Next, we examined the possibility that Cfz may undergo rapid metabolic inactivation in H727 cells. We treated H727 and H23 (Cfz-sensitive) cells with 500 nM Cfz and collected culture media to measure the levels of remaining Cfz at 6 or 24 h post-treatment. The level of remaining drug was overall comparable between H727 and H23 cells although a slight difference was noted at 24 h (Figure 3.2C). Direct sequencing analyses also indicated that the PSMB5 (encoding $\beta5$) and PSMB8 (encoding $\beta5i$) genes in H727 cells harbor no mutations (Figure 3.3A-D). We attempted to compare the intracellular drug levels by quantifying the remaining drug levels in lysates of H727 and H23 cells, but the levels were below the lower limit of quantitation (< 5 nM) of our current analytical assay. Although it was not feasible to assess the intracellular drug levels, H727 cells contained Cfz in the culture media at the level comparable to or slightly higher than H23 cells. Assuming that Cfz primarily enters cells via passive diffusion (no report yet supporting the presence of uptake transporters for Cfz as far as we know), it appears unlikely that H727 cells have intracellular Cfz levels much lower than H23 cells. Taken together, de novo resistance of H727 cells was not explained by previously reported mechanisms such as P-gp upregulation, genetic mutations in proteasome catalytic subunits, or enhanced metabolic inactivation of Cfz.
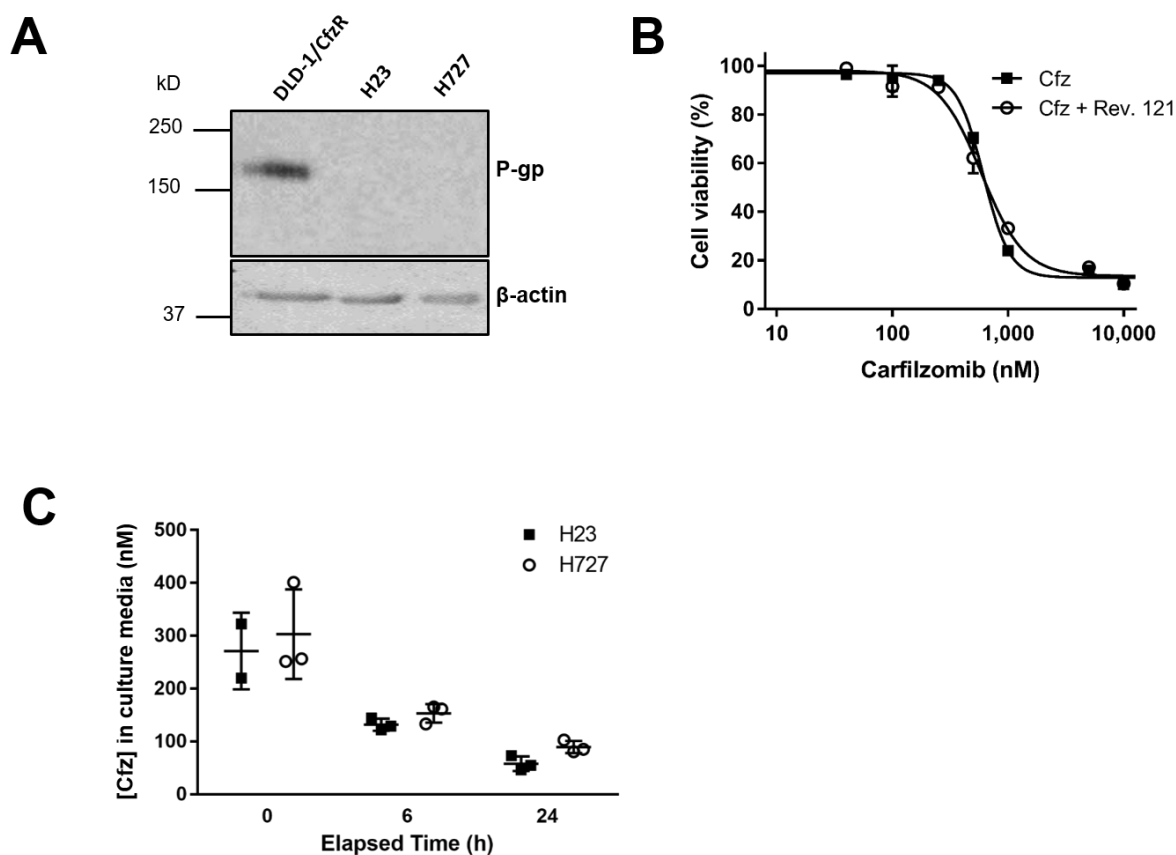
Figure 3.2 Independency of H727 cells in previously reported mechanisms

A. Immunoblotting results showing no detectable expression of P-glycoprotein (P-gp) in H727 cells. DLD-1 cells with acquired Cfz resistance via P-gp upregulation (DLD-1/CfzR) were used as a positive control. **B.** The co-treatment of reversin-121 (7.5 μM, P-gp inhibitor) did not affect the sensitivity of H727 cells to Cfz. The IC$_{50}$ values did not show statistically significant difference between in the presence and absence of reversin-121 (Student's t-test). **C.** The levels of remaining Cfz in culture media were comparable between H727 and H23 cells (no statistically significant differences, t-tests the Holm-Sidak method to correct for multiple comparisons with α = 0.05) (This experiment was performed by Ji Eun Park from Wooin Lee's group in the College of Pharmacy and Research Institute of Pharmaceutical Sciences, Seoul National University, Korea)

A
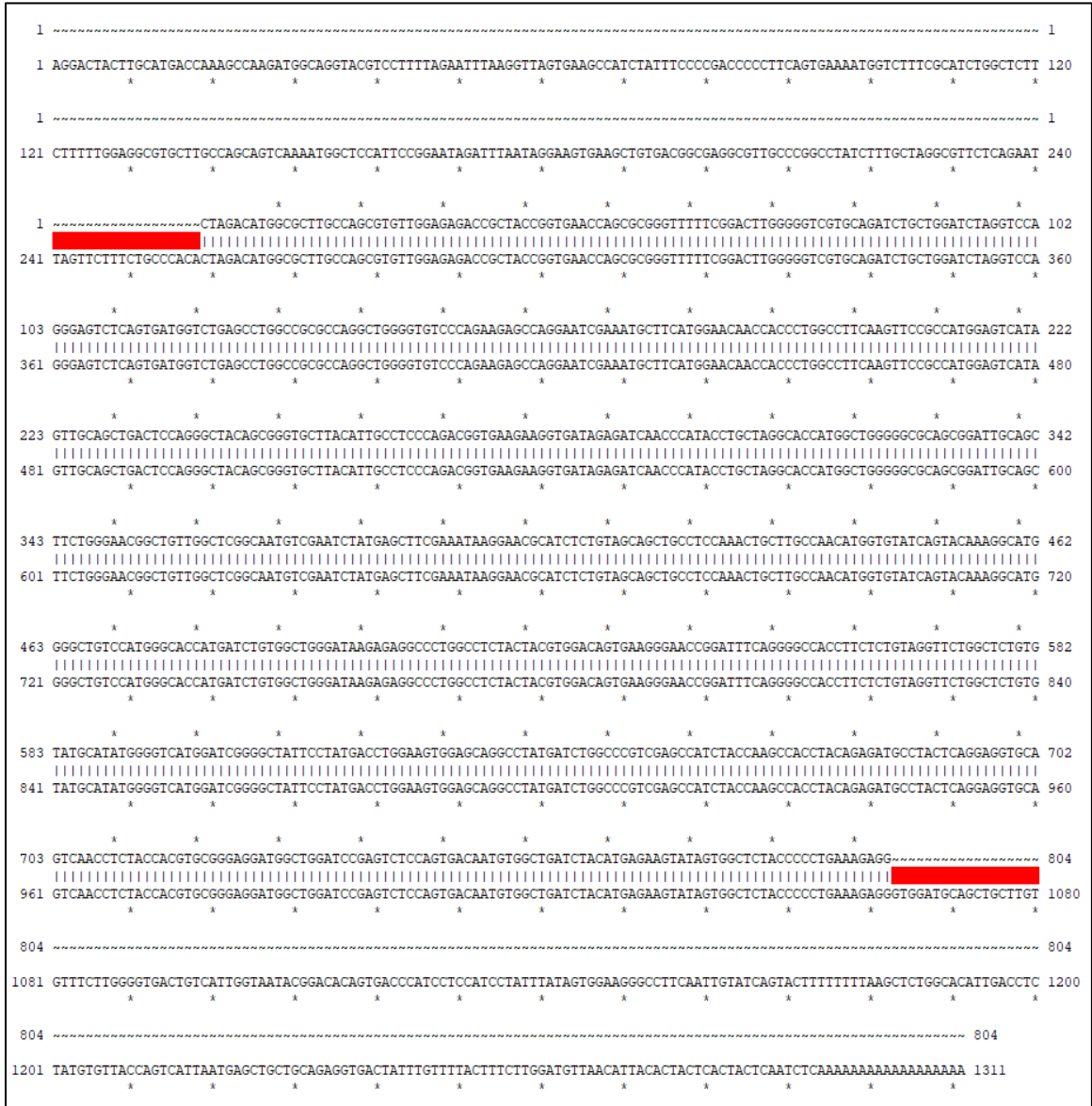
Figure 3.3† Sequencing analysis of the PSMB5 and PSMB8 genes in H727 cells
A. Alignment of truncated H727 PSMB5 forward sequencing read to PSMB5 NM_002797.4. **B.** Alignment of truncated H727 PSMB5 reverse sequencing read to PSMB5 NM_002797.4. **C.** Alignment of H727 PSMB8E2 forward sequencing read to truncated PSMB8E2 NM_148919.3 ORF. **D**. Alignment of H727 PSMB8E2 reverse sequencing read reverse-compliment to truncated PSMB8E2 NM_148919.3 ORF.

55

B

Figure 3.3† (continued)

C

Figure 3.3† (continued)

D

Figure 3.3† (continued)

† Sequencing analysis data of the PSMB5 and PSMB8 genes in H727 cells were acquired by Zachary Miller.

3.3.3 *The proteasome remains essential for the survival of H727 cells*

It is possible that cancer cells might have adaptations to endure reduced levels of 20S proteasome function and the rely on the non-proteasomal protein degradation pathways to reduce proteasome load. In order to verify whether the UPS is important for the survival and proliferation of Cfz-resistant H727 cells, as it is in Cfz-sensitive cell lines such as H23, we first transfected cells with siRNAs targeting the proteasome α7 subunit in H727 cells, thereby blocking the assembly of active 20S proteasomes. [270, 271]. As seen in Figure 3.4A, effective silencing of α7 resulted in almost complete cell death after 3 days post-transfection for both in H727 and H23 cells, indicating that active proteasomes remain indispensable for the survival of Cfz-resistant H727 cells. These results suggested that H727 cells may still respond to proteasome inhibitors other than Cfz. In order to examine this, we treated H727 cells with alternative PIs, particularly ones with differing pharmacophores or structures, such as Btz (a peptide boronic acid) and MG-132 (a peptide aldehyde). These PIs were indeed highly effective in killing H727 cells and their IC_{50} values were comparable between H727 and H23 cells (Figure 3.4B). We also used two inhibitors targeting various upstream components of the UPS, PYR-41, an inhibitor of ubiquitin E1 ligase and several DUBs, and P5091, a specific USP7/USP47 inhibitor [245]. Both PYR-41 and P5091 were cytotoxic in H727 and H23 cells with comparable potencies (Figure 3.4B). These results further support that H727 cells remain dependent on the ubiquitin-proteasome system, despite their *de novo* resistance to Cfz.

A.
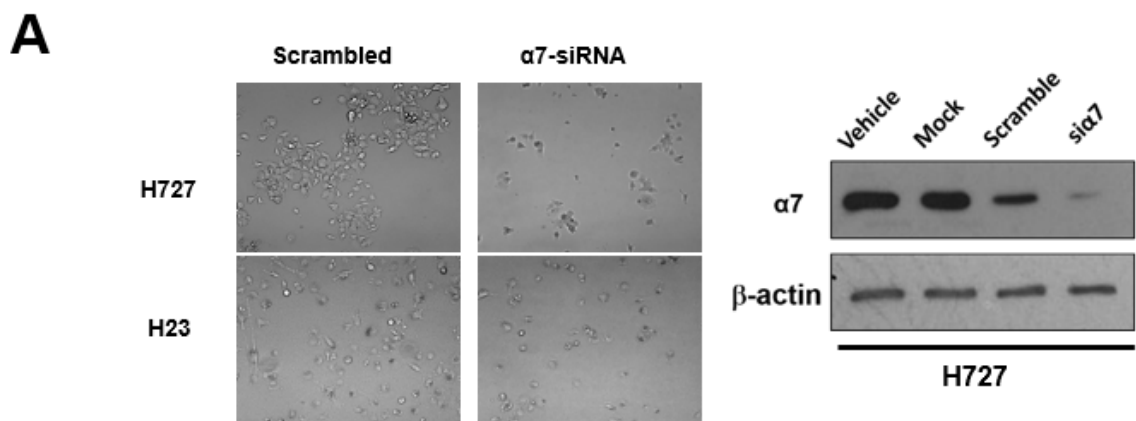
B.

	72-hour cell viability IC$_{50}$ (µM)				
	Carfilzomib (epoxyketone)	Bortezomib (boronic acid)	MG-132 (aldehyde)	PYR-41	P5091
H727	0.610 ± 0.152	0.025 ± 0.014	0.98 ± 0.27	23.77 ± 4.41	12.92 ± 5.05
H23	0.018 ± 0.009	0.010 ± 0.007	0.43 ± 0.14	18.02 ± 3.61	6.49 ± 0.95
Fold difference (H727/H23)	34	2.5	2.0	1.3	2.0

Figure 3.4 Cytotoxic effect of targeting the UPS in H727 cells

A. Knockdown of proteasome α7 subunit in H727 cells effectively induced cell death to a similar extent as observed in H23 cells (images taken 48 h post-transfection). Immunoblotting analysis was performed to verify the efficient knockdown of α7 in H727 cells. **B.** Comparison of the sensitivity (IC$_{50}$ values) of H727 and H23 cells to carfilzomib, bortezomib, MG 132, PYR-41 (an E1 inhibitor) and P5091 (an USP7/USP47 inhibitor). Data are shown as mean ± SD derived from a non-linear regression based on n=3-4 replicates per compound per concentration.

3.3.4 *H727 cells have a distinct composition of proteasome catalytic subunits*

To account for the sensitivity of H727 cells to other PIs, we hypothesized whether the subunit composition at the 20S proteasome level may contribute to *de novo* resistance of H727 cells to Cfz. To test this hypothesis, we compared the proteasome catalytic subunit expression and activity profiles of H727 and H23 cells via immunoblotting analysis and kinetics assays using fluorogenic substrates for individual subunits (β1, β5, β1i, β5i). In the case of the β2 and β2i subunits, their combined trypsin-like activity was assessed due to the lack of a specific fluorogenic substrate that can distinguish the two subunits. As shown in Figure 3.5A., the expression pattern of proteasome catalytic subunits in H727 cells differed from that in Cfz-sensitive H23, panc-1, and RPMI 8226 cells. H727 cells expressed high levels of β1, β2, and β5i, while β1i expression was undetectable. The expression profile of catalytic subunits in H727 cells was not consistent with those typically expected for the two main 20S proteasome subtypes, namely a set of β1-β2-β5 for cP or an immuno-subunit set of β1i-β2i-β5i for iP. Substantial differences were also noted when the activity profiles of proteasome catalytic subunits were compared between these two cell lines using subunit-selective fluorogenic substrates (Figure 3.5B). Interestingly, the activity profiles of individual catalytic subunits showed discrepancies with the protein levels of the respective catalytic subunits. We suspect that the observed differences may reflect the complex relationship between proteasome structure and function (e.g. contributions of post-translational modifications, regulatory particles, or non-standard composition of proteasome catalytic subunits to the hydrolysis rates of fluorogenic substrates).

We next examined whether individual subunits of proteasomes in H727 cells may display different proteasome inhibition profiles than those of H23 cells. We treated H727 and H23 cells with 20 nM of Cfz for 4 h and measured the remaining activities of individual catalytic subunits relative to vehicle-treated control cells. As shown in Figure 3.5C (left panel), more than 80% of β5, β5i and β1i activities were blocked by Cfz for both H727 and H23 cells. On the contrary, over 50% of β1 activity

persisted in H727 cells, but not in H23 cells (Figure 3.5C, left panel). It remains unclear whether the remaining β1 activity contributes to *de novo* resistance of H727 cells to Cfz. On the other hand, Btz treatment resulted in over 80% inhibition across all catalytic subunits in both H727 and H23 cell lines, which may explain the high sensitivity of both cell lines to Btz (Figure 3.5C, right panel). These results support that the 20S proteasomes present in H727 cells may be functionally different from those in Cfz-sensitive H23 cells.

A.

	H727	H23	Panc-1	RPMI 8226	kDa
β5					20
β2					25
β1					25 / 20
β5i					25 / 20
β1i					25 / 20
α5					25
β-actin					37
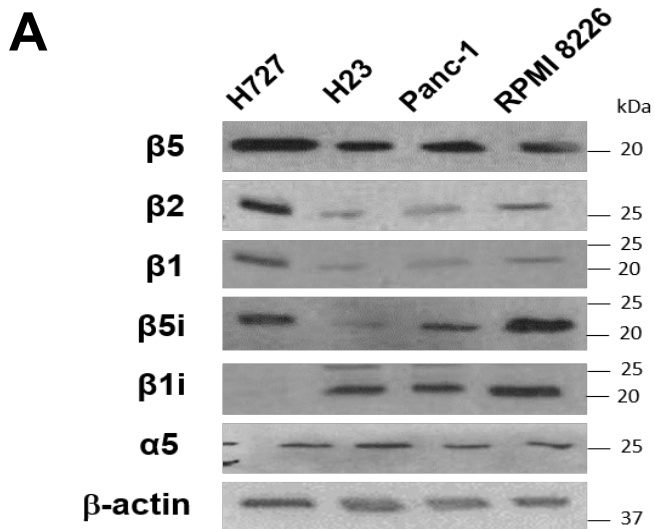
B.

Proteasome activity (RFU/min)				
	CP	IP	H727	H23
β5/β5i	25.06	58.47	4.51	3.49
β5	6.25	1.08	6.02	15.13
β1	41.88	14.51	46.16	56.23
β2/β2i	7.00	27.15	58.97	122.33
β5i	5.71	69.55	6.04	9.86
β1i	14.88	96.13	1.08	21.93

C.

Carfilzomib (20 nM)   Bortezomib (20 nM)
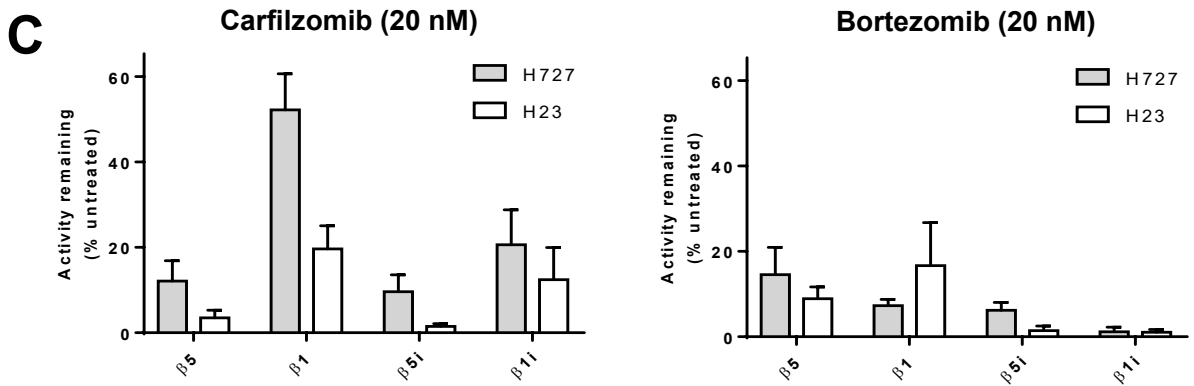
Figure 3.5 Distinct composition of proteasome catalytic subunits in H727 cells

A. Immunoblots showing the differential expression of cP and iP catalytic subunits in

H727 and H23 cells as well as Cfz-sensitive panc-1 and RPMI 8226 cells. **B.** Differential

proteasome activity profiles in H727 and H23 cell lines. Purified human 20S cP and iP were used as controls for individual subunits: 20S cP for β5 and β1 and 20S iP for β5i and β1i. The numbers represent hydrolysis rates of respective substrates (RFU/min, mean values derived from three technical replicates) **C.** Remaining catalytic activities of individual proteasome subunits in H727 and H23 cells 4 h after treatment with 20 nM of carfilzomib (left panel) or 20 nM bortezomib (right panel). Data are presented as mean ± SD derived from three technical replicates.

3.3.5 *A distinct composition of proteasome catalytic subunits in H727 cells*

Based on the differential expression pattern of proteasome catalytic subunits in H727 as compared to H23, we hypothesized that the composition of proteasome catalytic subunits may impact the sensitivity of H727 cells to Cfz. To test this hypothesis, we altered catalytic subunit composition in H727 using interferon-γ (IFN-γ) treatment. IFN-γ's ability to upregulate immuno-subunits (β1i, β2i, and β5i) and to induce IP formation has been well-documented [37, 38]. As shown in Figure 3.6A, incubation of H727 cells with IFN-γ (150 U·ml^{-1}) 24 h prior to Cfz treatment resulted in upregulation of immune-subunit expression and corresponding increases in their activity. IFN-γ pre-treatment caused a significant decrease in Cfz IC_{50} values from 621.1 to 189.5 nM in H727 cells. When H23 cells were pre-treated with IFN-γ, the Cfz IC_{50} values changed in the opposite direction (IC_{50} values increased from 18.6 to 44.1 nM, Figure 3.6B). With IFN-γ pre-treatment, the fold differences in IC_{50} values between the two cell lines were reduced from 33-fold to 4.2-fold. Consistently, IFN-γ pre-treatment also had effect on viability of RPMI 8226 cells with acquired Cfz resistance. Human RPMI 8226 multiple myeloma cells with acquired resistance to Cfz were established by adapting them in the presence of escalating concentrations of Cfz up to 80 nM over 6 months. RPMI 8226 Cfz-resistant cells were cultured in 80 nM of Cfz and then grown in the absence of Cfz for two weeks prior to the use. We have observed the P-glycoprotein was overexpressed in RPMI 8226 Cfz-resistant cells (Data shown in chapter 4). Regardless of P-glycoprotein overexpression, IFN-γ (150 U·ml^{-1}) pretreatment could mediate the cellular response to Cfz (from 239.2 nM to 135.1 nM) in this cell line.

A

IFN-γ

β1i
β1
β5i
β5
β-actin

H727

H727 (+ IFN-γ)

H727

	IC$_{50}$ (nM)
- IFN-γ	621.1
+ IFN-γ	189.5

**

[Carfilzomib] (nM)

B

IFN-γ

β1i
β1
β5i
β5
β-actin

H23

H23 (+ IFN-γ)

H23

	IC$_{50}$ (nM)
- IFN-γ	18.6
+ IFN-γ	44.1

**

[Carfilzomib] (nM)

66
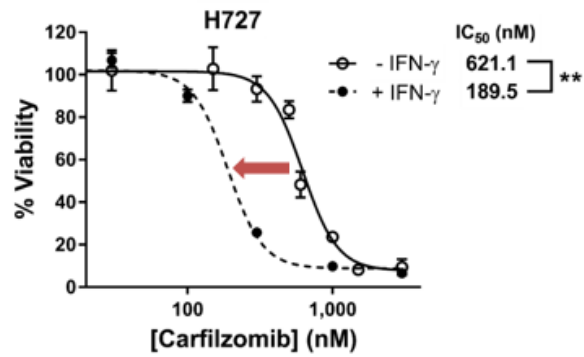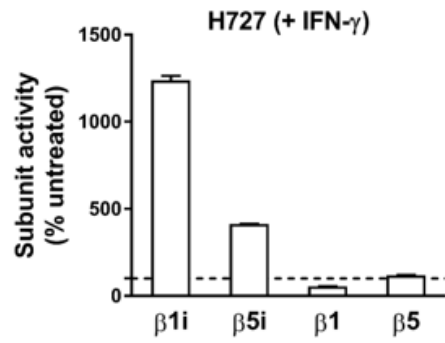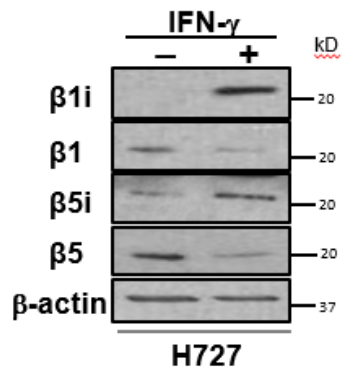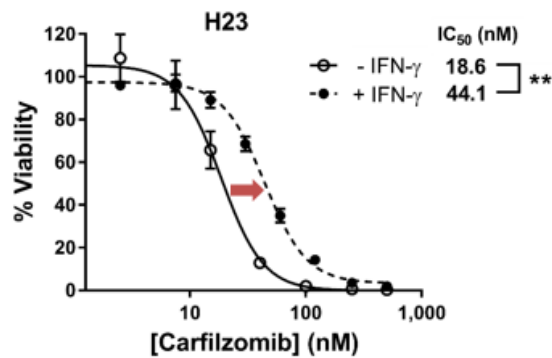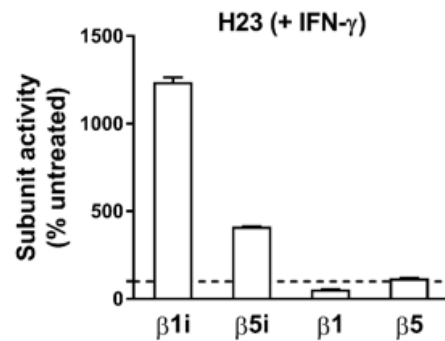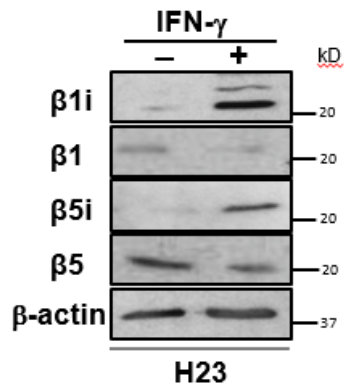
Figure 3.6 Effect of IFN-γ pretreatment on H727 and H23 cells

A. IFN-γ (150 U·ml-1) pretreatment for 24 h led to increased expression (top left panel) and activity (top right panel) of proteasome immuno-subunits. and sensitized H727 cells to Cfz (bottom) **B.** IFN-γ (150 U·ml-1) pretreatment for 24 h desensitized H23 cells towards Cfz. The IC_{50} values displayed a statistically significant difference between IFN-γ-pretreated cells and vehicle control in both of H727 and H23 cells. (P value < 0.01, n=3, Student's t-test comparing the log transformed IC_{50} values obtained from three independent runs).

3.3.6 *Alteration of proteasome catalytic subunit composition affects H727 Cfz sensitivity*

In order to further investigate a causal relationship between the composition of proteasome catalytic subunits and Cfz sensitivity, we sought to alter the composition of proteasome catalytic subunits in H727 cells in a more selective manner using an siRNA pool targeting the abundantly expressed β5 subunit. We expected that β5i will substitute for β5 during proteasome assembly, forming 20S complexes with altered catalytic subunit composition. When β5 was knocked down (verified via immunoblotting and activity assays, Figure 3.7A & B), H727 cells grew normally with modest upregulation of β5i. Despite their normal growth, H727 cells were significantly sensitized to Cfz by β5 knockdown, shifting the IC_{50} value from 622 to 99.9 nM (Figure 3.7C). In contrast, the IC_{50} for Btz was only modestly affected, decreasing from 26 to 12 nM (Figure 3.7D). Knockdown of other catalytic subunits such as β5i and β2 resulted in minimal changes in the IC_{50} values for Cfz. A similar pattern was observed in H23 cells where knockdown of β5i and β2 had little effect on Cfz sensitivity but β5 knockdown triggered a five-fold reduction in Cfz IC_{50} from 26.7 to 5.0 nM (Figure 3.7C).
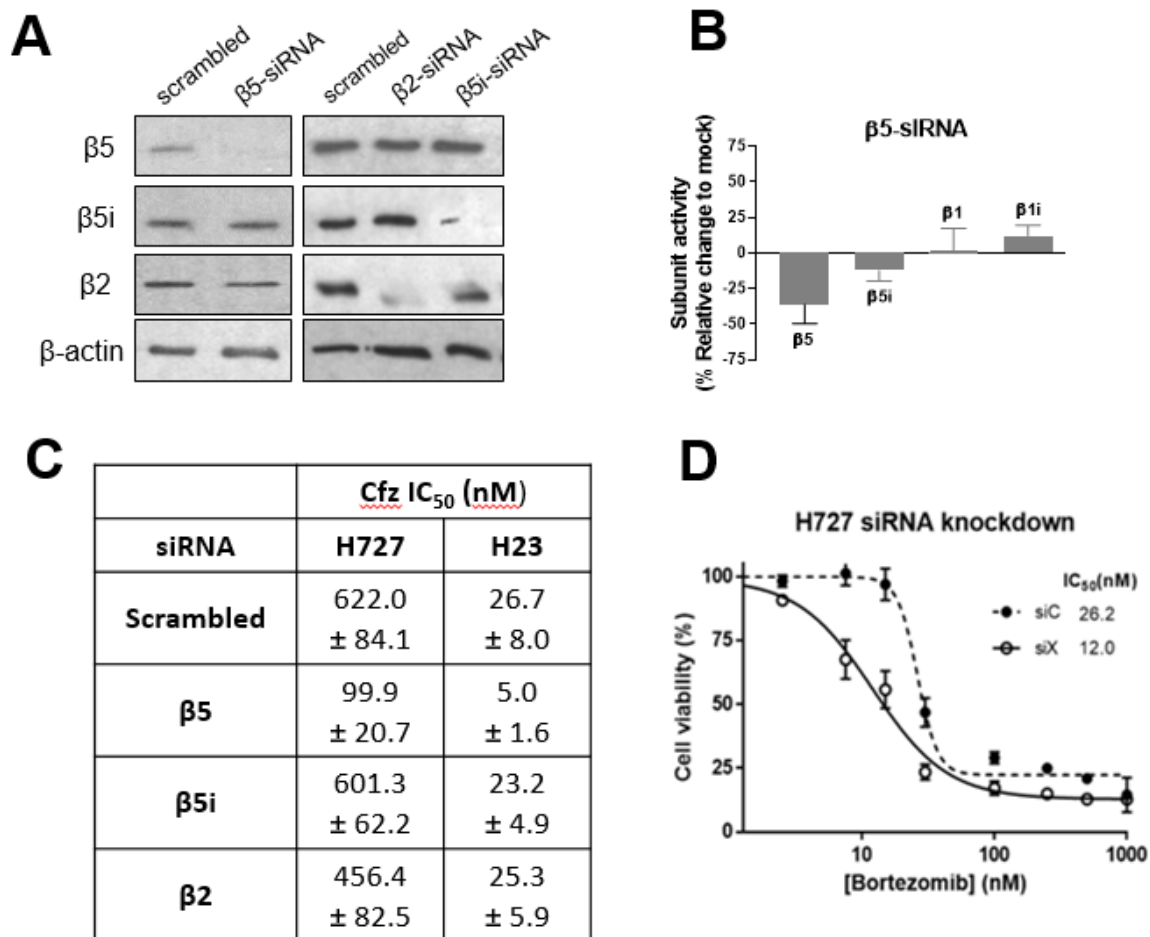
Figure 3.7 The effect of catalytic subunit knockdown on H727 cells

A. Immunoblots of proteasome catalytic subunits in H727 cells transfected with siRNA targeting β5, β2 or β5i. **B.** The catalytic activity of β5 subunit was decreased in H727 cells transfected with siRNA targeting β5 compared with H727 cells transfected with scrambled siRNA. **C.** Effects of siRNA knockdown of β5, β5i, or β2 on Cfz sensitivity (IC$_{50}$ values) in H23 and H727 cells. Data are shown as mean ± SD derived from a non-linear regression based on n=3 replicates per compound per concentration. **D.** 72 h cell viability for Bortezomib 48 h after siRNA knockdown β5 in H727 cells

3.3.7 *The proteasome activity profiles of primary MM cells is highly variable*

In order to assess whether the observed variability in proteasome activity profiles in PI-naïve cell line models reflects the Cfz sensitivity of clinical MM samples, we examined the proteasome activity profiles and degree of Cfz sensitivity using 6 MM samples from patients who have received no prior PI therapy. Similar to the results obtained using cell line models, the clinical samples also showed considerable variability in catalytic subunit activity profiles and Cfz sensitivity (Figure 3.8 A & B). Due to the limited sample quantities, we were not able to perform any further investigations on these samples. Based on these initial assessments, we cautiously speculate that differential Cfz sensitivity in these patient samples may be influenced by variability in proteasome catalytic subunit composition, perhaps partially accounting for the varied responses to Cfz observed in clinical trial results [260, 263, 264].

A. Heat map

Subunit responsible	Patient					
	1	**2**	**3**	**4**	**5**	**6**
β5/β5i	321.4	134.7	186.9	9.5	98	85.2
β5	16.9	15.8	13.9	2.6	7.2	5.7
β1	42.5	50.1	38.1	4.3	22.4	10.4
β2/β2i	86.8	27.9	144.2	17.8	16.1	40.4
β5i	263.1	102.4	165.9	3.3	53.9	58.4
β1i	332.3	112.4	97.0	5.4	71.8	14.1
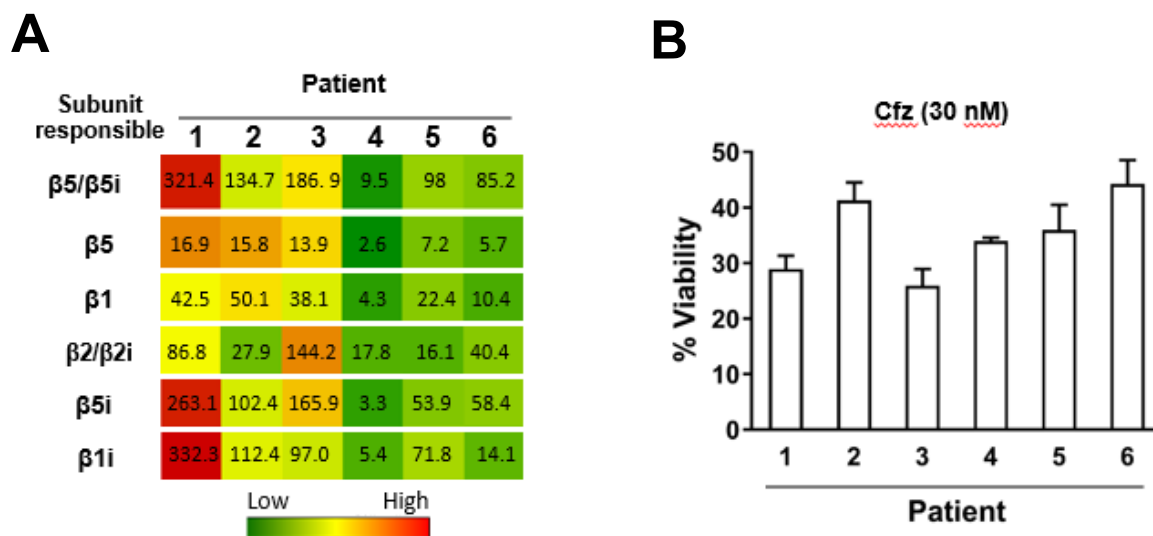
Figure 3.8 Activity profile and viability for Cfz in primary MM samples

A. Heat map showing proteasome catalytic subunit activity profiles of 6 PI-naïve patient MM samples purchased from Conversant Biologics and AllCells. The numbers represent hydrolysis rates of respective substrates (RFU/min, mean values derived from three technical replicates) and were converted to color format and clustered by using the program "R" (http://www.R-project.org) **B.** Carfilzomib (Cfz) cell viability of the same 6 patient MM cells was measured via CellTiter-Glo Luminescent Cell Viability Assay.

3.4 Discussion

Cfz has contributed to a substantial advancement in multiple myeloma treatment by improving patient survival and quality of life. A considerable portion of patients however display intrinsic resistance to Cfz. A significant portions of MM patients previously treated with Btz-containing regimens do not respond to Cfz and even those who initially respond to Cfz almost ultimately develop resistance in the course of their treatment [260, 266]. In order to design new and effective therapeutic strategies to overcome resistance, it is important to better understand the mechanisms of Cfz resistance. To date, investigations of Cfz resistance have largely focused on acquired resistance due to the relative ease of generating Cfz-adapted cancer cell lines and the availability of clinical samples derived from patients who have developed resistance after prolonged Cfz therapy. On the other hand, mechanistic investigations of de novo Cfz resistance have been scarce, due to the lack of appropriate cell line models and patient samples.

In the current study, we report that H727 cells are intrinsically resistant to Cfz, potentially serving as a useful model for mechanistic investigations of de novo Cfz resistance. Given that H727 cells were sensitive to inhibitors of non-proteasomal targets in the UPS and PIs other than Cfz, we surmise that H727 cells harbor functionally active proteasomes and that complete or near-complete inhibition of proteasome catalytic activity is incompatible with survival in these cells. Based on our current results, a shift towards non-UPS protein degradation pathways appears unlikely since H727 cells remain highly sensitive to the inhibition of UPS components including the proteasome itself.

Despite their similar degrees of dependence on the proteasome or UPS for survival and growth, H727 and H23 cells respond differently to Cfz, to a degree of 33-fold difference in IC_{50} values. This may be in part due to cell line-dependent cell growth rates or genetic/molecular differences. However, the high sensitivity of H727 cells to other PIs suggests that Cfz resistance in H727 cells may be mediated at the 20S proteasome level. It has been reported that proteasome inhibitor resistance is

often associated with increased levels of proteasome subunit catalytic activity, especially in models of acquired bortezomib resistance [117, 272]. However, H727 cells displayed substantially low activities of individual catalytic subunits as compared to H23 cells. At present, it is unclear whether the low proteasome activities in H727 cells are involved in conferring Cfz resistance. Previously it was reported that 20S proteasomes harboring a mixed assortment of cP and iP catalytic subunits exist in cancer cells and that their PI sensitivity differs from those of standard cP or iP5. Our results also indicated not only differing expression levels of proteasome catalytic subunits between H727 and H23 cells, but also differing levels of subunit catalytic activity. These findings are consistent with the presence of non-standard 20S proteasome subtypes (other than cP and iP). Determination of the 20S proteasome subtypes present in H727 cancer cells may shed further light on the underlying mechanisms of de novo Cfz resistance in H727 cells. Determination of the subunit composition of intact 20S proteasomes in cells is challenging and several groups including ours are currently trying to develop bi-functional or fluorescent probes to facilitate these efforts [273, 274].

CHAPTER 4. DEVELOPMENT OF NOVEL EPOXYKETONE-BASED PROTEASOME INHIBITORS AS A STRATEGY TO OVERCOME CANCER RESISTANCE TO CARFILZOMIB AND BORTEZOMIB

Some of the work in this chapter has been accepted in *Journal of Medicinal Chemistry* 2019 [334].

4.1   Introduction

In 2003, the FDA approval of first-in-class Proteasome inhibitor (PI) bortezomib (Velcade®, Btz) for treating patients with multiple myeloma (MM) validated the proteasome as an anticancer target. A decade later, the FDA approved a second-in-class PI—carfilzomib (Kyprolis®, Cfz) and ixazomib (Ninlaro®, Ixz)—for treating patients with relapsed MM, firmly establishing the proteasome as an exciting target in treating cancer. Although the use of PIs in MM patients has successfully improved clinical outcomes, a subset of PI-naïve patients failed to respond to these inhibitors, and almost all patients who do respond eventually acquire PI resistance [105, 261, 263]. Recently, three non-PI drugs, daratumumab (a monoclonal antibody (mAb) targeting CD38), elotuzumab (mAb targeting SLAMF7) and panobinostat (HDAC inhibitor) were approved for treatment of relapsed MM. While these non-PI drugs provide additional options for MM patients relapsed on current PI-based therapies, a portion of patients still do not respond to these therapies. The results from recent clinical trials show that the response for these non-PI drugs is rather transient with the median duration of ~7-20 months before relapsing [275-277]. Therefore, it is now critically important to develop new therapeutic strategies that can overcome the limitations of the FDA-approved PIs and deliver the therapeutic benefits of PIs to cancer patients who have exhausted current treatment options.

The ubiquitin proteasome system (UPS) remains essential for cancer cells regardless of resistance to existing PI drugs. The UPS upstream components of the proteasome such as ubiquitin E3 ligases and deubiquitinases are being explored as potential anti-cancer therapeutic targets [245, 246, 278], but not be successful yet. Alternatively, it remains to be seen whether the proteasome itself can be subsequently re-targeted to achieve further therapeutic gains for MM patients relapsed on existing PI drugs.

Most of PIs have been developed through medicinal chemistry approach, optimizing amino acid side chains (P1, P2, P3) which interact with the substrate binding pockets (S1, S2, S3, etc.) of proteasome catalytic subunits. This binding configuration is further stabilized by anti-parallel β-sheet conferring hydrogen bonding interactions between the inhibitor's peptide backbone and conserved residues such as Thr21, Gly47, and Ala49 of proteasome catalytic subunits [279-281]. When combined with a C-terminal warhead which targets the catalytic Thr1 residue, this strategy typically yields potent inhibitors including the three FDA-approved PIs: Btz, Ixz (peptide boronic acids) and Cfz (a peptide epoxyketone). However, this strategy might have unintentionally contributed to an increased cross-resistance among them. A potential strategy to overcome PI cross-resistance is to identify and exploit a structural niche not utilized by existing PIs. In that regard, previously unexplored are P1′ binding sites which lie on the C-terminal side of the proteasome catalytic subunit's cleavage site.

Here, we have developed peptide epoxyketones having a P1′-targeting moiety. The anticancer efficacy of these compounds was superior to their non-P1′-targeting parent compounds when evaluated against models of intrinsic and acquired Cfz resistance. The identified lead compound, Cfz-OH, an analog of Cfz containing a hydroxyl group at the P1′ position, displayed potent proteasome inhibitory activity and cytotoxicity in both Cfz-sensitive and Cfz-resistant cancer cell lines.

4.2 Material and Methods

4.2.1 *Chemistry*

Peptide epoxyketones having a P1′-targeting moiety were synthesized by Dr. Deepak Bhattarai.

4.2.2 *Enzyme kinetic assay*

Purified human 20S immunoproteasome (Boston Biochem) or RPMI 8226 cell lysates were diluted in 20S proteasome assay buffer (20 mM Tris-HCl, 0.5 mM EDTA, 0.035% SDS, pH 8.0) and incubated with various concentrations of each inhibitor for 1 h in a 96-well plate. The fluorogenic substrates Suc-Leu-Leu-Val-Tyr-AMC (Bachem) or Ac-Pro-Ala-Leu-AMC (Boston Biochem) were used at the final substrate concentration of 100 μM to measure the remaining levels of chymotrypsin-like activity or LMP2-specific catalytic activity, respectively. Fluorescence signals from the release of free AMC (7-amino-4-methylcoumarin) were monitored every minute for 1 h via a SpectraMax M5 microplate reader (Molecular Devices) using excitation and emission wavelengths of 360 and 460 nm, respectively. The initial hydrolysis rates (slopes) for individual wells were calculated via linear regression and normalized to the values from vehicle-treated control wells. Non-linear regression analysis was performed using GraphPad Prism 7 to calculate an IC_{50} value for each compound in inhibiting proteasomal CT-L or LMP2 activity.

4.2.3 *Cell culture*

Human cancer cell lines H23, H727, and RPMI8226 were obtained from the ATCC (American Type Culture Collection) and maintained in the ATCC recommended media, RPMI1640 supplemented with 10% fetal bovine serum (Gibco, and Atlanta Biologicals). RPMI8226 cells with acquired resistance to Cfz were established by adapting them in the presence of stepwise increasing concentrations of Cfz up to 80 nM over a period of approximately 6 months. Cfz-resistant cells were maintained in

80 nM Cfz and then grown in the absence of Cfz for approximately one week prior to the experiments.

4.2.4   *Isolation of primary MM samples*

Bone marrow (BM) aspirates were obtained from patients after approval by the UC Cancer Institute Institutional Review Board followed by positive selection with CD138 microbeads developed for the isolation of plasma cells. Immunophenotyping by flow cytometry was performed to confirm the purity and quantity of selected CD138+ plasma cells.

4.2.5   *Cell Viability*

4.2.5.1   Established cancer cell lines

H23 cells or H727 cells were plated at 5,000 or 10,000 cells per well, respectively. RPMI8226 cells and Cfz-resistant RPMI8226 sublines growing in suspension were plated at 10,000 cells per well. Twenty-four hours after plating, media containing the test compounds were added to each well to deliver the intended final concentration. After 72 h, cell viability was determined using the assay protocol recommended by the manufacturer (CellTiter 96 Aqueous One Solution Cell Proliferation assay, Promega). The resulting signals were measured using a SpectraMax M5 microplate spectrophotometer (Molecular Devices). Non-linear regression analysis was performed using GraphPad Prism 7 to calculate an IC_{50} value for each compound to incur cell death.

4.2.5.2   Primary MM cells

Purified primary MM cells were plated on 96-well plates at a density of 20,000 cells per well in IMDM media (Gibco) supplemented with 10% FBS. After cells were treated with test compounds for 48 h, the percentage of viable cells was determined using the CellTiter Glo Luminescent Cell Viability Assay (Promega) and a Veritas microplate luminometer (Promega).

4.2.6 *Immunoblotting*

Cell lysates were prepared using ice-cold RIPA lysis buffer (50 mM Tris–Cl, 150 mM NaCl, 1% NP-40, 1% Triton X-100) supplemented with 1% protease inhibitor cocktail (Sigma–Aldrich). After centrifugation at 14,000g at 4 °C for 20 min, the resulting supernatant was collected and subject to the total protein assay using Protein Assay Dye Reagent Concentrate (Bio-Rad). Proteins were resolved by 7.5% SDS-PAGE, and transferred onto PVDF membranes (Bio-Rad) via semi-dry transfer. After blocking in 5% nonfat dry milk, membranes were incubated with primary antibodies (anti-P-gp (Abcam) or anti-β-actin (Enzo)) at 4 °C overnight. Membranes were washed and incubated with appropriate peroxidase-conjugated secondary antibodies for 1 h at room temperature. Proteins were visualized on Kodak BioMax XAR Films (Sigma–Aldrich) using ECL.

4.2.7 *In vitro metabolic stability*

To assess whether Cfz-OH has indeed an improved metabolic stability over Cfz, we compared the rate by which Cfz-OH or Cfz disappears in the presence of rat liver homogenates, as previously reported [282]. Briefly, the liver was obtained from male Sprague-Dawley rats (8 week-old, Nara Biotech Co. Ltd., Seoul, Korea) using the protocol approved by the Seoul National University Institutional Animal Care and Use Committee (approval No. SNU-160512-5-1). The harvested liver was washed with phosphate-buffered saline (PBS, pH 7.4) and homogenized using 5-fold excess volume of PBS per g tissue. After pre-incubation at 37 °C, an aliquot of liver homogenates was spiked with the stock solution of Cfz or Cfz-OH to achieve the final concentration of 1 M (total volume of 400 μl, n=3). At the pre-designated time (0, 5, 10, and 20 min), an aliquot (40 μl) was collected and mixed with 4-fold excess volume of ice-cold acetonitrile containing chlorpropamide (an internal standard, IS, 0.5 μM). After vortexing and centrifugation, the drug levels in the resulting supernatant were analyzed via HPLC interfaced with mass spectrometry (LC-MS/MS).

Cfz-OH was quantified using the slightly modified analytical conditions via LC-MS/MS (1260 infinity HPLC system interfaced with 6430 Triple Quad LC-MS system, Agilent Technologies, Palo Alto, CA) in a positive ion mode. The chromatic separation was performed using a Poroshell 120 EC-C18 column (4.6 x 50 mm, 2.7 μm, Agilent Technologies, Palo Alto, CA) and an isocratic mobile phase composed of acetonitrile and water (75:25, v/v) at a flow rate of 0.3 mL/min. The retention time of Cfz-OH was 1.7 min and the gas temperature was set at 300 °C. The source-dependent parameters, the fragment voltage, collision energy and cell accelerator voltage were set as follows: 170 V, 75 V, and 1 V for Cfz-OH and 90 V, 30 V and 7 V for chlorpropamide (IS). Quantification was performed in the selected reaction monitoring (SRM) mode using the following transitions: m/z 736.2 > 99.9 for Cfz-OH and m/z 276.9 > 110.8 for chlorpropamide (IS). The calibration samples were prepared in the range of 1 to 200 nM and the signals showed linearity with the r^2 value greater than 0.98. The data were processed using the MassHunter Workstation Software Quantitative Analysis (vB.05.00; Agilent Technologies).

4.3   Results

4.3.1   *Initial screening for proteasome inhibitors that overcome intrinsic Cfz resistance*

As described in chapter 3, H727 human lung adenocarcinoma cell line is intrinsically resistant to Cfz (IC_{50} of 611 nM) compared to a panel of cancer cell lines (IC_{50}'s in the low nM range). Thus, we selected the H727 cell line as our cell line model of intrinsic resistance to Cfz in which to identify PIs that can overcome de novo resistance to Cfz. As a control, we used another lung cancer cell line model of H23 cells, which are highly sensitive to Cfz (IC_{50} of 18 nM). We treated theses Cfz-sensitive H23 and Cfz-resistant cancer H727 cell lines with PIs that have distinct chemical structures and pharmacophores—The peptide epoxyketone inhibitor carfilzomib, the peptide boronate inhibitor bortezomib, the peptide aldehyde inhibitor MG-132, the in-house-generated peptide epoxyketone inhibitors UK-101 and UK-102, and the β-

lactone inhibitor lactacystin (Figure 4.1)—for 72 hours. We then measured the effects of each inhibitor on cell viability. UK101 and UK102 were previously developed in our laboratory [283]. Interestingly, compared to Cfz, UK-101 and UK-102, displayed relatively smaller differences in their IC_{50} values between Cfz-sensitive and Cfz-resistant cancer cells (Table 4.1). In other words, UK101 and UK102 displayed a comparable cytotoxicity in H727 and H23 cells. In addition, Cfz-resistant cancers may be minimally cross-resistant to UK-101 and UK-102. On the other hand, a β-lactone inhibitor lactacystin was not as effective in H727 cells as in H23 cells. These results suggest that targeting the proteasome using alternative PIs still can be a viable therapeutic option even in the presence of cancer resistance to Cfz and Identifying alternative PIs that remain effective in Cfz-resistant cancer cells.

Carfilzomib

Bortezomib

MG-132

Lactacystin

UK101

UK102
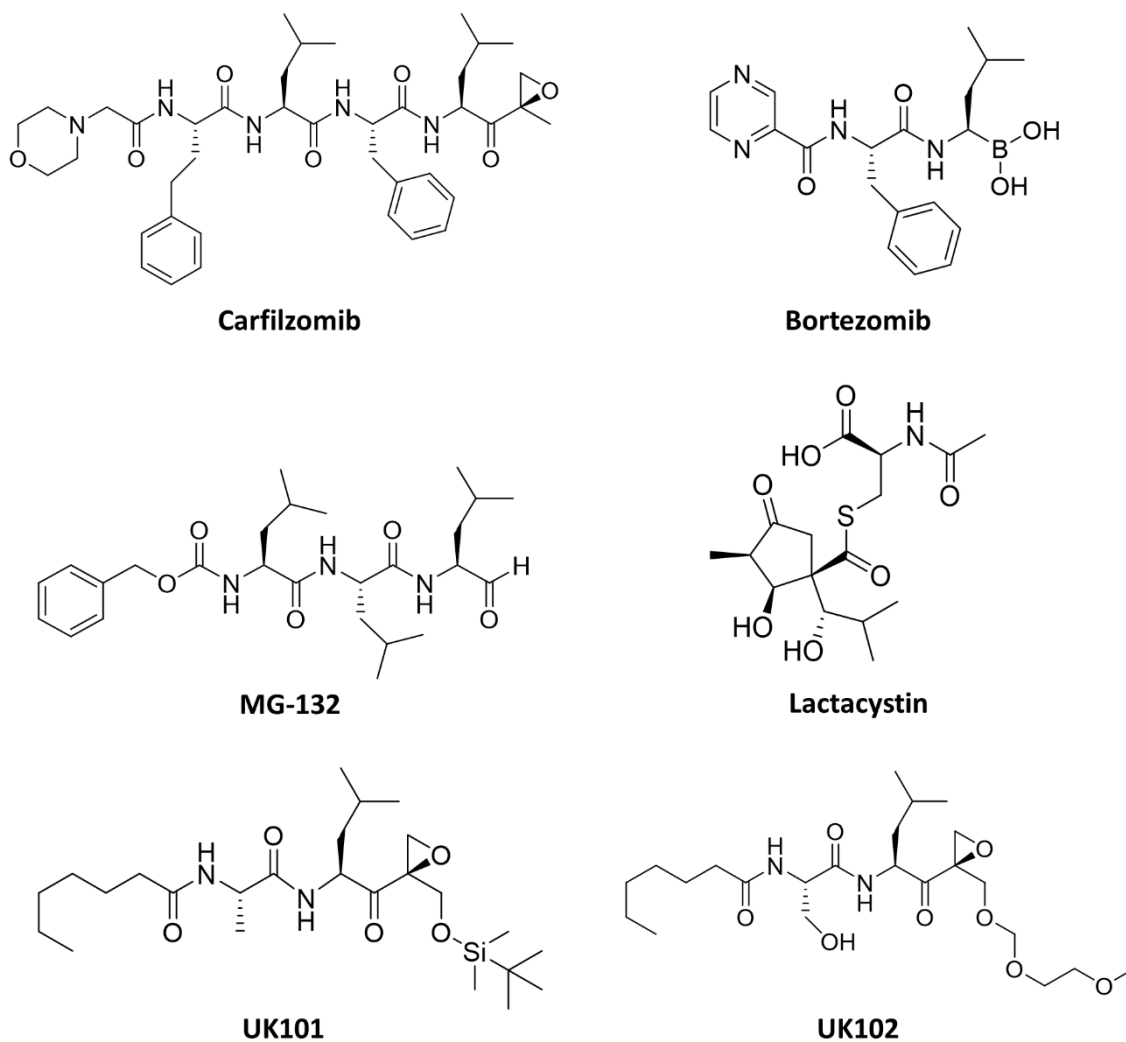
Figure 4.1 Structures of structurally distinct-proteasome inhibitors

Structures of the peptide epoxyketone inhibitor carfilzomib, the peptide boronate inhibitor bortezomib, the peptide aldehyde inhibitor MG-132, the β-lactone inhibitor lactacystin, and the in-house-generated peptide epoxyketone inhibitors UK-101 and UK-102 are shown

Table 4.1 Cytotoxicity of proteasome inhibitors in H727 and H23 cells

	IC$_{50}$ (μM)		
	H23	H727	Fold difference (H727/H23)
Carfilzomib	0.018 ± 0.004	0.611 ± 0.047	33.3
Bortezomib	0.010 ± 0.001	0.025 ± 0.006	2.5
MG-132	0.48 ± 0.01	0.98 ± 0.03	2
Lactacystin	5.23 ± 0.22	> 100	> 19
UK101	3.37 ± 0.19	5.21 ± 0.11	1.5
UK102	3.40 ± 0.18	4.49 ± 0.26	1.3

4.3.2   *The PIs with P1' (UK101 & UK102) exert the anticancer efficacies in acquired Cfz resistant cancer cells*

Since acquired cfz resistance is a major clinical challenge facing Cfz-based therapies, we wondered whether these P1′-targeting epoxyketones, UK101 and UK102 are also effective in acquired Cfz resistance cells. To test this, we established a Cfz-resistant subline of human MM RPMI8226 and U266 (RPMI 8226/CfzR and U266/CfzR) by culturing them in the continuous presence of gradually increasing concentrations of Cfz over 6 months. As shown in Figure 4.2 A&B, results from MTS cell viability assays revealed that, in comparison with those of their respective parental cell lines, the Cfz IC_{50} values of RPMI 8226/CfzR and U266/CfzR cells were 36-fold and 9-fold higher, respectively.

As described previously, several studies have shown that the efflux transporter P-gp can contribute to acquired resistance to Cfz observed in cancer cell line models and clinical samples from patients with prior Cfz therapy [132-135]. To test whether P-gp plays a role in these RPMI 8226/ CfzR and U266/ CfzR cell line models, we performed immunoblotting analysis to detect P-gp expression (Figure 4.3A). While there is no delectable level of P-gp expression in PRMI 8226 or U266 parental cells, the highly elevated expression of P-gp in both RPMI 8226/CfzR and U266/CfzR cells. Furthermore, treatment of RPMI 8226/CfzR cells with 7.5 μM of reversin 121, a dipeptide P-gp inhibitor, did not significantly impact the IC_{50} value of Cfz (Figure 4.3B), confirming the predominant contribution of P-gp in the current model of acquire Cfz resistance. Using these acquired Cfz resistant cell line modesl, we examined the effectiveness of P1′-targeting epoxyketones. As reported before, both epoxyketone PIs Cfz and epoxomicin displayed a marked increase in IC_{50} values, indicating there are P-gp substrate. On the other hand, compared to Cfz, UK-101 and UK-102, displayed relatively smaller differences in their IC_{50} values between Cfz-resistant cancer cells and their parental controls (Table 4.2).
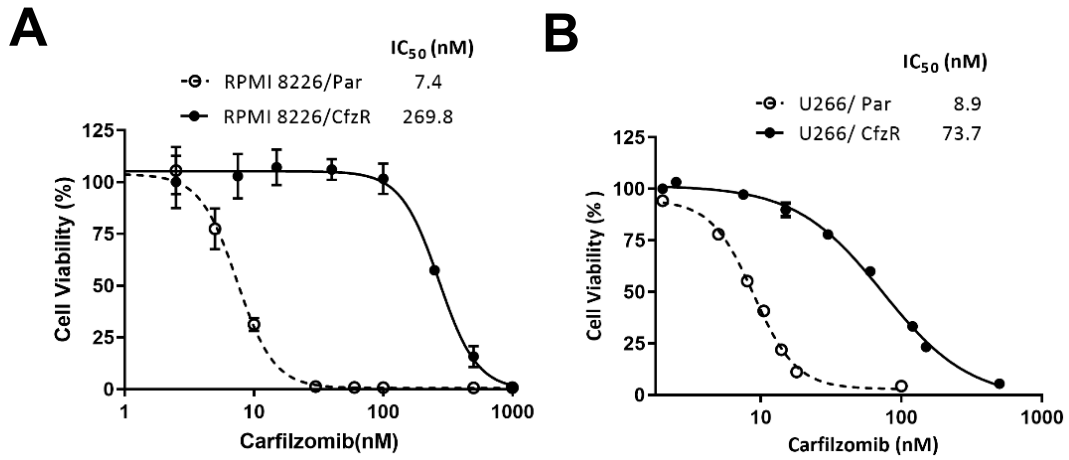
Figure 4.2 Establishment of MM cell lines with acquired resistance to Cfz

A. 72 h cell viability data for Cfz in RPMI 8226 parental and Cfz-resistant cells are shown. **B.** 72 h cell viability data for Cfz in U266 parental and Cfz-resistant cells are shown.
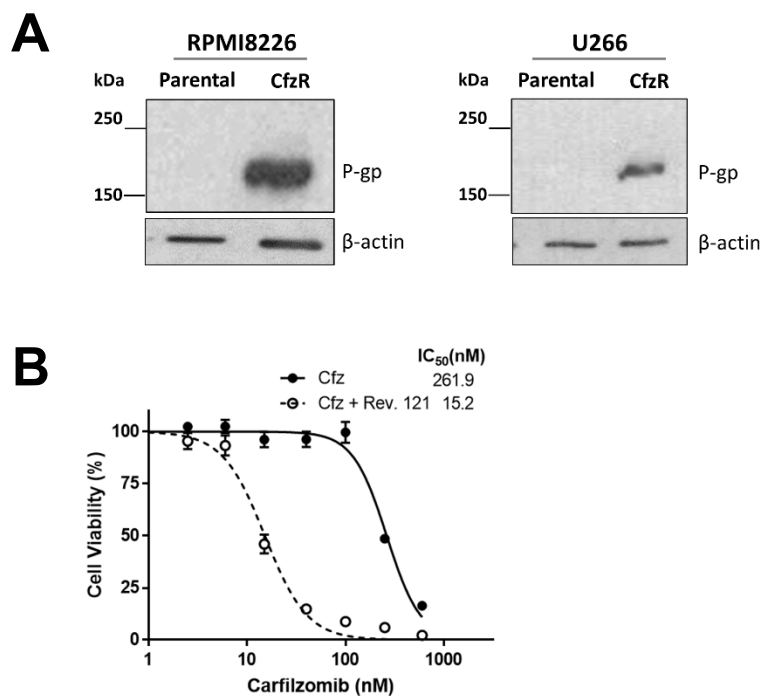
Figure 4.3 P-gp overexpression in acquired Cfz resistant MM cells

A. Immunoblotting results showing elevated expression of P-glycoprotein (P-gp) in RPMI 8227 and U266 cells with acquired Cfz resistance. **B.** The co-treatment of reversin-121 (7.5 μM, P-gp inhibitor) restored the sensitivity of RPMI 8226/CfzR cells to Cfz. Data shown are representative of biological triplicate experiments.

Table 4.2 Cytotoxicity of proteasome inhibitors in acquired Cfz resistant cells

	IC$_{50}$ (nM)			
	RPMI 8266	**RPMI 8266/CfzR**	**U266**	**U266/CfzR**
Carfilzomib	7.4 ± 1.5	269.8 ± 55.6	8.9 ± 1.1	73.7 ± 10.4
Epoxomicin	11.3 ± 5.9	540.9 ± 58.0	ND	ND
UK101	2147 ± 803	3728 ± 105	1818 ± 891	7096 ± 844
UK102	1753 ± 113	9651± 902	1809 ± 109	1284 ± 114

Data are reported as the mean ± SD. For epoxomicin and carfilzomib, the SD values were obtained from three independent experiments. For UK101 and UK102, the SD values were from non-linear regression analysis using three replicates.

4.3.3 *UK101 and UK102 exert the anticancer efficacy in acquired Btz resistant-primary MM samples*

In order to further validate that UK-101 and UK-102 have anticancer efficacy in Cfz-resistance, we examined whether UK101 and UK102 can be also effective in primary MM samples derived from patients who do not respond to Btz. Since we were unable to obtain MM samples from patients who are resistant to Cfz, we only obtained primary cells from two different patient groups: patients who did not respond to Btz therapy (Btz-resistant patients), and patients who were never treated with Btz or Cfz (PI-naïve patients), but it was previously reported that patients with MM refractory to or relapsed on Btz are often cross-resistant to Cfz [260]. Using the primary MM samples from 14 different donors (6 from PI-naïve patients and 8 from patients relapsed on Btz therapy), we treated these primary MM cells for 48 hours with Cfz, UK-101, or UK-102 at its *in vitro* IC_{80} concentration derived from viability assay in cell line models via CellTiter-Glo® Luminescent Cell Viability Assays. In this assay, we found varying degrees of sensitivity to Btz or Cfz, but the MM samples from the patients who relapsed on Btz tended to be less responsive to both Btz and Cfz than those from patients from the PI-naïve group (Figure 4.4 A & B). Due to limited quantities of primary MM samples from 6 patients (#1-#4, #9, and #10), we only utilized 10 primary MM samples (4 Btz-resistant and 6 PI-naïve) to examine the efficacy of UK101 or UK102. When 10 primary MM samples treated with UK101 or UK102 for 48 h, the results showed UK-101 and UK-102 remained much more active in primary MM cells derived from Btz-resistant patients and the PI-naïve patients in a dose dependent manner (Figure 4.4 C & D). These results suggest that alternative PIs such as UK-101 and UK-102 may have valuable clinical potential and warrant further investigation. Furthermore, the lack of apparent cross-resistance between Cfz/Btz and UK101/UK102 was encouraging although the current sample size was small.
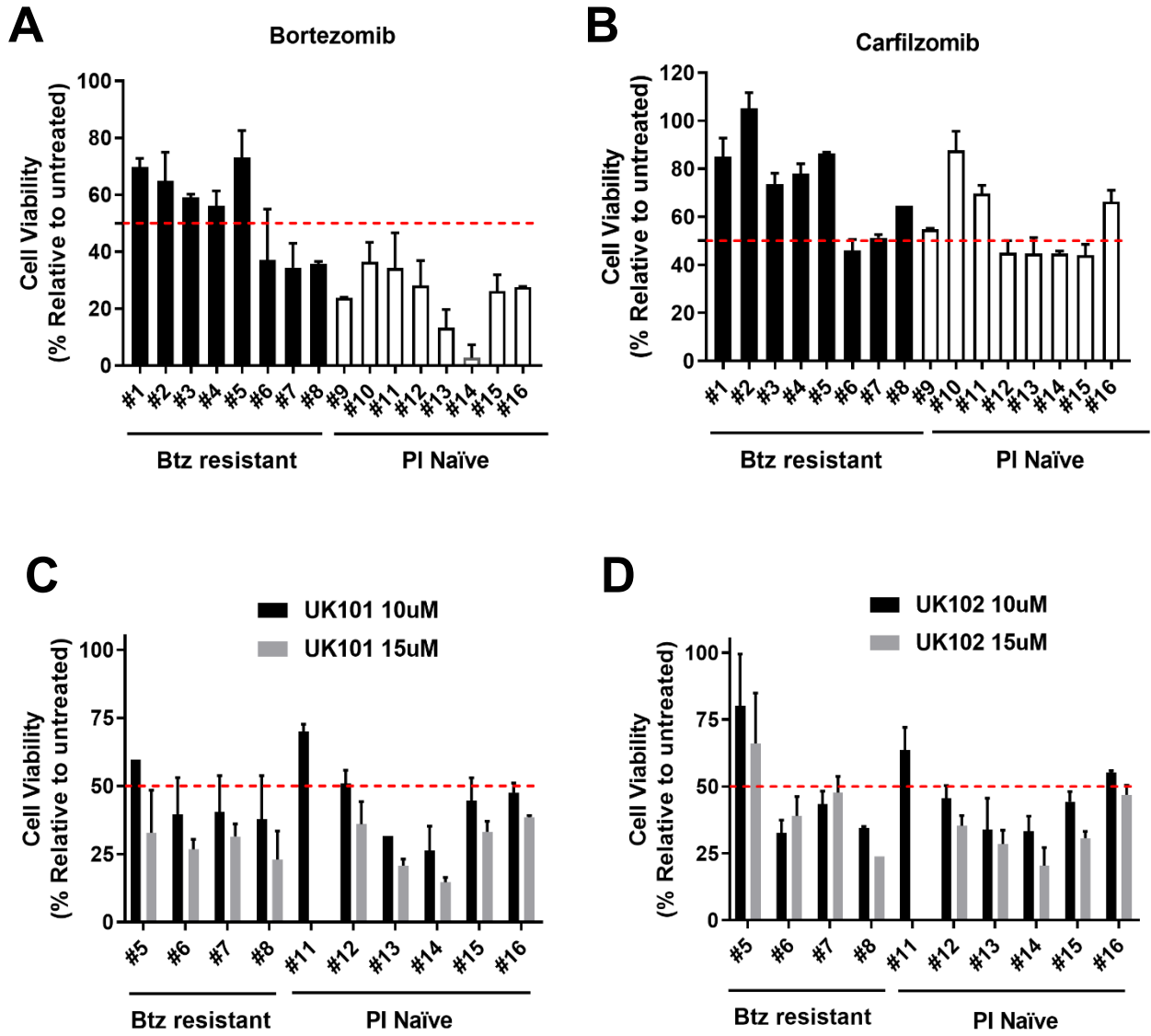
Figure 4.4 Cytotoxic effects of bortezomib, carfilzomib, UK101, and UK102 on primary MM samples

A. Viability for 50 nM of Btz in primary MM cells derived from Btz-resistant patients and PI-naïve patients **B.** Viability for 50 nM of Cfz in primary MM cells derived from Btz-resistant patients and PI-naïve patients **C.** Viability for 10 or 15 μM UK-101 in primary MM cells derived from Btz-resistant patients and PI-naïve patients **D.** Viability for 10 or 15 μM UK-102 in primary MM cells derived from Btz-resistant patients and PI-naïve patients.

4.3.4 *Introduction of hydrophilic residues at the P1′ position of peptide epoxyketones enhances the potency of the proteasome inhibition.*

Since we observed that UK101 and UK102 had anti-cancer efficacy in primary samples derived from Btz-resistant patients but displayed display much lower potencies than Btz and Cfz with IC$_{50}$ values, we first utilized a previously reported docking model of UK101 bound to β1i and β5, known targets of UK101 to improve the potency of UK101/UK102 and obtain structure-activity relationship (SAR) information [84, 283]. As shown in Figure 4.5, the P1-P3 residues of UK101 were predicted to occupy the S1-S3 pockets located deep inside of the active sites of the β1i and β5 subunits. However, unlike Cfz bound to β5, docking followed by molecular dynamics simulations indicated that UK101 occupies an additional binding pocket (S1′) of the β5 as well as β1i subunits via its P1′ group (highlighted in purple circles, Figure 4.5) which is not occupied by Cfz or Btz. Although the P1′ group (t-butyldimethylsilyl, TBDMS) of UK101 is not predicted to participate in any specific interactions upon binding to β1i, it fully occupies the S1′ pocket defined by the surrounding polar amino acids (Ser21, Ser48, Ser95, His97). In the case of UK101 bound to β5, a steric clash between the TBDMS group and Tyr169 is noted. The resulting change in conformation is predicted to abolish a potential hydrogen bond between UK101 and Gly47, a plausible contributing factor towards UK101's low potency against the β5 subunit [284]. We hypothesized that the optimization at the P1′ position could provide energetically-favorable interactions with the S1′ pocket of β1i and also avoid steric clash with Tyr169 of β5, potentially improving potency against both subunits. To test this, we replaced the bulky hydrophobic P1′ substituent (TBDMS) of UK101 with a hydroxyl group (scheme in Figure 4.6) and assessed its impact. This simple P1′ substitution increased in vitro 20S proteasome inhibitory potency by ~4-10 fold (Table 4.3). Moreover, the P1′ hydroxyl group also considerably improved the cytotoxic activity of UK101-OH (5) cancer cell lines, including our models of both de novo and acquired Cfz resistance. Based on this result,

we suspect that the P1' residue of peptide epoxyketones may play an important role in overcoming the resistance of cancer cells to Cfz.

β5:UK101

β5:Carfilzomib

β1i:UK101

β1i/β5 superimposed
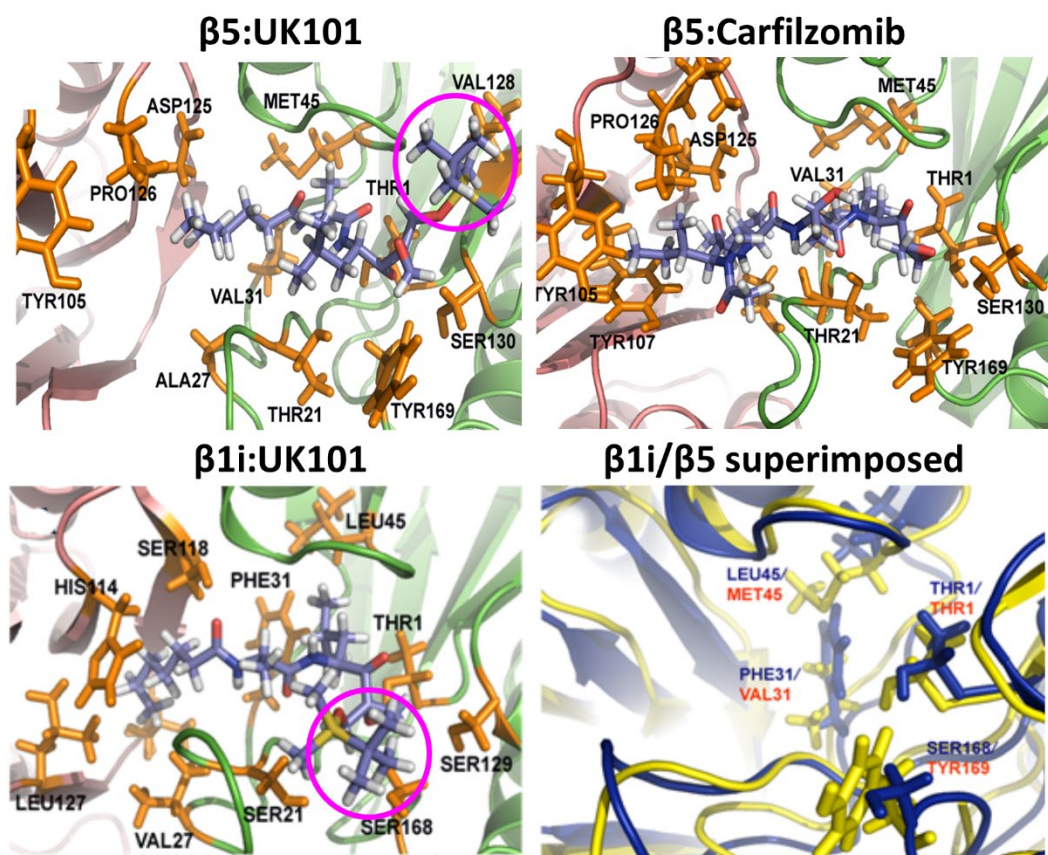
Figure 4.5 Predicted docking models of UK101 and Cfz bound to β5 or β1i

Predicted docking models of UK101 and carfilzomib (Cfz) bound to β5 or β1i. The superposition of the β5 and β1i active sites are shown based on molecular dynamics simulations. The location of UK101's TBDMS group positioned within putative P1′ pockets is highlighted using a purple-colored circle. X-ray structures of β1 (PDB ID: 3UNF) and β5/X (PDB ID: 3UNE) from mammalian 20S proteasomes were used as templates for modeling LMP2 and X. This experiment was performed by Dr. Chang-Guo Zhan's group in the College of Pharmacy, University of Kentucky.
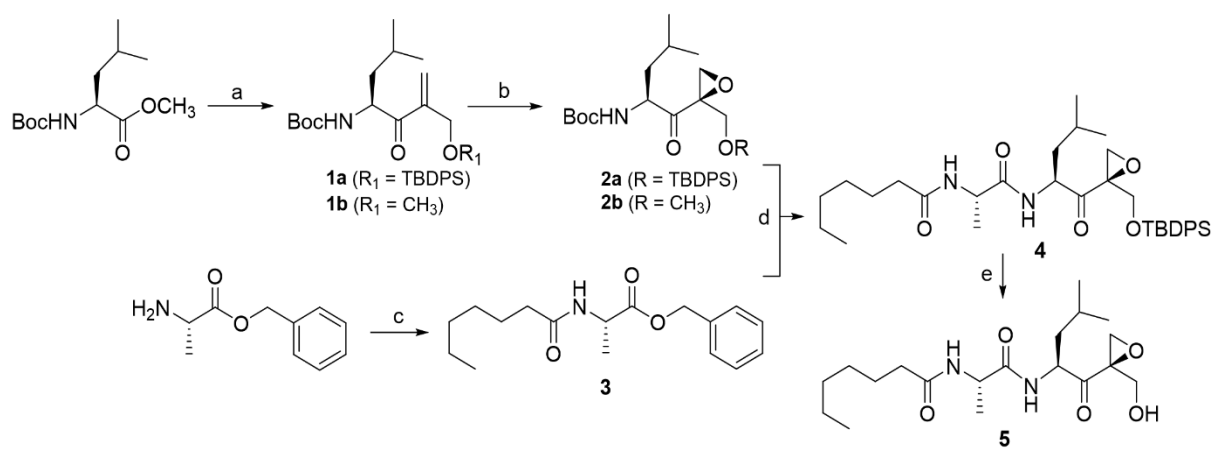
Figure 4.6 Synthetic scheme for UK101-OH (5)

These compounds including UK101-OH(5) were synthesized by Dr. Deepak Bhattarai.

Table 4.3 Cytotoxicity of proteasome inhibitors in H727, H23, RPMI 8226/CfzR cells

Proteasome inhibitors	IC$_{50}$ (μM)				
	CT-L	LMP2	H23	H727	RPMI 8266/CfzR
UK101	> 10	0.140 ± 0.01	3.37 ± 0.19	5.21 ± 0.11	2.14 ± 0.08
5 (UK101-OH)	1.7 ± 0.1	0.036 ± 0.01	0.58 ± 0.02	0.69 ± 0.01	0.31 ± 0.01

Data are reported as the mean ± SD.

4.3.5 *Development of Cfz analog with an improved potency in de novo and acquired Cfz resistant models*

In our efforts to further optimize UK101-OH, we deemed that the P1-P4 groups of Cfz have already been thoroughly optimized for the S1-S4 pockets of β5 and β5i (as well as β1i, to a lesser extent, based on the largely β1i/β5 superimposed model, Figure 4.5). We thus decided to attach several different P1′ moieties to Cfz. Since we have observed that Cfz analogs bearing a P1′-targeting group could overcome cross-resistance to Cfz, we also expected that a Cfz analog containing a polar P1′ moiety leading an improved inhibitory potency against both β5 and β1i compared to Cfz, due to additional P1′:S1′ interactions. Based on this, we prepared Cfz analogs having a series of P1′ moieties varying from bulky hydrophobic to small hydrophilic residues (synthetic scheme in Figure 4.7). We subsequently measured their activity against cell lysates to measure CT-L (β5/β5i) inhibition and against 20S purified immunoproteasomes to measure β1i inhibition. As predicted by molecular dynamics, Cfz-OH and Cfz-Sulfone having small polar moieties were most potent in vitro with IC$_{50}$ values similar to that of Cfz. When these two compounds were tested using Cfz-resistant H727 cells, Cfz-Sulfone (12) was less potent than Cfz against H727. On the other hand, Cfz-OH, a Cfz analog (9) with a hydroxyl group at the P1′ position, demonstrated an improved potency by ~10-fold relative to Cfz. When tested against RPMI8226 with acquired Cfz resistance, Cfz-OH (9) demonstrated an almost 3-fold improvement in potency against Cfz-resistant RPMI8226 cells as compared to Cfz (Figure 4.8).
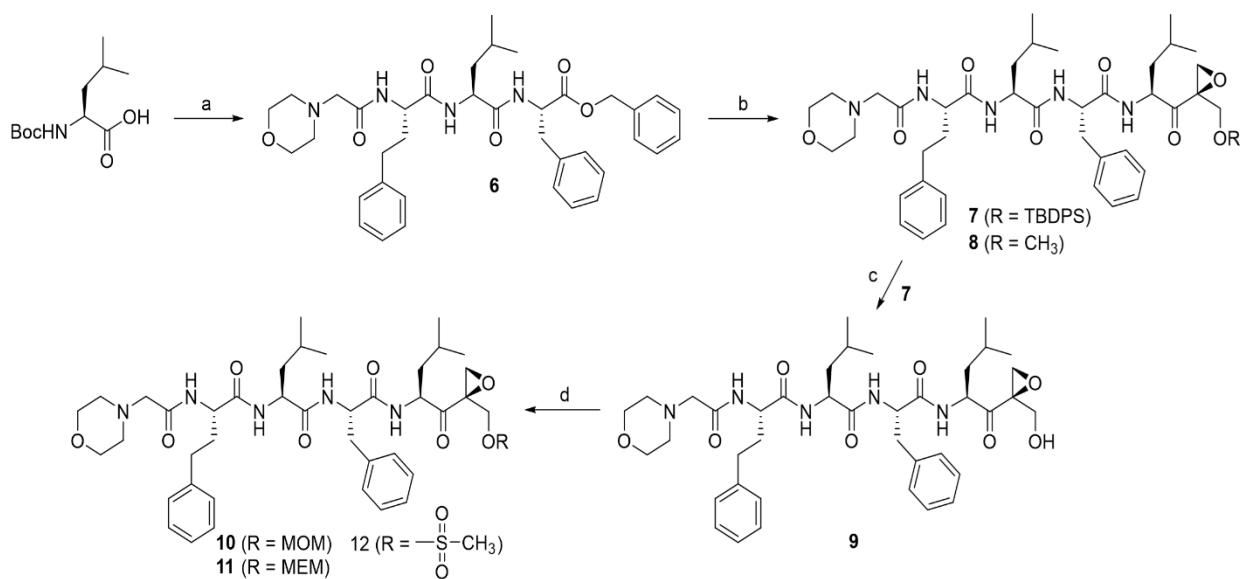
Figure 4.7 Synthetic scheme for Cfz-OH (9)

These compounds including Cfz-OH (9) were synthesized by Dr. Deepak Bhattarai.

R =

$-Si(Ph)_2$ tBu	**7**
$-CH_3$	**8**
$-H$	**9 (CFZ-OH)**
$-CH_2OCH_3$	**10**
$-CH_2OCH_2CH_2OCH_3$	**11**
$-SO_2CH_3$	**12**
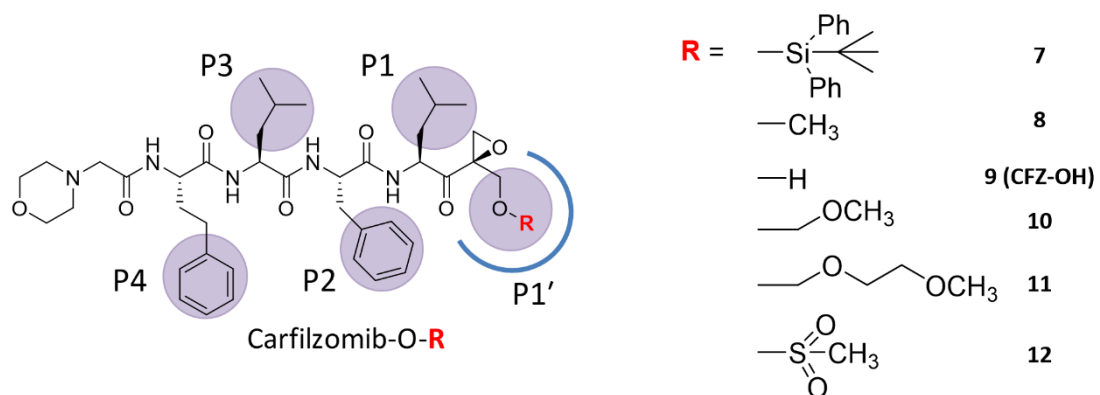
Carfilzomib-O-**R**

Proteasome inhibitors	IC_{50} (nM)				
	CT-L	**LMP2**	**H23**	**H727**	**RPMI 8266/CfzR**
Carfilzomib	2.7 ± 2.2	2940 ± 22.3	18.3 ± 6.6	610.2 ± 46.9	269.8 ± 54.8
7 (CFZ-TBDPS)	111.6 ± 11.1	-	$> 10,000$	$> 10,000$	-
8 (CFZ-CH$_3$)	>1000	-	-	-	-
9 (CFZ-OH)	2.1 ± 0.9	743.5 ± 10.7	29.4 ± 2.5	61.0 ± 10.7	106.2 ± 28.9
10 (CFZ-MOM)	> 1000	-	-	-	-
11 (CFZ-MEM)	> 1000	-	-	-	-
12 (CFZ-Sulfone)	8.0 ± 4.9	-	310.7 ± 12.3	834.4 ± 41.6	-

Figure 4.8 Effects of various substitutions at the P1′site of the compound on the potency in Cfz resistant cells

The potency (IC_{50} values) for compounds with various substitutions at the P1′site against proteasome chymotrypsin-like activity (RPMI8226 cell lysate), LMP2 activity (purified human 20S immunoproteasome), and cell viability of H23, H727, and Cfz-resistant RPMI8226 cells. Data reported as the mean ± SD (carfilzomib, n = 3 independent experiments) or from a single experiment (3 replicates, 7, 9, and 12).

4.3.6 *Cfz-OH has improved metabolic stability compared to Cfz*

Due to the presence of peptidase and microsomal epoxide hydrolase (mEH) enzymes throughout many of the body's tissues, the peptide epoxyketone inhibitor carfilzomib is metabolized extremely rapidly, likely contributing to poor activity against solid tumors [285-287]. While cytochrome P450 is well known as a major enzyme to metabolize most of drugs, metabolites formed via P450 enzymes were only detected at very low levels. An in vitro study using rat tissue homogenates has confirmed that carfilzomib metabolism is not restricted to the liver and that lung, kidney, and heart tissues all possess the ability to rapidly degrade carfilzomib to its inactive metabolites. In the case of mEH, the active site harbors two conserved Tyr residues which may contribute to substrate specificity and orientation of substrates within the active site [288, 289]. The prototypical substrates of mEH include planar hydrophobic compounds such as various epoxides of polycyclic aromatic hydrocarbons and steroids [290]. It is thus expected that the epoxide ring of Cfz occupies the active site of mEH with a position suitable for hydrolysis to yield Cfz-diol (Figure 4.9). We hypothesized that the addition of a hydroxyl group adjacent to the epoxide ring of Cfz, Cfz-OH, may hinder the hydrolysis of the epoxide ring by inhibiting access to the active site of mEH. To assess whether Cfz-OH has indeed an improved metabolic stability over Cfz, we compared the rate by which Cfz-OH or Cfz disappears in the presence of rat liver homogenates, as previously reported [282]. In the presence of rat liver homogenates, Cfz-OH was metabolized much more slowly than Cfz. In this case ~40% of Cfz-OH remained unmetabolized at 5 minutes as compared to just 7% of carfilzomib (Figure 4.9). Based on these preliminary results we found Cfz-OH was indeed more stable than Cfz.
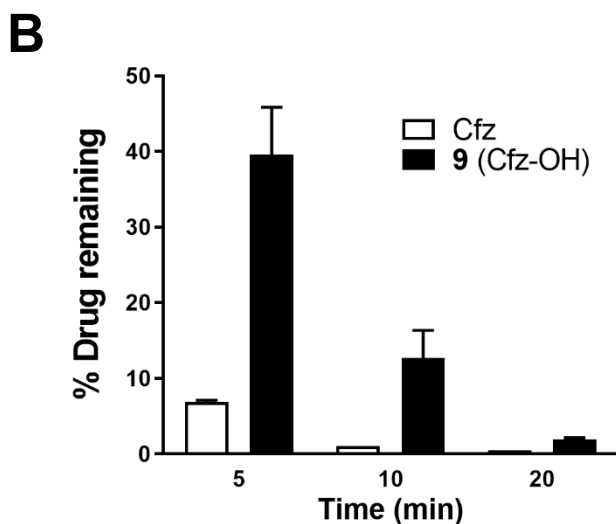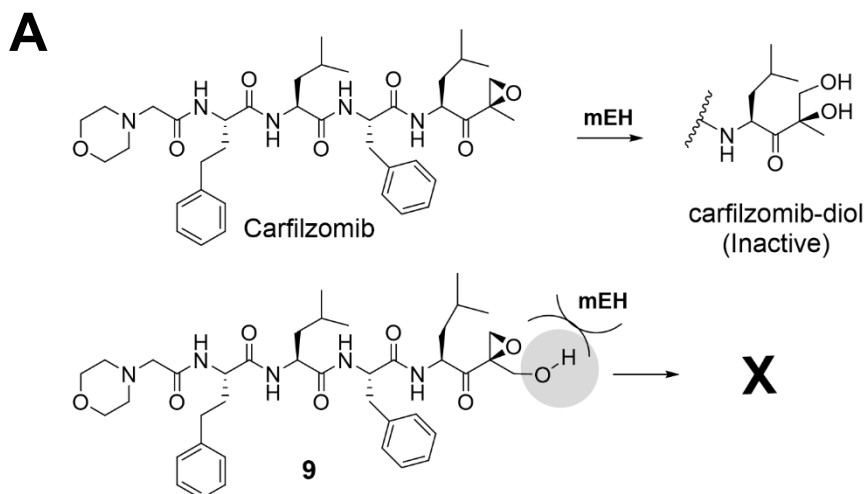
Figure 4.9 The metabolic stability of CFZ-OH

A. Schematic depicting the rapid metabolism of Cfz by microsomal epoxide hydrolase (mEH) to the inactive diol. **B.** Quantification of the remaining levels of Cfz or 9 following the incubation with rat liver homogenate containing active mEH and peptidase activities for 5, 10, and 20 minutes respectively. Data presented as mean ± SD. This experiment was performed by Zi Soo Yoo from Wooin's group in the College of Pharmacy and Research Institute of Pharmaceutical Sciences, Seoul National University, Korea.

4.4   Discussion

It is now well-understood that proteasome inhibitor resistance, either de novo or acquired, is a major limitation associated with the clinical use of PI drugs in treating cancers. In patients with refractory/relapsed MM, response rates for Btz and Cfz are less than 50% and 25%, respectively. Although the response rates can increase to ~70-90% when combined with other drugs including lenalidomide, all patients inevitably develop resistance to therapy and have a dismal prognosis once resistance emerges. While several PI resistance mechanisms have been proposed so far, their clinical relevance is yet to be validated. Currently, the lack of the mechanistic understanding of PI resistance is a major obstacle in improving MM patient care.

Mounting evidence has demonstrated that the proteasome remains necessary for cancer cells survival regardless of their resistance to PI drugs. The proteasome plays important roles in various cellular functions and to date there appears no pathway which can fully compensate for the loss of proteasome function. Several reports supported that proteasome inhibition may offer therapeutic gains even in patients with MM relapsed/refractory to currently used PIs in clinic.

In this study, we used two type of PI resistant cancer cell lines, de novo Cfz resistant H727 cells or acquired Cfz resistant RPMI 8226/CfzR, U266/CfzR cells. We identified an effective proteasome inhibitor compound against both de novo or acquired Cfz resistant cell lines. We found that epoxyketones with P1′ substituents can overcome both de novo and to a lesser degree, acquired Cfz resistance in cell line models. It is well known peptide epoxyketones harbor greater selectivity in their interactions with the proteasome catalytic subunit by forming an 1,4-oxazepane adduct with the N-terminal catalytic threonine residue of the proteasome [75], leading to the improved safety profiles of Cfz over other classes PIs including the peptide boronate Btz. We believe that the compound with improved metabolic stability and ability to overcome resistance mechanisms may offer valuable knowledge for further drug development. Future studies will address the in vivo

99

efficacy and metabolic stability of epoxyketones with previously underexplored P1′ substituents that can overcome both de novo and acquired Cfz resistance.

CHAPTER 5. A SELECTIVE INHIBITOR OF THE IMMUNOPROTEASOME SUBUNIT LMP2 ATTENUATES DISEASE PROGRESSION IN MOUSE MODELS OF ALZHEIMER'S DISEASE

Some of the work in this chapter has been submitted to Nature Chemical Biology.

5.1 Introduction

Alzheimer's disease (AD), the most common form of dementia, is a degenerative disorder of the brain that leads to memory loss. AD is a progressive, neurodegenerative disorder and is the sixth-leading cause of death across all ages. Currently there is there is no cure for AD, however, promising research and development for early detection and treatment is underway. Over the past decades, new therapeutic approaches targeting amyloid-β (Aβ) have been discovered and developed with the hope of modifying the natural history of AD. However, none of these drugs resulted in the positive cognitive improvement in most recent high-profile phase III clinical trials [171], raising the doubt about amyloid hypothesis. In addition to extracellular Aβ, intraneuronal neurofibrillary tangles (NFT) composed of hyperphosphorylated tau protein have been also identified as a major hallmark of AD, leading active development of AD therapies targeting tau aggregation. Unfortunately, anti-tau therapies are also not available yet [291]. Therefore, it is highly timely and important to design disease-modifying drugs that are not reliant on the amyloid or tau hypothesis and to validate their therapeutic potential in pre-clinical and clinical studies.

The 26S proteasome, an evolutionarily-conserved multiprotease complex, is largely responsible for controlled degradation of intracellular proteins, ranging from defective ribosomal products (DRiPs) to signaling proteins regulating numerous cellular processes (e.g., cell cycle control, immune response, apoptosis, stress response)[292]. Once poly-ubiquitinated, substrate proteins are recognized by the

19S regulatory particle and degraded by the 20S core particle of the 26S proteasome. In response to cellular stress or pro-inflammatory cytokines such as TNF-α or interferon (INF)-γ, cells upregulate variant forms of proteasome catalytic subunits, known as immuno-subunits (β1i/LMP2, β2i/MECL-1, β5i/LMP7). The resulting immunoproteasome (IP) harbors the immuno-subunits LMP2 and MECL-1 and LMP7 instead of constitutive counterparts Y, Z and X, respectively.

A previous study demonstrating the depletion of immunoproteasomes showed major changes in antigen presentation, indicating a fundamental role of the IP in antigen presentation by major histocompatibility complex (MHC) I class [293]. In addition, the IP also manages oxidative stress via degradation of misfolded and oxidant-damaged proteins [45]. In addition, LMP7, an immunoproteasome subunit, has been considered as an attractive therapeutic target for autoimmune disease due to the ability of regulating pro-inflammatory cytokine production in human tissues (T-cells, B-cells, neutrophils, monocytes etc)[52-57, 80]. LMP7-selective inhibitors (ONX0914, KZR-616) are currently in early phase clinical development for the treatment of rheumatic diseases, such as lupus nephritis (LN). For LMP2, there have been a few reports suggesting its involvement in processing of NFκB precursors (p100/p105) and degradation of IκBα [58-60]. However, recent studies dispute the involvement of LMP2 in inflammatory responses [56, 294 295].

Increasing evidence support an important role of inflammation in AD, thus many efforts to develop anti-inflammatory drugs targeting inflammation yielded several COX or TNF-α inhibitor for AD treatment. However, there is no clinically available AD therapies relied on inflammation so far [190]. While the role of IP in neuroinflammation is not clearly understood, it has been observed the elevated expression and activity of IP is correlated with enhanced microglial activation in AD patients and in a mouse model of brain injury [240-243]. Most recently, Wagner et al. reported LMP7 knockout improved cognitive impairment in a mouse model of Aβ deposition through altering microglial cytokine production profiles, suggesting a potential role of IP in Aβ-induced neuroinflammation [51]. In addition, moderate up-regulation of LMP2 expression in AD patients was also reported [244]. Despite these

data suggesting the involvement of IP in neuroinflammatory responses and therapeutic potential for AD treatment, the pharmacological inhibition of LMP7 or LMP2 has never been tested for the impact on AD pathology.

In this study, we investigated the effect of LMP2 inhibition on the symptom of AD, cognitive dysfunctions, in two different AD mouse models, LPS-induced inflammation model and APP transgenic mouse model. We found that a peptide epoxyketone inhibitor YU102 targeting LMP2 improved cognitive function in both of AD mouse models. These results were not affecting Aβ deposition or tau aggregation in a mouse model. Our *in vitro* cell line model data also showed YU102 suppresses production of pro-inflammatory cytokines. In summary, YU102 improves cognitive dysfunction by inhibiting pro-inflammatory cytokine production in microglial cells and these findings suggest that LMP2 may offer a valuable therapeutic target for AD treatment.

5.2   Material and Methods

5.2.1   *Cells*

BV-2, EOC BV-2, EOC-20, and WI-38 cells were seeded at 5,000 cells/well and RPMI 8226 cells. The murine microglial BV-2 cell line was a kind gift of Dr. Jin Tae Hong (College of Pharmacy, Chungbuk National University, Korea). The murine microglial cell line EOC-20, a human myeloma cell line RPMI 8226, and a human lung fibroblast cell line WI-38 cell line were obtained from American Type Culture Collection. BV-2 cells were cultured in DMEM containing 10 % fetal bovine serum, and 1 mM pyruvate. All other cells were cultured according to the manufacturer's protocol in 5% CO2 in medium. Cultured cell lines were tested for Mycoplasma contamination routinely every 2 months. BV-2 cells or EOC-20 cells were seeded at 2.5×10^5 cells/mL in 12-

well plates and were activated by incubation in medium containing 1 μg/mL of E. coli 055:B5 lipopolysaccharide (Thermo Scientific).

5.2.2   *Animals*

For YU102 efficacy studies, 9-month-old Tg2576 and 8-week-old ICR mice were purchased from the Division of Laboratory Animal Resources (Korea FDA, Osong, South Korea) and Samtako (Osan, South Korea), respectively. All animal studies were approved by Animal Care and Use Committee (IACUC) of Chungbuk National University (approval number: CBNUA-144-1001-01). Animals were housed three per cage, allowed access to water and food ad libitum, and maintained on a 12-h light/dark cycle regulated at 23°C. Experiments were performed at least 1 week after their arrival in individual home cages.

5.2.3   *Animal behavioral analysis*

5.2.3.1   *The Morris watermaze test*

The Morris water maze test was performed following a procedure described previously [296]. Briefly, a circular plastic pool was filled with water maintained at 22-25°C. An escape platform was submerged 1-1.5 cm below the surface of the water. The learning trials were conducted over 5 days, with three randomized starting points. The position of the escape platform was kept constant. Each trial lasted for 60 sec or ended as soon as the mice reached the submerged platform. Swimming pattern of each mouse was monitored and recorded by a camera mounted above the center of the pool, and the escape latency, escape distance and swimming speed were assessed by the SMART-LD program (Panlab, Spain). A quiet environment and constant water temperature were maintained throughout the experimental period. To assess memory consolidation, a probe test was performed 24 hr after the water maze test (i.e. Day 6). For the probe test, the platform was removed from the pool and

mice were allowed to swim freely. The swimming pattern of each mouse was monitored and recorded for 60 sec using the SMART-LD program. Consolidated spatial memory was estimated by the time spent in the target quadrant area.

5.2.3.2   The passive avoidance test

5.2.3.2   The passive avoidance test

The passive avoidance test was performed 48 hours after the probe test. The passive avoidance response was determined using a "step-through" apparatus (Med Associates Inc., Vermont, USA) that is divided into an illuminated compartment and a dark compartment (each 20.3 × 15.9 × 21.3 cm) adjoining each other through a small gate with a grid floor, 3.175-mm stainless steel rods set 8 mm apart. On the first day (i.e. Day 7), the mice were placed in the illuminated compartment facing away from the dark compartment for the learning trial. When the mice moved completely into the dark compartment, it received an electric shock (0.45 mA, 3 s duration). Twenty-four hours after learning trial (i.e. Day 8), each mouse was placed in the illuminated compartment and the latency period until the animal entered the dark compartment was determined and defined as the step-through latency (i.e. Testing trial). The cut-off time for the examination was 180 seconds.

5.2.4   *Tissue extraction from Tg2576 mouse*

The hippocampus was dissected from parasagittal brain slices; nucleus accumbens (NAc) and striatum were dissected from coronal brain slices; the ventral tegmental area (VTA) was dissected from horizontal brain slices. Tissues were homogenized in RIPA buffer (containing 50 mM Tris-HCl (pH 7.5), 150 mM NaCl, 5 mM $MgCl_2$, 1 mM EDTA, 1% Triton X-100, 0.25% sodium deoxycholate, 0.1% SDS, 1 mM sodium orthovanadate, 5 mM β-glycerophosphate, 5 mM NaF and protease inhibitor cocktail), sonicated and incubated on ice for 30 min. The samples were then centrifuged at 14,000g for 20 min and protein concentrations of the supernatant were determined by the Bradford method.

5.2.5   *Proteasome activity assay*

5.2.5.1   *Using the purified human 20S proteasome*

Purified 20S human proteasomes (from Boston Biochem) were used to assess the in vitro activity of proteasome inhibitors. In 96-well format, 20S proteasomes (0.5 μg/mL) were mixed with proteasome inhibitors in assay buffer (20 mM Tris-HCl, 0.5 mM EDTA, 0.035% SDS) at room temperature for 30 min, prior to the addition of fluorogenic substrates to a final assay volume of 100 μL. Fluorogenic substrates used in this study are: Suc-LLVY-AMC (CT-L activity, 100 μM), Ac-PAL-AMC (LMP2, 100 μM), Ac-WLA-AMC ($\beta 5$, 20 μM), Ac-nLPnLD-AMC ($\beta 1$,100 μM), and Ac-ANW-AMC ($\beta 5i$, 100 μM). The fluorescence of liberated AMC was measured over a period of 90 min at 360 and 460 nm on a SpectraMax M5 fluorescence plate reader (Molecular Devices).

5.2.5.1   *Using the isolated mouse tissue samples*

To measure proteasome activity in brain tissues isolated from Tg2576 mice, tissues were homogenized in RIPA buffer (50 mM Tris Cl, pH 7.4, 150 mM NaCl, 5 mM EDTA, 1% Nonidet P-40, 1% sodium deoxycholate, 0.1% SDS, 1% aprotinin, 50 mM NaF) and sonicated. Samples were then centrifuged for 20 min at 14,000g (4 °C). After the Bradford protein assay of the supernatant, samples were loaded onto a 96-well plate prior to the addition of the substrate (Ac-PAL-AMC) at 37 °C. Fluorescence was recorded for 90 min using a Synergy-HT (Bio Tek) plate reader. To exclude non-proteasomal substrate degradation, control samples were incubated with YU102 (1 μM) for 60 min at 37 °C before loading on the plate and values were subtracted from lysates incubated with DMSO control.

5.2.6   *Immunoblotting analysis*

Total cell lysates containing equivalent protein content were separated by 12% SDS-PAGE and transferred to polyvinylidene difluoride membranes (Millipore) via a semi-

dry transfer. Membranes were then blocked in 5% non-fat dry milk (Bio-Rad) in Tris-buffered saline with 0.05% Tween-20 (TBST) for 1 h at room temperature. After 5 times wash with PBS, membranes were probed with primary antibodies (anti-LMP2, anti-LMP7, and anti- β-actin, Abcam) in 3% BSA followed by a rabbit horseradish peroxidase-conjugated secondary antibody (GE Healthcare). β-actin was used as a gel loading control. SuperSignal West Femto Chemiluminescent Substrate (Thermo Scientific) and X-ray film (Thermo Scientific) were used for visualization.

5.2.7 *Measurement of Aβ*

Hippocampal $A\beta_{1-42}$ levels were determined using an ELISA Kit (Cusabio Biotech Co., Ltd., Wilmington, DE, USA). Experiments were performed according to the manufacturer's instructions. In brief, samples and standards were added into the pre-coated plate and incubated for 2 hours at 37°C. Biotinylated antibodies (1x) were added to each well and incubated 1 hour at 37°C. After washing, HRP-avidin (1x) was added and incubated for 30 minutes at 37°C. After washing, TMB substrate was added to each well. After the addition of stop solution, the absorbance was measured at 450 nm using a microplate reader (Sunrise™, TECAN, Switzerland).

5.2.8 *Thioflavin T staining*

Frozen hippocampal tissues were cut into 30 μm sections by using cryostat microtome (Leica CM1850; Leica Microsystems). The pieces of tissues were thoroughly washed with distilled water for 5 min, and then transferred to gelatin coated slides and placed in 1% Thioflavine T for 5 min, followed by dehydration using ascending grades of ethanol (50%, 70%, 90%, and 100%) for 2 min in each grade. The dehydrated samples were then mounted with mounting medium (FluoromountTM, Sigma). Thioflavin T staining was examined by using a fluorescence microscope.

5.2.9 *Cresyl violet staining*

Frozen hippocampal tissues were cut into 30 μm sections by using cryostat microtome (Leica CM1850; Leica Microsystems, Korea). The pieces of tissues were thoroughly washed with PBS to remove excess fixative agent, and then transferred to gelatin coated slices and stained with 0.1% Cresyl violet (2-5 minutes) to identify cortical layers and cytoarchitectural features of isocortical region. Next, the resulting sections were washed with distill water and dehydrated by using ascending grades of ethanol (50%, 70%, 90%, and 100%) for 2 min in each grade followed by a 1-min immersion in a 1:1 mixture of absolute alcohol and xylene. The sections were then rinsed with xylene for 5-10 min and mounted with mounting medium (CYTOSEALTM XYL; Thermo Scientific, USA). The same areas of tissues were photographed (100x).

5.2.10 *Tau aggregation assay*

For microscopic image analysis, cells were plated in a black transparent 96-well plate. The next day, tau-BiFC cells were treated with the okadaic acid or forskolin at various concentrations. After, 2, 9, 19, and 24 hr of incubation, the entire 96-well plate was automatically imaged under same exposure by using Operetta® High Contents Screening System (equipped with a 10x and 20X dry lenses). The cellular intensities of tau-BiFC fluorescence were analyzed using Harmony 3.1 software. Error bars indicate s.d. from two independent experiments. Each experiment was performed as triplicate.

5.2.11 *Immunohistochemical staining*

Frozen hippocampal tissues were cut into 30 μm thick sections and stored free floating in cryoprotectant solution (30% ethylene glycol, 20% glycerol, 50 mM sodium phosphate buffer, pH 7.4) at 4 °C until further use. For immunohistochemical staining, sections were rinsed in 1× PBS, incubated in blocking buffer (1× PBS

containing 0.3% Triton X-100 and 10% normal goat serum) for 1 hr at room temperature and further incubated overnight with primary antibodies for GFAP (1:1000; Abcam) or Iba-1 (1:500; Abcam) diluted in 1× PBS/ 0.3% triton X-100/ 5% normal goat serum at 4 °C. Sections were washed with 1× PBS to remove excessive primary antibodies, incubated with species specific peroxidase-coupled secondary antibodies (goat anti-mouse or goat anti-rabbit (1:300, Abcam)) diluted in 1× PBS/ 0.3% Triton X-100/ 5% normal goat serum. The resulting sections were incubated for 1 h on a shaker at RT and developed with liquid diaminobezadine (DAB) (Dako, K3647). Sections were then counterstained with matured hematoxylin, followed by dehydration in an ascending alcohol series before covering using Roti®-Histokitt II mounting medium. For Congo red staining, free-floating cerebral sections were mounted on glass slides and incubated in stock solution I (0.5 M NaCl in 80% ethanol, 1% NaOH) for 20 min and subsequently stock solution II (8.6 mM Congo red in stock solution I, 1% NaOH) for 45 min. After rinsing twice in absolute ethanol, sections were counterstained with mature hematoxylin and dehydrated in ascending alcohol series before rinsing twice in 98% xylene for 1 min, and finally mounted with Roti®-Histokitt II mounting medium. Stereological analysis was performed using a Stereo Investigator system (MicroBrightField) and DV-47d camera (MicroBrightField) mounted on an Olympus BX53 microscope (Olympus, Germany). Fluorescence imaging was performed using an Olympus XM10 monochrome fluorescence CCD camera (Olympus, Germany).

5.2.12 *Membrane-based cytokine array*

A cytokine antibody array assay was performed with a mouse cytokine array kit (R&D Systems) according to the manufacturer's protocol. Briefly, BV-2 cells, seeded in a 12-well plate at 2×10^5 cells per well, were incubated with 1 µg/mL of E. coli 055:B5 lipopolysaccharide (Thermo Scientific) and 3 µM of YU102 or ONX 0914 for 24 hr. The supernatants from BV-2 cells were collected and centrifuged to remove cell debris. The resulting supernatants were then incubated with assay membranes

precoated with capture antibodies overnight at 4°C. After rinsing the membranes with wash buffer, a detection antibody was added using streptavidin–horseradish peroxidase (HRP) and Chemi Reagent Mix. The immunoblot images were visualized using SuperSignal West Femto Chemiluminescent Substrate (Thermo Scientific) and X-ray film (Thermo Scientific or GeneMate).

5.2.13 *Enzyme-linked immunosorbent assay (ELISA)*

BV-2 microglial cells (2.5×10^5 cells/well) were seeded in 12-well culture plates. After overnight incubation, cells were simultaneously treated with 1 µg/mL of E. coli LPS and various concentrations of YU102, YU102 epimer, or ONX 0914 for 24 h. Supernatants were analyzed for the quantification of released pro-inflammatory cytokines, using Mouse IL-1α, IL-6, or CCL12/MCP-5 uncoated sandwich ELISA Kit (Thermo Scientific) on high-binding ELISA plates according to the manufacturer's protocol. Briefly, standards and samples were incubated on capture antibody coated plate for 2 h at room temperature, followed by incubation with detection antibody for 1 h and then Avidin-HRP for 30 minutes. For visualization, substrate solution was added to each well, and then the reaction was stopped by the addition of stop solution (2N H_2SO_4). Absorbance was measured by ELISA microplate reader at 450 nm wavelength.

5.2.14 *RPE flat mounts*

Retinal pigment epithelium (RPE) of Tg2576 was isolated and incubated with β-catenin (1:100 diluted) overnight at 4°C. After incubation with primary antibody, the RPE tissues were further incubated with Alexa 555-conjugated secondary antibody (Invitrogen; A21422; 1:1000 diluted) at room temperature for 2 hours. Sample was observed by using a confocal microscope (Carl Zeiss, LSM 800)

5.2.15 *Cell-based RPE degeneration assay*

ARPE-19 cells were seeded at 80,000 cells/well in 24-well plate with auto-coverglass. Cells were treated with 50 ng/mL of TNF-α and incubated for additional 24 hr before treatment with vehicle, 1 μM of YU102 or YU102 epi. After incubation, cells were fixed with 4% paraformaldehyde for 1 h at room temperature. Cells were then blocked with 3% BSA for 1 h after permeabilized with 0.2% Triton X-100 for 15 min. Cells were incubated overnight at 4°C with the primary antibodies (1:100; E-cadherin; Abcam; ab1416, 1:100; Vimentin; Abcam; ab92547) and treated with the fluorescence-conjugated secondary antibodies (1:1000; Alexa Fluor 488 and 555) for 2 h at room temperature in the dark. The cells were washed 3 times with PBS for 10 min each after every step, and the nuclei were stained with DAPI (1:1000; Invitrogen, D1306). Cells were mounted on the coverslip with ProLong Gold antifade reagent (Invitrogen Life Technologies, P36934) and observed with a confocal microscope (Carl Zeiss, LSM800).

5.2.16 *Cell viability assay*

BV-2, EOC-20, and WI-38 cells were seeded at 5,000 cells/well and RPMI 8226 cells were seeded at 10,000 cells/well in 96-well plates. Following overnight incubation, cells were treated with carfilzomib, ONX0914 or YU102 at indicated concentrations for 72 h. Cell viability was determined by CellTiter 96 AQueous One Solution Cell Proliferation assay (Promega) following manufacturer's protocol. Absorbance at 490 nm was measured using a SpectraMax M5 microplate reader (Molecular Devices).

5.2.17 *Statistics*

Results are expressed as means $\pm$ S.D. Statistical significance of the observed group differences was determined using Student's t-test or two-way ANOVA followed by

Dunnette's post hoc test. Significance was set at $p < 0.05$ for all tests. All statistical analyses were carried out using GraphPad Prism 8.0.1 (GraphPad Software).

5.3   Results

5.3.1   *YU102 improves cognitive function in an LPS-induced mouse model of neuroinflammation*

Since previous data suggested an increase in iP gene expression during aging and in plaque-associated glia cells in APP/PS1 mice we examined the impacts of proteasome inhibition on cognitive impairments using several subunit-selective proteasome inhibitors [240] (Figure 5.1A). We first ensured that cP or iP selective inhibitors displayed the expected inhibitory profile by conducting proteasome activity assays with subunit-selective fluorogenic substrates in purified human 20S constitutive and immunoproteasomes (Figure 5.1B). We set out to examine whether inhibition of IP activity might reduce or eliminate cognitive impairments caused by AD. For an initial assessment, we chose to use a lipopolysaccharide (LPS)-induced inflammation mouse model, known to display AD-like cognitive impairment [297, 298]. Specifically, 8-week old ICR mice were treated with daily injections of LPS for 5 days (250 µg/day), followed by i.p. delivery of iP-selective YU102 (10 mg/kg), PR-924 (10 mg/kg), CP-selective PR-825 (2 mg/kg) or conventional PIs (carfilzomib 5mg/kg, bortezomib 1 mg/kg) twice a week for 3 weeks. At the end of treatment period, the Morris water maze test was performed to evaluate cognitive functioning in mice. All mice were trained three times on the same day prior to daily measurements of escape latency and distance traveled over 5 consecutive days. Of note, none of the tested mice displayed any irregularity in their motility. Unfortunately, almost all the mice treated with general PIs (carfilzomib, bortezomib; inhibit both CP and IP) did not survive to complete the test. In contrast, the mice

treated with YU102 displayed no signs of overt toxicity and exhibited improved distance and escape latency compared to mice treated with LPS alone. Mice treated with PR-825 (X-selective) or PR-924 (LMP7-selective) displayed only mild improvement in performance relative to LPS-treated control mice (Figure 5.2 A&B). Next, we conducted probe trials to measure the ability of memory. As shown in Figure 5.2C, YU102-treated group displayed the better performance, spending longer time in the target quadrant compared to the control groups. One day after the probe tests, we performed the passive avoidance assay by measuring an average step-through latency of YU102-treated group or control groups (vehicle only or LPS treated group) (Figure 5.3). Consistent with previous the Morris water maze assay data, YU102 treated group showed the improved performance compared to LPS-treated group. This result was intriguing in that LMP2 inhibition through pharmacological inhibition or genetic knockout of LMP2 previously showed no effect on proinflammatory cytokine release from LPS-stimulated human PBMCs or mouse peritoneal macrophages [56, 294]. Taken together, we suggested that IP inhibition, especially LMP2 inhibition could improve cognitive impairment caused by a LPS-induced neuroinflammation.

A

YU102

YU102 Epimer

IPSI (PR-924)

PR-825

B
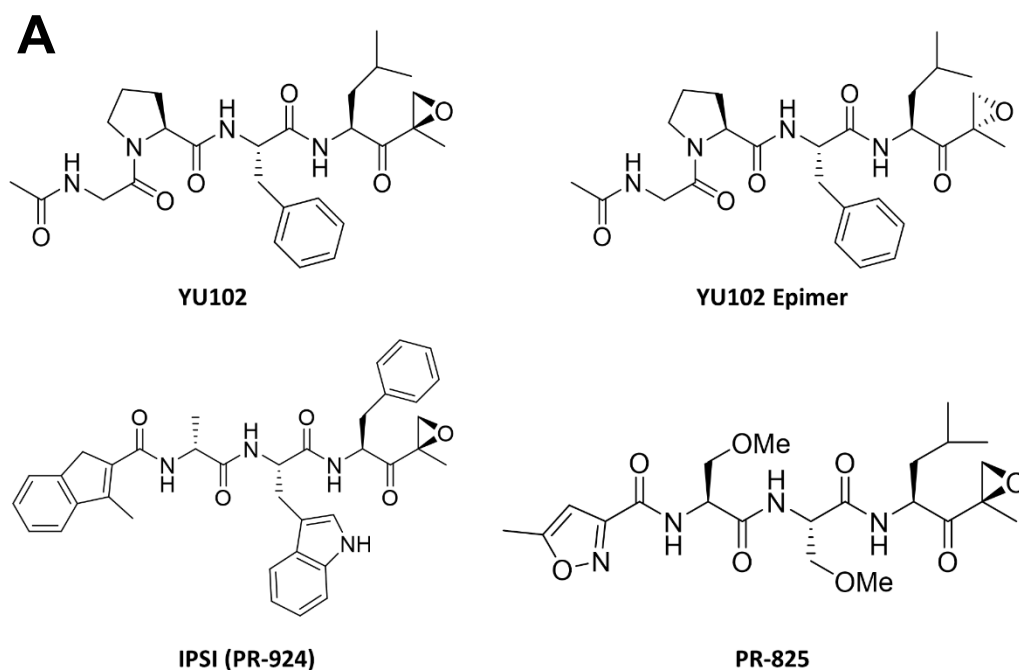
Proteasome Inhibitor	IC$_{50}$ (nM)			
	LMP2/β1i	Y/β1	X/β5	LMP7/β5i
YU102	105.2 ± 28.6	206.7 ± 173.3	>10,000	>10,000
YU102 epi	>10,000	>10,000	>10,000	>10,000
PR-924	3500[a]	>10,000[a]	227[a]	2.5[a]
PR-825	~150[b]	~1500[b]	17 ± 10[c]	238 ± 114[c]

Figure 5.1 Structures and Proteasome inhibitory activity of PIs

A. structures of immunoproteasome inhibitors (YU102, PR-924), YU102 epimer (an inactive stereoisomer of YU102), and constitutive proteasome inhibitor (PR-825) are shown. **B.** Proteasome inhibitory activity profiles of YU102, YU102 epimer, PR-924, and PR-825 in human purified 20S proteasome are shown. Data is shown as mean ± SD derived from a non-linear regression based on n=3 replicates per compound per concentration. [a]IC$_{50}$ values were determined from competition assays in Raji cell lysates [84]. [b]IC$_{50}$ values were approximated from ProCISE assay using A20 murine lymphoma cells [52]. [c]IC$_{50}$ values were from ProCISE ELISA using MOLT-4 human leukemia cells [332].
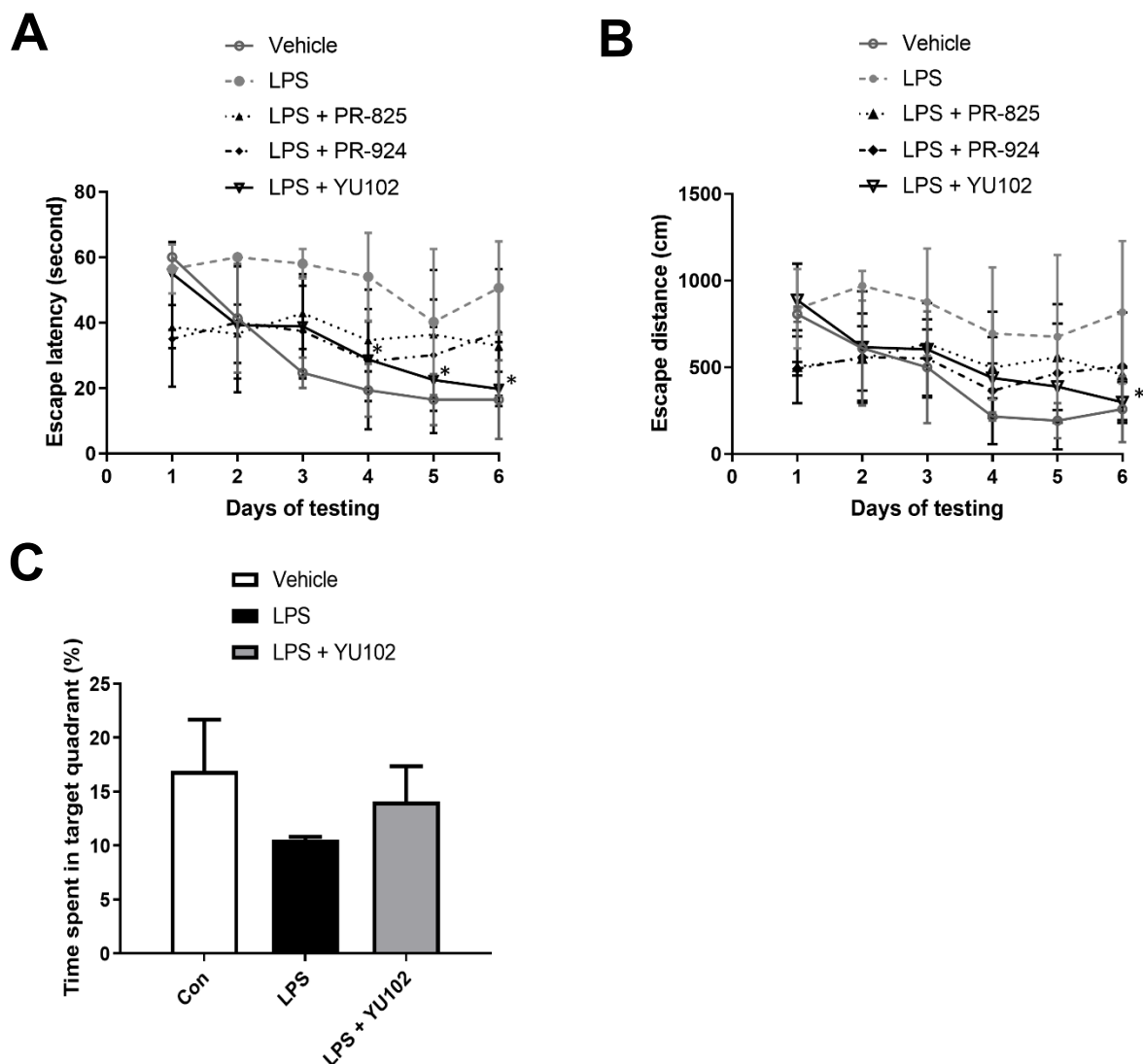
Figure 5.2 The Morris water maze tests in LPS-induced mouse model

YU102 (10mg/Kg), PR-924 (10mg/kg), PR-825 (2mg/kg), carfilzomib (5mg/kg) and bortezomib (1mg/kg) were treated in LPS-induced mouse model. Mice treated carfilzomib or bortezomib could not survive. Escape latency time in the target quadrant (**A**) and escape distance (**B**) of the mice were shown. Statistical analysis was performed via two-way ANOVA. *Differences in escape latency on days 4-6 and distance on day 6 between LPS-treated and YU102 treated were statistically significant (p-value < 0.05, n=5). **C.** Tg2576 mice were evaluated in the probe trial. (This experiment was performed by In Jun Yeo from Dr. Jin Tae Hong's group in the college of Pharmacy, Chungbuk National University, Korea)
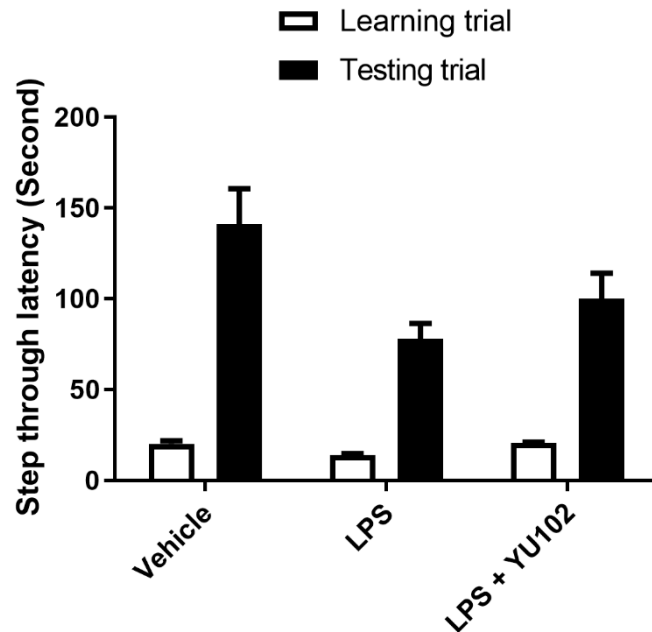
Figure 5.3 The passive avoidance test in LPS-induced mouse model

One day after the probe trials, LPS-induced mice were evaluated in passive avoidance test among vehicle only, LPS-injected (250 µg/day, for 5days), or LPS injected and then YU102-treated group (10mg/kg, twice a week for 3 weeks). (This experiment was performed by In Jun Yeo from Dr. Jin Tae Hong's group in the college of Pharmacy, Chungbuk National University, Korea)

5.3.2 *YU102 ameliorates AD-related cognitive impairment in the Tg2576 mouse model*

Encouraged by our initial assessment showing the promising activity of YU102 in a mouse model of LPS-induced inflammation (Figures 5.2 and 5.3), we wanted to further verify its efficacy using a more relevant animal model of AD. To this end, we chose the APP transgenic mouse model (also known as Tg2576), which exhibit age-associated deficits in learning and memory with Aβ deposits as a result of expression of KM670/671NL mutant human APP. To demonstrate target engagement and specificity of YU102, an inactive stereoisomer of YU102 (YU102 epi, a negative control) were also included. First, 10-month old APPsw mice (Tg2576 mice) were treated with YU102 via the intraperitoneal (i.p.) twice a week for 3 weeks and then the Morris water maze test was performed, followed by a single probe trial 24 hours later o and passive avoidance test to investigate the impacts of YU102 treatment on spatial learning and memory in a Tg2576 mouse model. Specifically, all mice were trained for three times for 5 days before behavior investigation. Initially, escape latency and distance traveled were measured on a daily-basis over a 5-day period. Remarkably, as shown in Figure 5.4, consistent with the results obtained from the LPS-induced inflammation model, mice treated with YU-102 exhibited significantly shorter distance and escape latency than those treated with inactive YU102 epi or vehicle (Figure 5.4 A & B). This strongly supports that the efficacy of YU102 is mediated through LMP2 inhibition. One day after the Morris water maze test, we next measured the ability of mouse to maintain memory on probe trials. In line with the results from the water maze tests, YU102-treated mice performed significantly better than control groups: the percentage of time spent in the target quadrant was 21.25 ± 2.71% for YU102-treated group and ∼10-14.50 ± 1.03% for control groups (Figure 5.4C). Sequentially, a step-through latency test was performed a day after the probe trial. While Tg2565-vehicle treated group showed an average step-through latency of ∼44 sec, YU102-treated group had ∼128 sec, displaying considerably improved fear-

associated short-term memory, suggesting LMP2 activity improves cognitive function in Tg2576 mice (Figure 5.5).
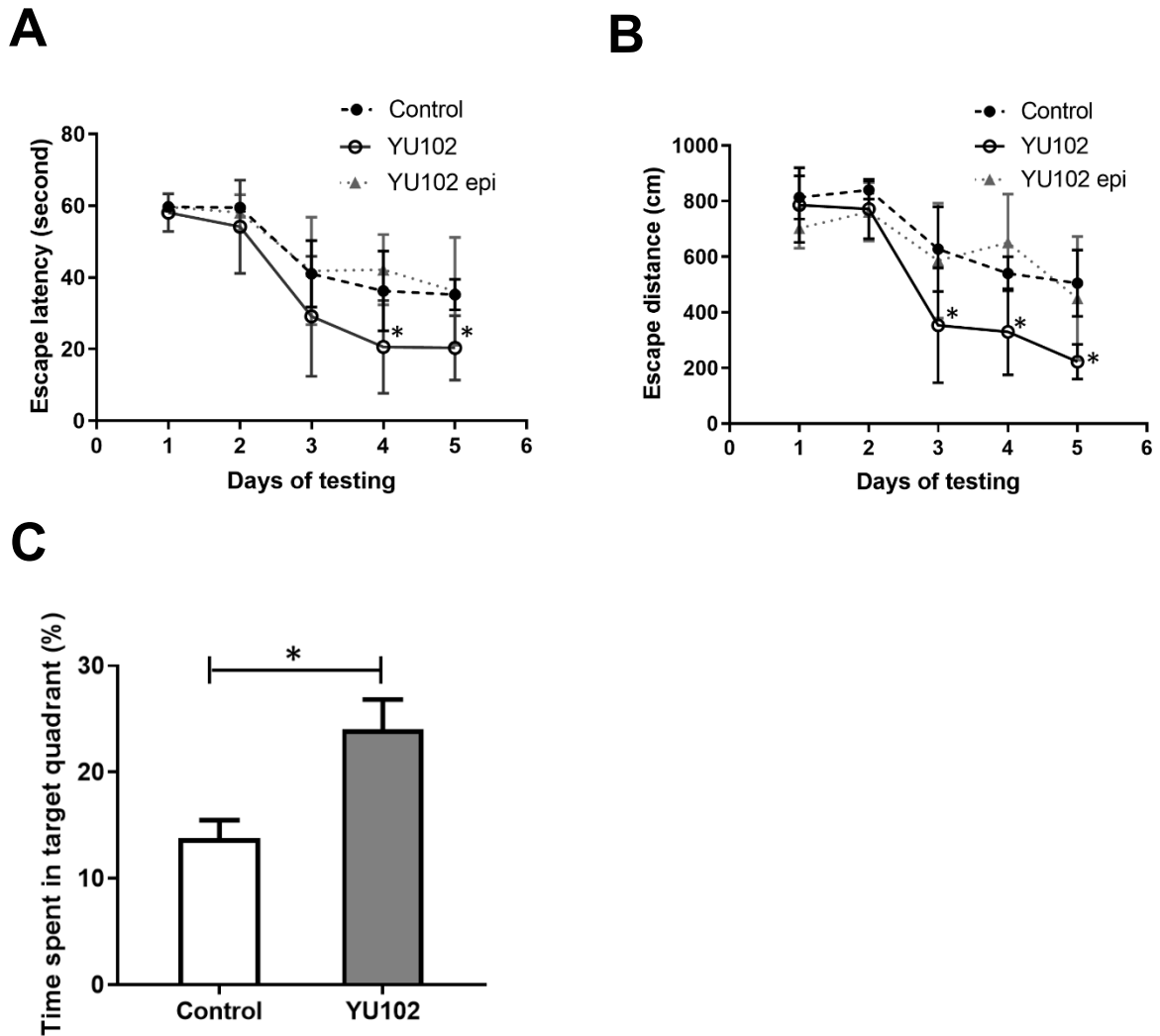
Figure 5.4 The Morris water maze tests in Tg2565 mice

YU102 ameliorates cognitive deficits in Tg2576 mice. Escape latency time in the target quadrant (A) and escape distance (B) were shown. Statistical analysis was performed via two-way ANOVA. *Difference in escape latency on days 4-5 or distance on days 3-5 between control and YU102-treated mice was statistically significant (p-value < 0.05, n=8). C. Upon the completion of the Morris water maze test, Tg2576 mice were evaluated in the probe trial. Statistical analysis for probe trial was performed via Student-t test. Differences in time spent in target quadrant between control and YU102-treated mice were statistically significant (p-value < 0.05, n=8) (This experiment was performed by In Jun Yeo from Dr. Jin Tae Hong's group in the college of Pharmacy, Chungbuk National University, Korea)

119
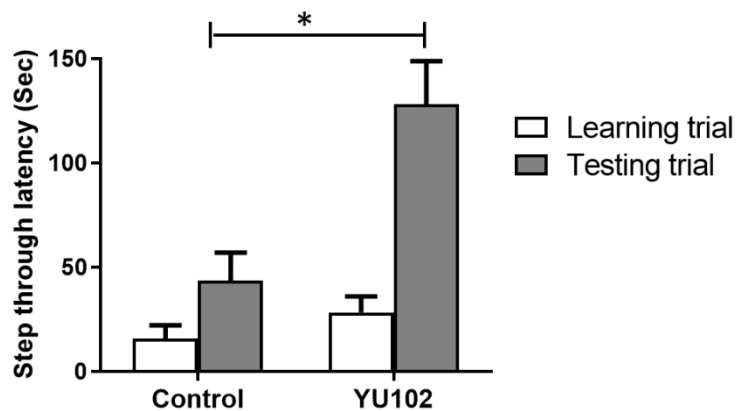
Figure 5.5 The passive avoidance test in Tg2576 mice

One day after the probe trials, Tg2565 mice were evaluated in passive avoidance test between vehicle only and YU102-treated group (10mg/kg, twice a week for 3 weeks). Statistical analysis for passive avoidance was performed via Student-t test. Difference in step through latency between control and YU102-treated mice were statistically significant (p-value < 0.05, n=8) (This experiment was performed by In Jun Yeo from Dr. Jin Tae Hong's group in the college of Pharmacy, Chungbuk National University, Korea)

5.3.3 *YU102 selectively inhibits LMP2 activity in the Tg2576 mouse model*

After behavioral testing, mice were sacrificed and proteasome activities in different organ tissues were measured to examine target engagement and specificity of YU102 by measuring the remaining LMP2 activity in mice. As shown in Figure 5.6, YU102 inhibited LMP2 but not Y or LMP7/X-associated proteasome activity (measured as the CT-L activity). This target engagement investigation was possible due to the irreversible covalent binding of YU102 to LMP2. It should be also noted that the family of peptide α,β-epoxyketones such as YU102 have been shown to be highly selective for the proteasome with no significant off-targets reported so far 44-48. As such, we expect that YU102 will likely have no major off-target interactions. The relatively modest LMP2 inhibition observed in monitored tissues is likely due to the synthesis of new proteasome catalytic subunits during the gap between the final YU102 treatment and sacrifice. Taken together, the results support that selective inhibition of LMP2 activity improves cognitive function in the APP transgenic mouse model of AD.
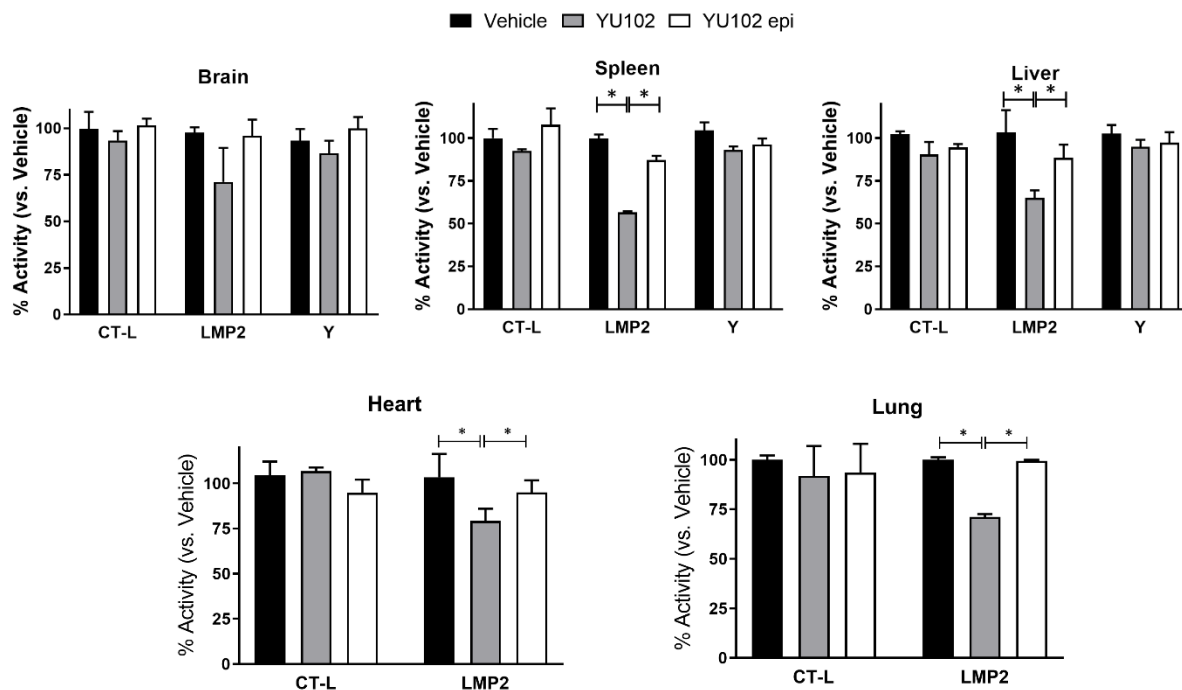
Figure 5.6 The proteasome activities in organ tissues collected from Tg2565 mice

Upon the completion of the behavior test, proteasome activities in heart and lung collected from Tg2576 mice treated with vehicle, YU102 (10 mg/kg), or YU102 epimer (10 mg/kg) were measured using fluorogenic substrates. Error bars are standard deviation derived from three technical replicates. *Differences in LMP2 inhibitory activity in spleen, liver, heart, and lung tissues between YU102-treated and YU102 epi-treated group were statistically significant ($p\text{-value} < 0.05$, $n=3$).

5.3.4   *YU102 exerts its efficacy independently of Aβ deposition*

Given the data showing improved learning and memory of LMP2 inhibitor-treated mouse models of AD, we initially suspected that YU102 exert their activity by promoting Aβ clearance in the brain of Tg2576 mice via an undefined mechanism. To examine such a possibility, we measured the levels of soluble Aβ in hippocampal tissues isolated from the brain of Tg2576 mice using an enzyme-linked immunosorbent assay (ELISA) and levels of amyloid fibrils were measured via the fluorescent dye Thioflavin T. Interestingly, we observed no difference in Aβ deposition between the mice treated with YU102 and vehicle-treated mice (Figure 5.7 A & B). The results can be cautiously interpreted that YU102 may exert its anti-AD efficacy in the Tg2576 model independently of Aβ deposition or clearance. This result is highly intriguing considering that several drugs with proven Aβ-clearing ability have failed to demonstrate clinically meaningful efficacy in recent high-profile phase 3 clinical trials [171].
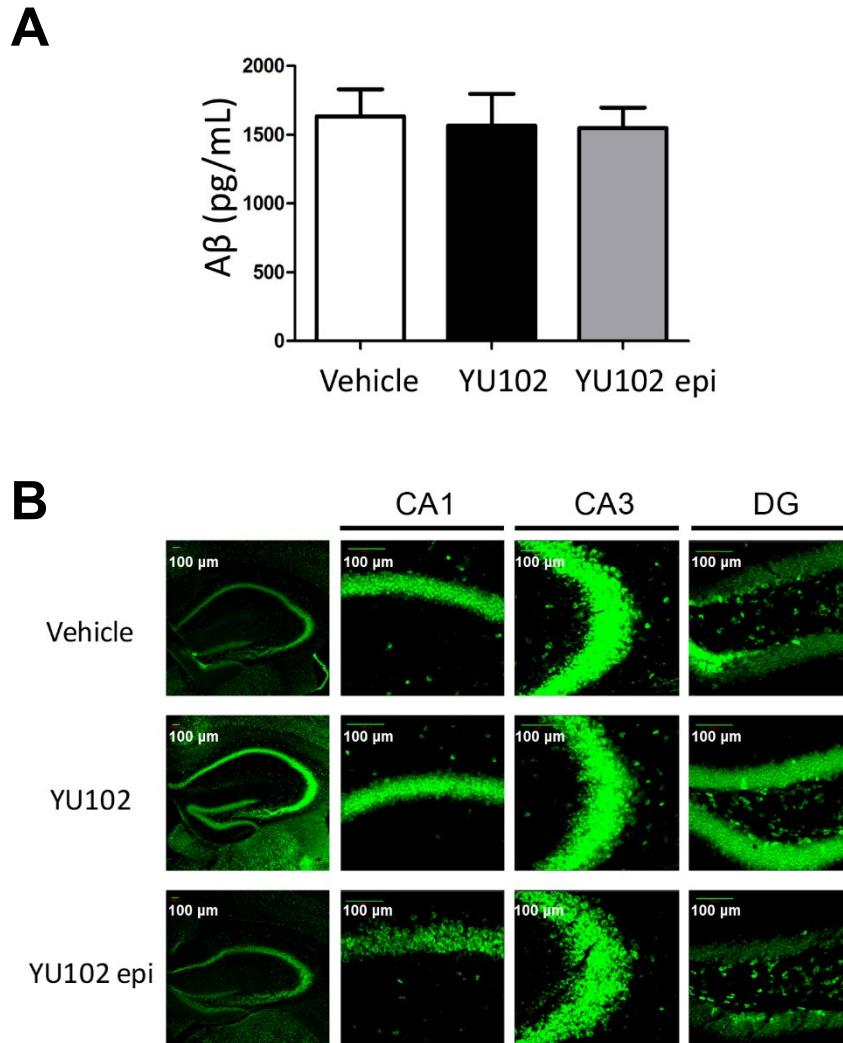
Figure 5.7 Efficacy of YU102 in Tg2576 mice on Aβ deposition

A. ELISA-based quantification of $A\beta_{1\text{-}42}$ in hippocampal tissues isolated from Tg2576 mice. The difference in the levels of $A\beta_{1\text{-}42}$ between vehicle control and YU102-treated mice was not statistically significant (p-value > 0.1, n=3). Statistical analysis of ELISA results was performed via Student t-test. **B.** Thioflavin T staining of Aβ fibrils in hippocampal tissue sections from Tg2576 mice. (This experiment was performed by In Jun Yeo from Dr. Jin Tae Hong's group in the college of Pharmacy, Chungbuk National University, Korea)

5.3.5 *Efficacy of YU102 is unrelated to tau or neuroprotection*

5.3.5.1 *Effect of YU102 on Tau aggregation*

Tau polymerization has been considered as one of main culprits behind AD etiology and a potential target for therapeutic intervention [299]. In Tg2576 mice, hyperphosphorylated tau oligomerizes in an age-dependent manner that coincides with the appearance of Aβ oligomers and declining cognitive function [300-304]. Given this, we wondered whether YU102 exerts its anti-AD efficacy by inhibiting the oligomerization of hyperphosphorylated tau. To quickly test this possibility, we used HEK293-tau-BiFC (bimolecular fluorescence complementation) cell-based assay, in which tau oligomerization and aggregation induced by an activator of protein kinase A (PKA) such as forskolin or thapsigargin can be detected via the reconstitution of the fluorescent protein Venus. As shown in Figure 5.8, YU102 did not inhibit thapsigargin or forskolin-induced tau aggregation. Low tau-BiFC intensity observed at high concentration of LMP2 inhibitors (30-100µM) were due to cell death. Taken together, these results demonstrate that the YU102-induced improvement in cognitive behavior in Tg2576 mice is independent of Aβ deposition and tau aggregation.

5.3.5.2 *Effect of YU102 on neuroprotection*

Since accumulation of misfolded proteins such as Aβ in cells induces immune response and cell death, we next tested whether YU102 has neuroprotective effects in Tg2576 mice. To examine this, we performed Cresyl violet staining experiments on neuronal tissues isolated from the brains of Tg2576 mice. We found no noticeable difference in the total number of neurons between mouse groups treated with YU102, YU102 epi, or vehicle (Figure 5.9). Although we found no evidence that YU102 affects neuron survival, these results could also be affected by the relatively short drug treatment period (~3 weeks).
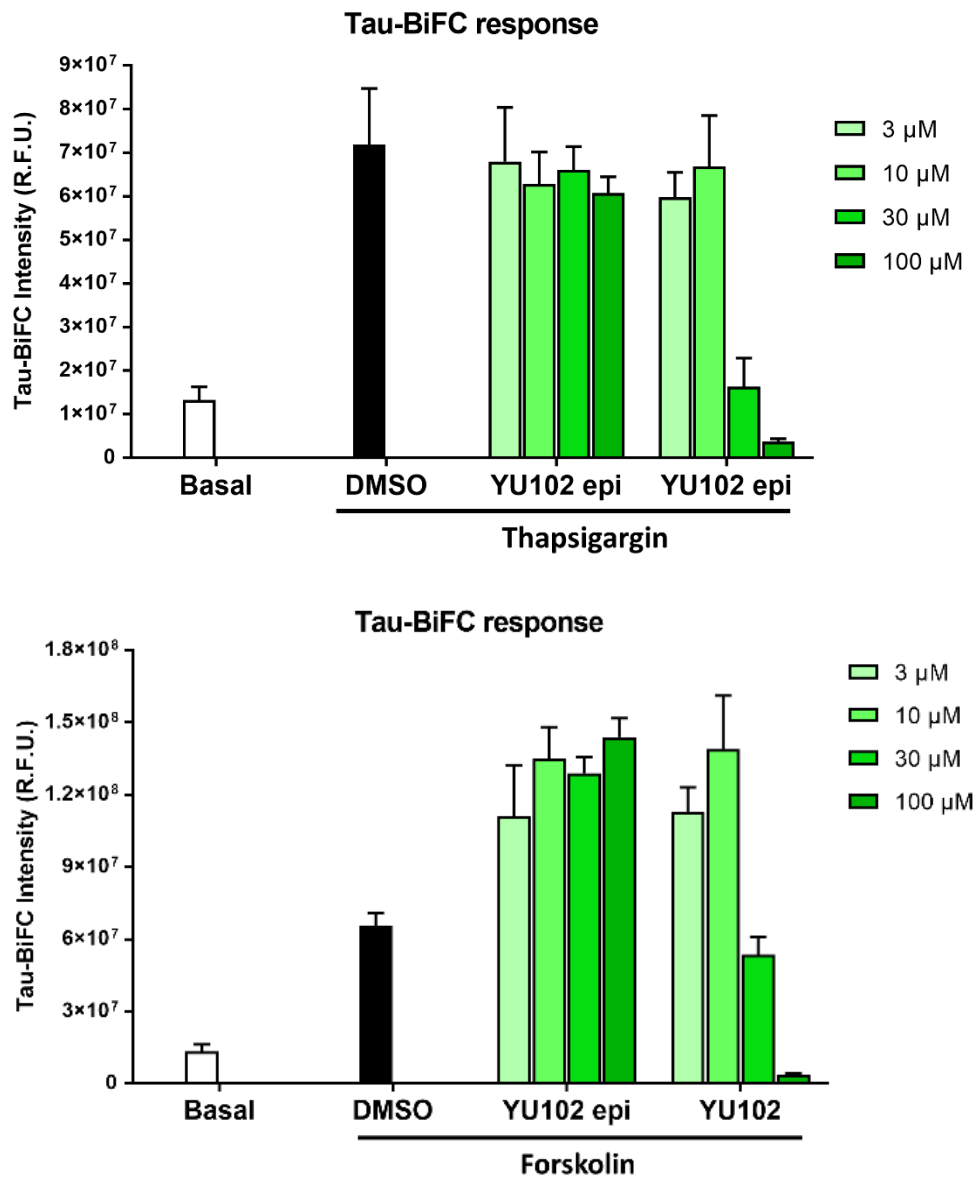
Figure 5.8 Efficacy of YU102 in Tg2576 mice on tau aggregation

YU102 has no effect on tau aggregation. Thapsigargin (1μM) or forskolin (1μM) induces tau aggregation in tau-BiFC cells, activating a tau BiFC fluorescence signal that can be detected. (This experiment was performed by Hyun Jung Jeong from Dr. Yun Kyung Kim at KIST, Korea.)
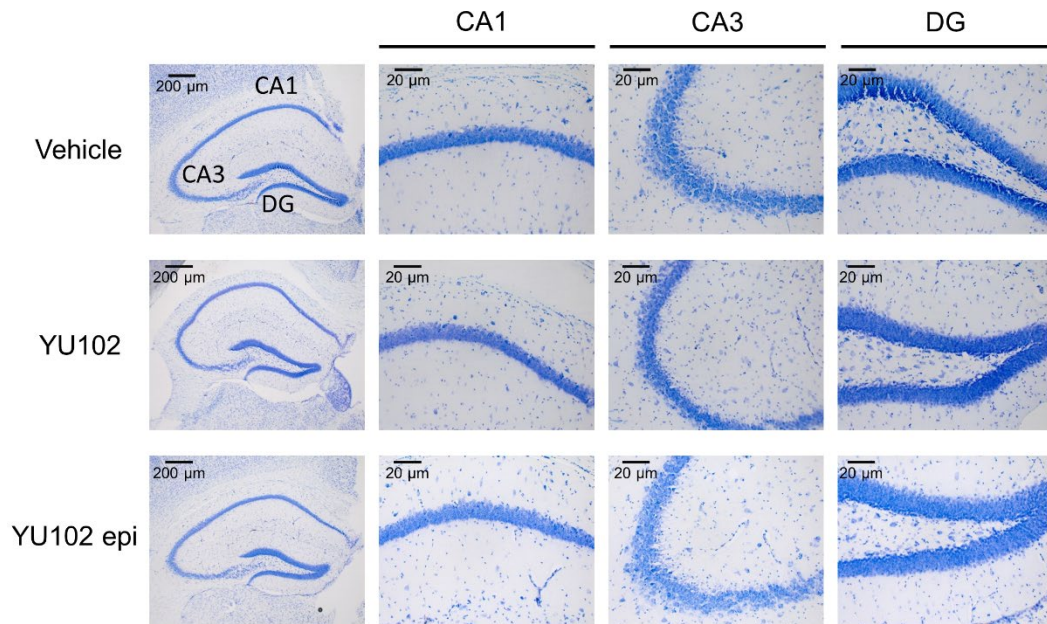
Figure 5.9 Efficacy of YU102 in Tg2576 mice on neuroprotection

YU102 displays no neuroprotective effects during the experimental period. Hippocampal tissues isolated from the brains of Tg2576 mice were stained with Cresyl violet, a marker for Nissl substance in neurons. (This experiment was performed by In Jun Yeo from Dr. Jin Tae Hong's group in the college of Pharmacy, Chungbuk National University, Korea.)

5.3.6   *YU102 reduces the number of reactive astrocytes and microglia in Tg2576 mice*

Neuroinflammation is reported to be closely linked to the development and progression of AD and inflammation in the brain is characterized by the activation of neuroglia cells (microglia and astrocytes), which was considered as a major culprit behind AD pathology and a key drug target in neurodegenerative diseases [249, 305-307]. Also, Aβ and LPS have been shown to distinctly alter cytokine production profiles and induce innate immune signaling and microglial activation [308-311]. Therefore, we set out to investigate whether YU102 blocks the activation of glial cells in brain tissues of Tg2576 mice. When immunostaining for GFAP and Iba1, known markers of reactive astrocytes and microglia, respectively, was performed, we observed that the numbers of positively stained cells in hippocampal tissues were significantly fewer in mice treated with YU102 than in the control group (Figure 5.10A). COX-2 also known as a proinflammatory enzyme is overexpressed in human AD and mouse AD models [312-314]. As shown in Figure 5.10B, expression of COX-2 was also significantly lower in hippocampal tissues of mice treated with YU102 compared to control mice. Taken together, these data suggest that LMP2 is involved in the activation of glia cells and that LMP2 inhibition suppresses activation of astrocytes and microglia and thus suppresses neuroinflammation.
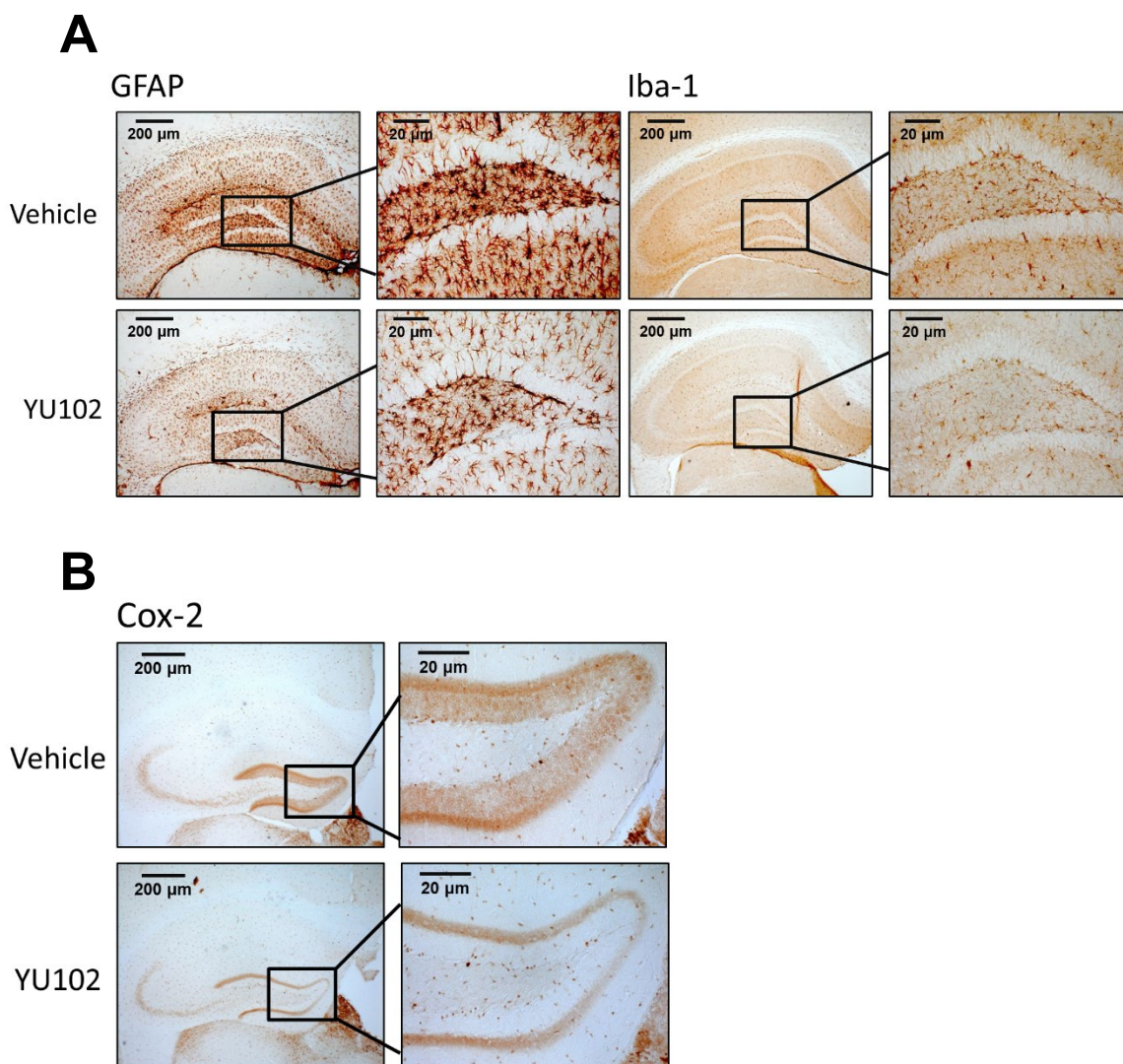
Figure 5.10 YU102 reduces the numbers of activated astrocytes and microglia
A. Reactive astrocytes (left) and microglial cells (right) were visualized using respective markers (GFAP and Iba1) in hippocampal tissues from Tg2576 mice. **B.** Expression levels of COX-2 in hippocampal tissues in Tg2576 mice treated with YU102 are lower than in the control Tg2576 mice. (This experiment was performed by In Jun Yeo from Dr. Jin Tae Hong's group in the college of Pharmacy, Chungbuk National University, Korea)

5.3.7 *LMP2 inhibition attenuates pro-inflammatory cytokine production in microglial*
       cells

5.3.7.1 *Membrane-based cytokine array*

It is well-documented that activated microglia synthesize and release pro-inflammatory cytokines and play an important role in AD progression. Furthermore, secretion of pro-inflammatory cytokines by microglia and associated changes in phagocytic and neuroprotective properties are a major contributing factor to the recently recognized "cellular" phase of Alzheimer's disease [315, 316]. Since YU102 reduced the number of activated microglia cells in Tg2576 mice, we suspected that it could exert their anti-AD efficacy by suppressing pro-inflammatory cytokine production. Therefore, we examined whether YU102 can suppress the production of pro-inflammatory cytokines in microglial cells. To do this, we used an immortalized murine microglial cell line BV-2, commonly used as a substitute for primary microglia in many experimental settings [317]. BV-2 cells were pre-incubated with YU102 for 2 hr before LPS treatment to upregulate cytokines. After additional 24 hr incubation, cell supernatants were collected and analyzed for the levels of 40 cytokines and chemokines using a membrane-based mouse cytokine antibody array (Figure 5.11A). BV-2 cells treated with LPS only exhibited elevated levels of multiple pro-inflammatory cytokines and chemokines compared to unstimulated cells (Figure 5.11 B & C). As previously reported, ONX 0914, a selective inhibitor of immuno-subunit LMP7, suppressed LPS-induced production of pro-inflammatory cytokines, such as IL-1β, CCL12/MCP-5, IL-6 and CCL5/RANTES [52]. Similarly, YU102 also significantly attenuates production of IL-1α, CCL12/MCP-5, and to a lesser degree, IL-6 which were induced by LPS. The result that YU102, a LMP2 inhibitor, strongly suppressed the production of several proinflammatory cytokines was highly intriguing. Previously, inhibitors of LMP2, such as KZR-504, displayed little to no suppression of cytokine production (e.g. IL-1β, IL-6, IL-8, TNF-α) in human peripheral blood mononuclear cells (PBMCs) [56]. We suspect these contradictory results are due to cell type

130

(organ)-specific role of LMP2, indicating a distinct role of LMP2 in microglia inflammatory response. Altogether, these findings demonstrate that inhibition of LMP2 ameliorates disease in mouse models of AD and may offer a promising strategy for AD treatment.

5.3.7.2 *Enzyme-linked immunosorbent assay (ELISA)*

Since we observed the effect of YU102 on the production of pro-inflammatory cytokines and chemokines in LPS-stimulated BV-2 microglial cells using a mouse cytokine membrane array, we further verified the effect of YU102 on microglia cytokine release in vitro by measuring the levels of individual cytokines in LPS-stimulated BV-2 cells treated with vehicle or YU102 via enzyme-linked immunosorbent assay (ELISA). Consistent with membrane-based cytokine array, as shown in Figure 5.12, LPS-activated BV-2 cells secreted significantly increased amounts of pro-inflammatory cytokines IL-α and IL-6 and mildly upregulated the level of pro-inflammatory chemokine CCL12. Most notably, inhibition of LMP2 by YU102 substantially attenuated the levels of IL-α, IL-6, and CCL12 production. Taken together, our results suggest a specific role for LMP2 in modulating the glial response during LPS-induced neuroinflammation.
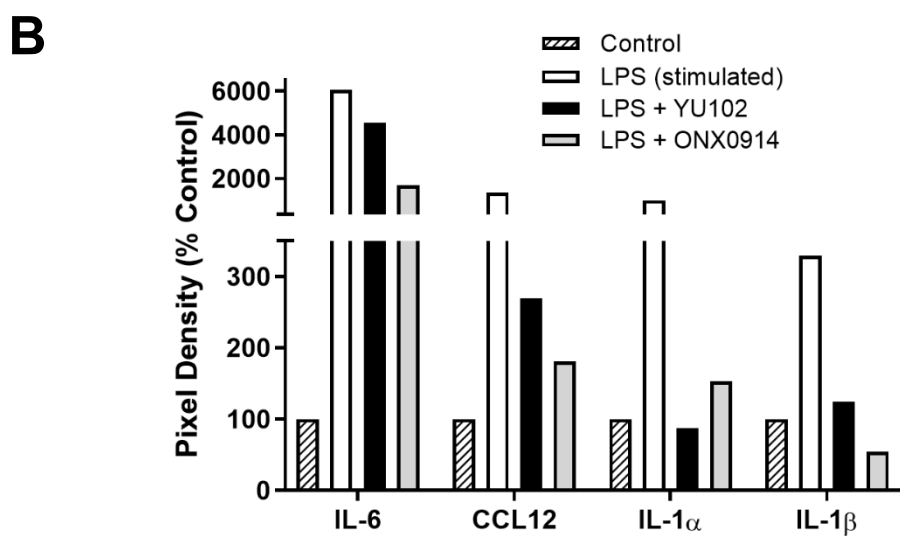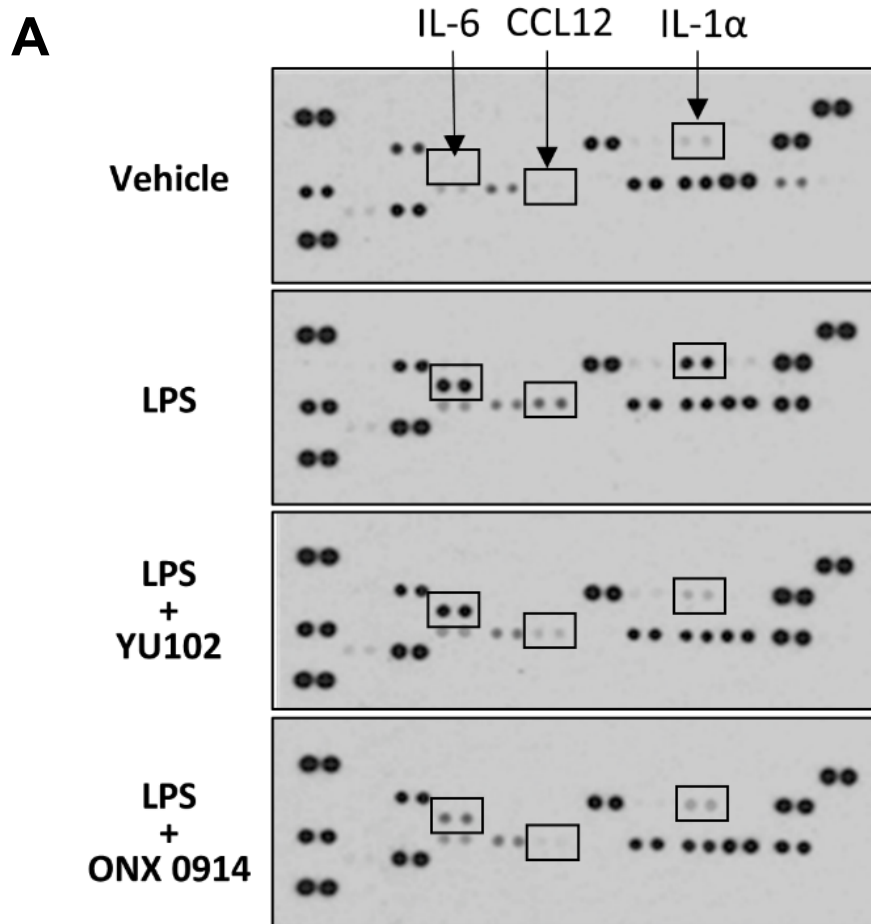
Figure 5.11 Mouse cytokine array in microglial BV-2 cells

C
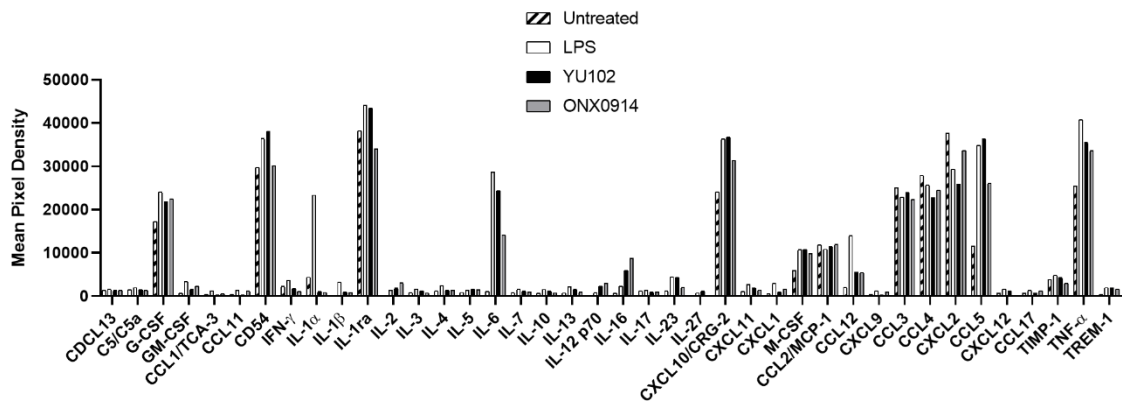
Figure 5.11 Mouse cytokine array in microglial BV-2 cells (continued)

Suppression of cytokine production by YU102 in LPS-stimulated BV-2 cells. **A.** Cytokine and chemokine protein array blots of BV-2 cells treated with vehicle, LPS (1μg/mL) alone, and YU102 (3μM) or ONX0914 (3μM) with LPS (1μg/mL). **B.** The amount of each cytokine or chemokine was relative to the mean of the intensity of corresponding spots from vehicle control sample. Each cytokine or chemokine has duplicate detection spots. Graph depicts the fold change of each cytokine or chemokine (mean). Arrow labels indicate cytokines that are most significantly impacted by YU102. **C.** Full suppression profile of cytokine production by YU102 in LPS-stimulated BV-2 cells using a mouse cytokine array kit (R&D Systems). The amount of each cytokine or chemokine was relative to the mean of the intensity of corresponding spots from vehicle control sample. Each cytokine or chemokine has duplicate detection spots. The graph depicts the mean spot pixel density from the arrays using Quantity One software (Bio-rad) analysis.
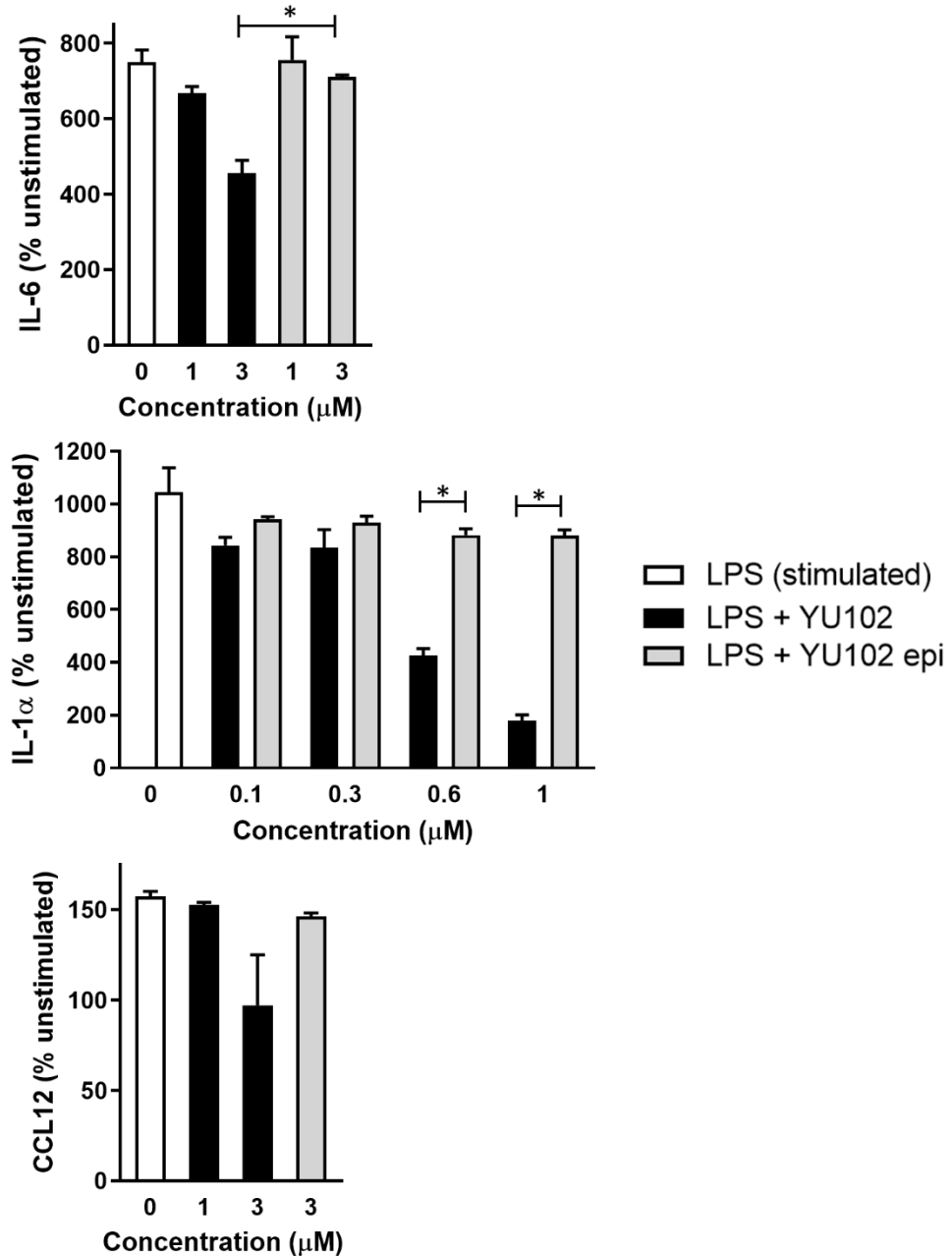
Figure 5.12 Enzyme-linked immunosorbent assay (ELISA) in BV-2 cells

Cytokine production in LPS-stimulated BV-2 cells with and without YU102 was determined by ELISA. Effect of YU102 on the release of cytokines in LPS-stimulated BV-2 cells. BV-2 cells were incubated with LPS (1μg/mL) and YU102 or YU102 epimer for 24 h. All values are expressed as mean ± SEM from three independent experiments. *Differences in suppression of IL-1α and IL-6 levels between YU102-treated and YU102 epi-treated group were statistically significant (p-value < 0.05, n=3).

5.3.8 *YU102 selectively inhibits LMP2 subunit in microglial cells*

In line with selectivity data of YU102 in different organ tissues isolated from Tg2576 mice after behavior test, we confirmed selective LMP2 inhibition by YU102 using microglial cell line model BV-2 cells. First, we conducted proteasome activity assay with subunit-selective fluorogenic substrates in BV-2 cells. YU102 significantly inhibits LMP2 subunit at low concentrations (0.1 and 0.3μM), while ONX0914, a LMP7-selective inhibitor, achieved > 50% inhibition of both LMP2 and LMP7 activity at 0.3μM concentration in BV-2 cells (Figure 5.13A). We next assessed the specificity of YU102 toward the LMP2 subunit by mobility shift assays with western blot to visualize the YU102-LMP2 covalent adduct (Figure 5.13B). For mobility shift assay, where indicated, BV-2 cells were treated with DMSO, 0.1-3μM YU102 or YU102 epimer for 4 h. For competition assay, BV-2 cells were pre-treated with 1μM YU102 for 1 h, prior to the addition of the addition of 0.1-3μM YU102 epimer. The covalent binding of YU102 to LMP2 is shown by a complete upward shift of the LMP2 band in BV-2 cells upon treatment with YU102 compared to YU102 epimer. Conversely, covalent modification of proteasome catalytic subunits LMP7 and X by YU102 was not observed (data now shown). These results clearly showed that YU102 covalently binds LMP2, but not the other catalytic subunits of proteasomes in BV-2 cells, indicating its high specificity toward the LMP2 subunit.
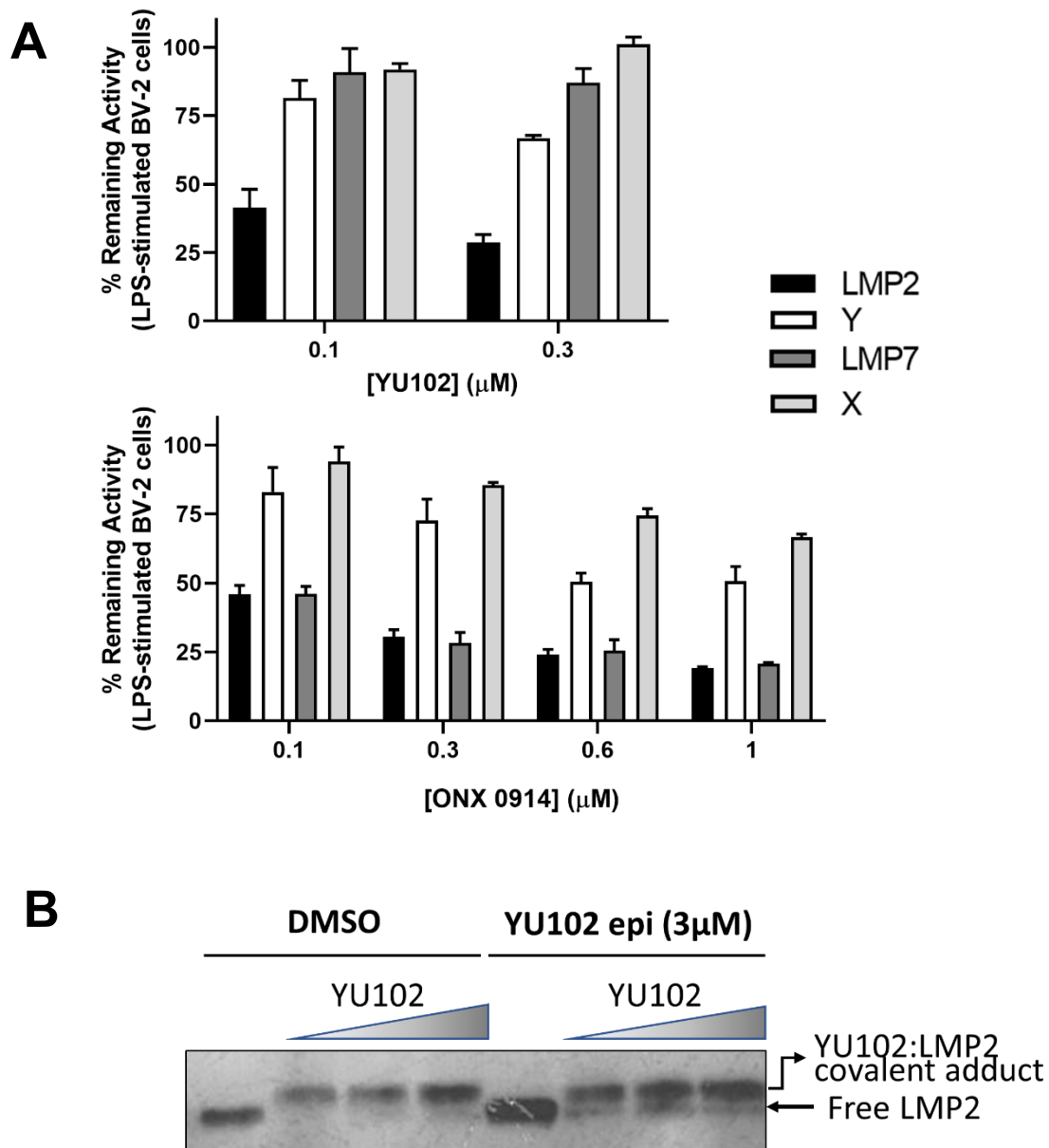
Figure 5.13 Selectivity of YU102 in BV-2 cells

A. Remaining catalytic activities of individual subunits in LPS-stimulated BV-2 cells 4 h after treatment with YU102 (top) or ONX0914 (bottom) at various concentrations. Data are presented as mean ± SEM from three independent experiments. **B.** Visualization of target engagement via immublotting YU102: LMP2 covalent adduct on the SDS-PAGE. BV-2 cells were treated with YU102 for 1 h at 0.3, 1, or 3μM concentrations.

5.3.9 *Broad impacts of YU102 on neuroinflammatory disorders in Tg2576 mice*

Several recent studies demonstrated that Aβ deposits are consistently found in the retina from patients with age-related macular degeneration (AMD) and can be positively correlated with the disease progress [318]. In addition, it has been reported that inflammation triggered by Aβ is a major contributor to RPE (retinal pigment epithelium) abnormalities in APP transgenic animal models including Tg2576 [319-321]. Given this, we investigated the effects of YU102 on RPE degeneration in Tg2576 mice, a characteristic of age-related macular degeneration (AMD) [318]. RPE samples were collected from Tg2576 mice treated with vehicle, YU102, or YU102 epi and subjected to immunohistochemical staining with an anti-β-catenin primary antibody followed by Alexa 555-conjugated secondary antibody. As shown in top, Figure 5.14, the orderly mosaic structure of RPE typically observed in non-transgenic mice was severely damaged in Tg2576 mice treated with vehicle only, as previously reported [322]. However, YU102 provided Tg2576 mice with almost complete protection from RPE damage, showing the typical mosaic structure of RPE (middle, Figure 5.14). In contrast, YU102 epi (an inactive stereoisomer of YU102) provided no protection from RPE mosaic disruption (bottom, Figure 5.14), indicating that YU102 protected the structure integrity of retina from degeneration through LMP2 inhibition.

5.3.10 *The effect of YU102 on human RPE cells degeneration*

In order to further verify *in vivo* observation in Figure 5.13, we conducted *in vitro* studies using the human RPE cell line ARPE-19, known to form a mosaic-like monolayer. Inflammatory stimuli, such as TNF-α, induce epithelial-to-mesenchymal transition (EMT) with concomitant morphological and molecular changes in ARPE-19. Normal ARPE-19 cells maintain the epithelial morphology and show high expression of E-cadherin in cell-cell junction with little expression of Vimentin in the

cytoplasm [323]. However, in response to TNF-α, ARPE-19 cells underwent EMT and exhibited downregulation of E-cadherin and overexpression of Vimentin in the cytoplasm. Notable, when the RPE cells were treated with LMP2 inhibitor, YU102, TNA-α-induced EMT was significantly suppressed through the maintenance of E-cadherin expression and inhibition of Vimentin expression (Figure 5.15). These results suggest suppression of TNF-α-induced inflammatory response. These findings are in line with a previous report that in response to TNF-α, RPE cells isolated from LMP2 knockout mice exhibit diminished NF-κB activation [324]. In summary, the result supports that LMP2 inhibition may control inflammatory response of RPE cells
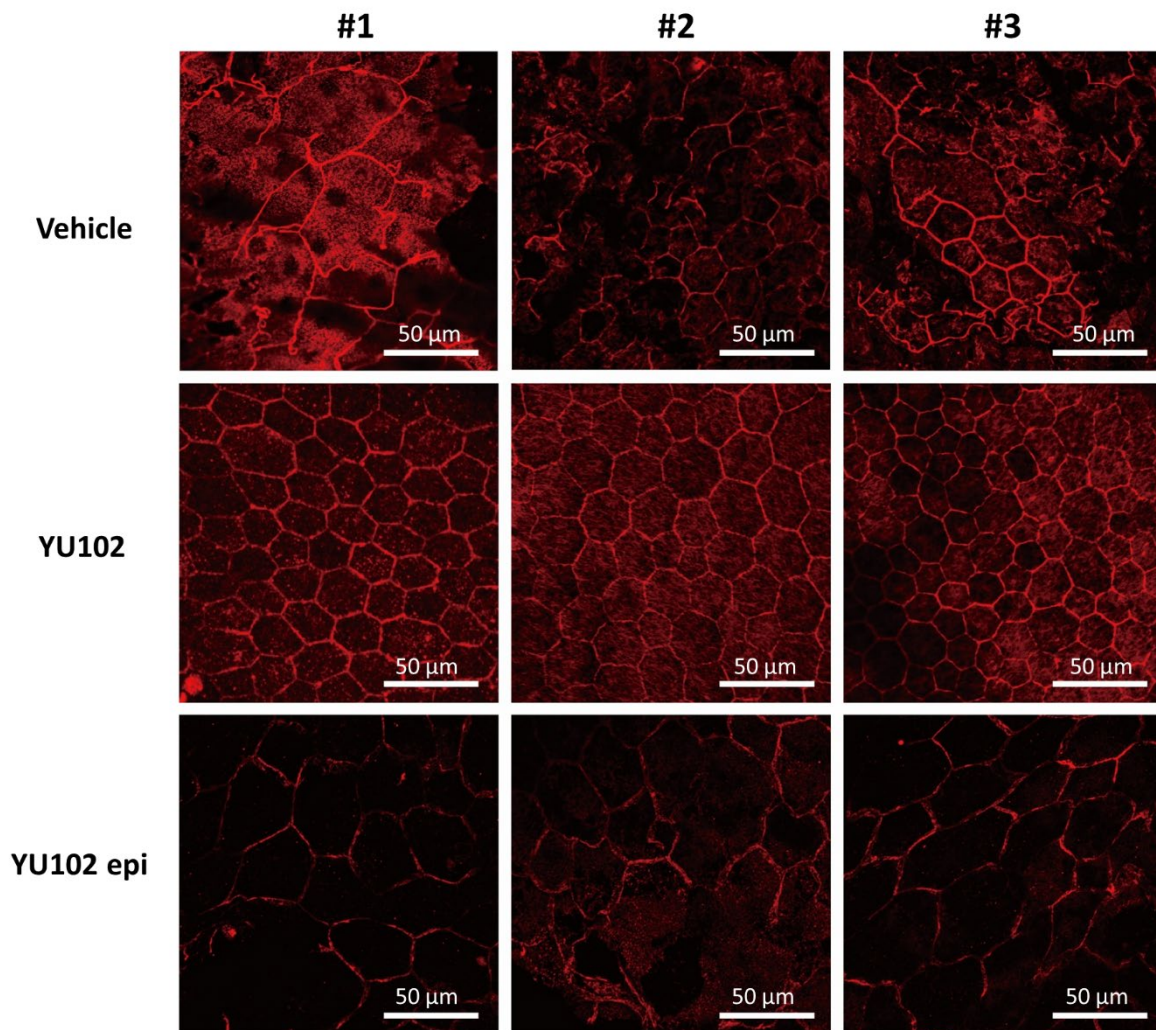
Figure 5.14 Effect of YU102 on *in vivo* RPE degeneration

YU102 inhibits *in vivo* RPE (retinal pigment epithelium) degeneration. RPE from eyes of Tg2576 mice treated with vehicle, YU102 or YU102 epi were isolated and immunostained to establish boundaries of RPE monolayers. (This experiment was performed by Areun Baek from Dr. Dong Eun Kim's group in the department of Bioscience and Biotechnology, Konkuk University, Korea)

| | E-cadherin | Vimentin | Merge |
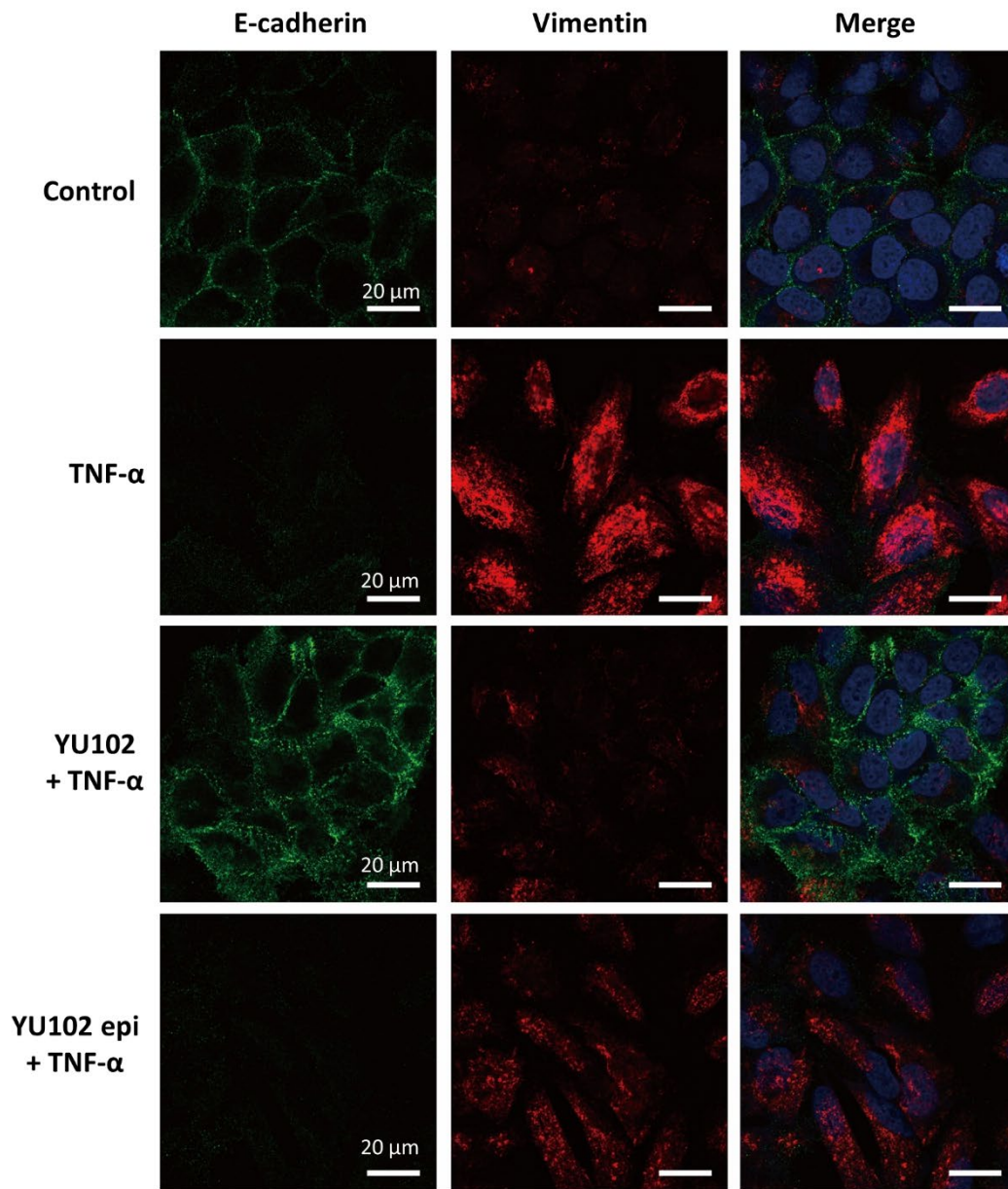
Figure 5.15 Effect of YU102 on *in vitro* RPE degeneration

YU102 inhibits *in vitro* RPE degeneration. EMT in the human RPE cell line ARPE-19 was induced by TNF-α. TNFα-induced EMT in ARPE-19 cells was attenuated by YU102 but not YU102 epimer. EMT is detected by upregulation of vimentin and downregulation of E-cadherin. (This experiment was performed by Areun Baek from Dr. Dong Eun Kim's group in the department of Bioscience and Biotechnology, Konkuk University, Korea)

5.3.11 *YU102 has no cytotoxic effect*

It is critical that LMP2 inhibition leads no major adverse effects in the body for the use of chronic AD therapy. Throughout our *in vivo* efficacy studies of YU102, we observed no signs of overt toxicities in mice treated with YU102. To further verify the non-toxicity of YU102 in cell culture, we incubated a panel of cell lines (WI-38, a human lung fibroblast cell line; RPMI 8266, a human myeloma cell line; BV-2 and EOC-20, two murine microglial cell lines) with YU102, ONX 0914 (an LMP7 inhibitor), or carfilzomib (an FDA-approved inhibitor targeting multiple proteasome subunits including β5 and β5i, a positive control known to induce cell death) for 2-3 days. We then performed cell viability assays using CellTiter 96 AQueous One Solution. YU102 showed no negative impact on the viability of all four cell lines at relevant concentrations (Table 5.1 and Figure 5.16). In comparison, ONX 0914 was much more toxic to these cell lines than YU102 and has a low therapeutic margin. Intriguingly, activation via LPS pretreatment further sensitized the two microglial cell lines (BV-2, and EOC-20 cell lines) to ONX0914, not to YU102, which is in line with previous reports demonstrating near complete cell death in a primary neuron model with 48 hours of 500 nM ONX0914 (Figure 5.16) [325]. Taken together, these results potentially indicate that LMP2 inhibition may offer a safer therapeutic strategy for neurodegenerative diseases than LMP7 inhibition.

Table 5.1 Cytotoxicity of proteasome inhibitors in BV-2, EOC20, RPMI 8226, and WI-38 cells

Inhibitor	Cell viability (IC$_{50}$, nM)			
	BV-2	EOC-20	RPMI8226	WI-38
Carfilzomib	1576.2 ± 300.8	781.1 ± 154.7	8.7 ± 3.1	17.9 ± 5.9
ONX 0914	1,327 ± 374.8	1030 ± 552.3	154.1 ± 23.4	682.7 ± 66.4
YU102	>10,000	>10,000	>10,000	>10,000

Data is shown as mean ± SD derived from a non-linear regression based on n=3 replicates per compound per concentration
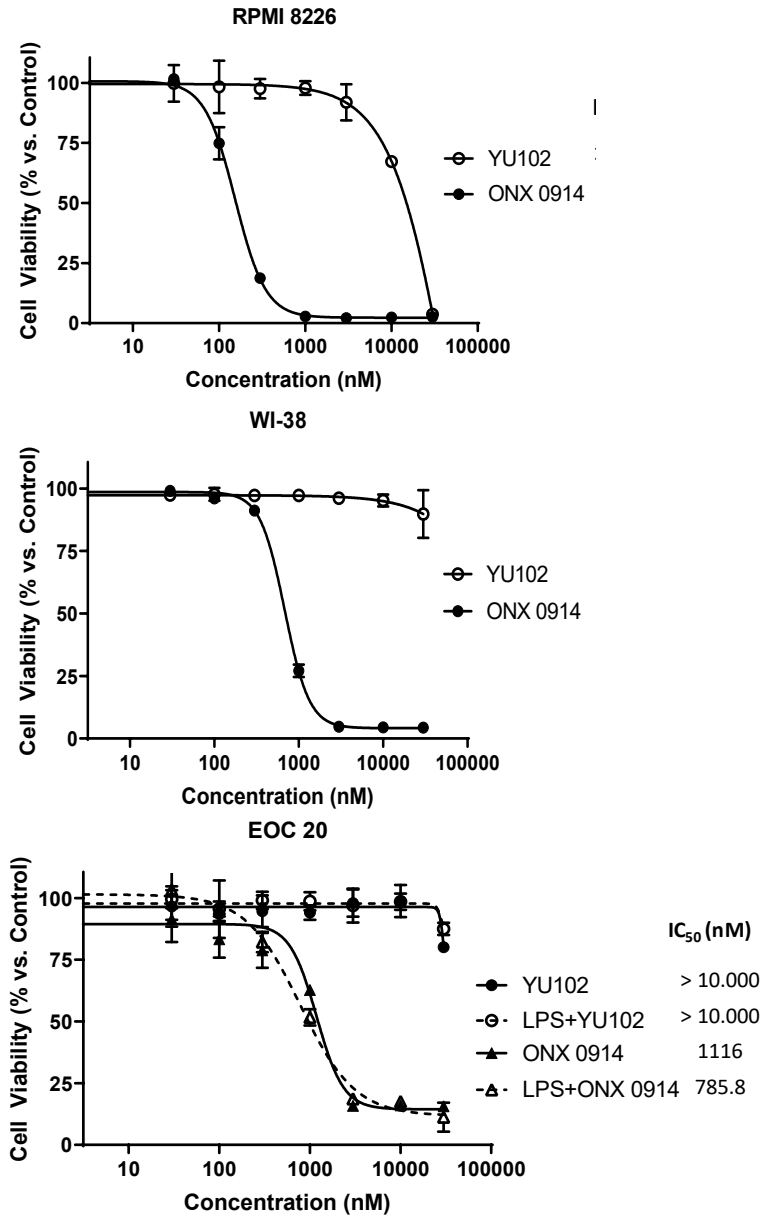
Figure 5.16 Cell viability graphs for YU102, and ONX0914 in various cell lines
EOC-20 and WI-38 cells were seeded at 5,000 cells/well and RPMI 8226 cells were seeded at 10,000 cells/well in 96-well plates. Following overnight incubation, cells were treated with YU102 or ONX0914 at indicated concentrations for 48 h (EOC-20 with or without 24h 1µg/mL LPS pretreatment) or 72 h (RPMI 8266 and WI-38). Cell viability was determined by CellTiter 96 AQueous One Solution Cell Proliferation assay (Promega) following manufacturer's protocol. Absorbance at 490 nm was measured using a SpectraMax M5 microplate reader (Molecular Devices).

5.4 Discussion

Alzheimer's disease is increasing rapidly in frequency as the world's population ages and more people enter the major risk period for this age-related disorder. Current drug treatment for AD patients, essentially symptomatic, is based on three cholinesterase inhibitors (rivastigmine, donepezil and galantamine) and memantine, affecting the glutamatergic system. These drugs do not represent a cure, as they do not arrest the progression of dementia, but rather, they lead to a temporary slowdown in the loss of cognitive. In recent years, several drug candidates (either monoclonal antibodies or small molecules) have been pursued based on the amyloid hypothesis. However, none of these drugs displayed meaningful cognitive improvement in phase III clinical trials, threatening the validity of the amyloid hypothesis. Therefore, new therapies are urgently needed to treat affected patients and to prevent, or improve the symptoms of AD.

In the current study, we report that YU102, inhibiting LMP2 subunit selectively in brain, ameliorates memory dysfunction in Tg2576 independent of Aβ deposition and tau aggregation. In addition, we demonstrated that YU102 blocks activation of astrocytes and microglia in Tg2576 mice and inhibits LMP2 subunit selectively in BV-2 microglia cells with high specificity. We also utilized a mouse cytokine array kit and ELISA assays, measuring the levels of pro-inflammatory cytokines and chemokines response following LPS-induced microglial activation in cells. Our data showed that YU102 suppresses the production of IL-1α, IL-1β, IL-6, and CCL12 in microglial cells, which are important factors involved in the progression of neuroinflammatory disease, indicating LMP2 inhibition can exhibit anti-neuroinflammatory activity in vitro by attenuating the production of pro-inflammatory cytokines and chemokines. This result was particularly surprising given previous reports demonstrating that LMP2-selective inhibitors have no effect on pro-inflammatory cytokine production 25 or NF-kB activation in human PBMCs or cancers [56, 295]. In microglial BV-2 cells, the potent LMP7-selective inhibitor ONX 0914 appears to be nearly as effective in suppressing pro-inflammatory cytokine production as YU102. At the same time, ONX

144

0914 was much more cytotoxic than YU102 in all tested cell lines. Overall, it seems that LMP2 may offer a better therapeutic target than LMP7 for the development of drugs to treat neurodegenerative diseases.

Several studies have shown that Aβ deposition was detected in the retinas, which might be responsible for the pathogenesis of AMD by causing RPE degeneration from different AD transgenic mouse models, resulting in both functional and structural retinal abnormalities [319, 326-330]. In this study, we also observed RPE damage in eyes isolated from Tg2576 mice and found YU102 protected from blocking RPE degeneration. This was further verified by the effect of YU102 on RPE degeneration in human ARPE-19 cells. We found YU102 suppressed TNF-α-induced EMT induction, suggesting YU102 may alter signaling pathways which mediate TNF-α-induced EMT such as TGF-β signaling pathway [331].

In summary, we showed that YU102, a LMP2-selective inhibitor, improves cognitive dysfunctions in AD mouse models without affecting Aβ deposition and tau polymerization. In addition, we found that YU102 suppresses production of pro-inflammatory cytokines in microglial cells, revealing a previously unrecognized role of LMP2 in microglia-mediated innate immune responses. Finally, the present study demonstrated that inhibition of LMP2 possesses anti-neuroinflammatory properties that suppress microglial activation and represents a potential therapeutic target for neuroinflammatory diseases such as AD and AMD.

CHAPTER 6. SUMMARY

Therapeutic agents targeting specific molecular lesions in cancer cells have substantially improved the survival of cancer patients. But, the inevitable emergence of drug-resistance presents a formidable challenge for clinicians. Currently, there are no available strategies in the clinic to combat PI-resistance due to a lack of knowledge regarding the PI response mechanisms. In order to address this problem, extensive effort has been put forth over the last decade toward improving our understanding of the mechanisms responsible for PI resistance. Although several mechanisms of PI resistance have been proposed previously, these mechanisms have not been validated clinically and cannot explain all PI resistance observed. Recently, several studies have shown that UPS-targeting inhibitors including PIs other than Btz retain anticancer activity in Btz-resistant MM cells, indicating that the UPS remains essential in these cells and alternative PIs can overcome Btz resistance. However, mechanistic understanding of intrinsic Cfz resistance is limited due to a lack of suitable cell-based models.

To elucidate intrinsic Cfz resistance in cancer cells, we identified that H727 human bronchial carcinoid cells are inherently resistant to Cfz and utilized this cell line to test our hypothesis. We found that proteasome function remained vital to the survival of Cfz-resistant cancer cells, and that targeting the proteasome using alternative PIs is a good strategy to overcome Cfz resistance. Additionally, results obtained from alterations in the composition of proteasome catalytic subunits in the cell line model showed a potential link may exist between the composition of proteasome catalytic subunits and the cellular response to Cfz. These findings support that proteasome catalytic subunit composition may play a major role in differential responses to PIs among MM patients. Thus, it is crucial to determine composition of proteasome subunits in cancer cells with intrinsic/acquired PI resistance to design a new effective treatment for MM patients who do not respond or have developed resistance to PIs. In addition, this study demonstrates that proteasome inhibition by alternative PIs may still be a valid therapeutic strategy for

patients with relapsed MM after having received treatment with Cfz. Although we believe that cell line model studies provide solid proof of concept evidence for the use of PIs in Cfz-resistant cells, it will be important to validate these findings using clinical samples.

Our studies may provide important insights into the design and further optimization of PIs with improved potency in Cfz-resistant cells. With this in mind, we designed and synthesized novel epoxyketone-based PIs by structural modifications at the P1′ site. We observed that a Cfz analog, harboring a hydroxyl substituent at its P1′ position, was highly cytotoxic against *de novo* or acquired Cfz resistant cell lines. These findings support that peptide epoxyketones incorporating P1′-targeting moieties may have the potential to bypass resistance mechanisms associated with Cfz and to provide additional clinical options for patients resistant to Cfz. Moving forward, further studies regarding the efficacy of peptide epoxyketones incorporating P1′-targeting moieties should be investigated in animal models and ultimately in clinically-relevant primary cells derived from patient who do not respond to PI therapies.

Despite extensive efforts to develop therapies for neurodegenerative diseases such as AD and AMD, effective treatments are not yet available. As such, there is an urgent need to reshape the drug target landscape and develop therapies against these diseases. In recent years, dysregulated immune response in the CNS has garnered increased attention as a target of neurodegenerative diseases. The IP, understood to contribute to and regulate immune response, has only recently become targetable by selective inhibitors. While inhibitors targeting the IP catalytic subunit LMP7 are currently being investigated in preclinical and clinical models of multiple inflammatory diseases, their efficacy in neurodegenerative diseases has never been evaluated. Although the IP found to be highly expressed in microglial cells from AD patients and mouse models, the exact role of IP in AD pathology remains poorly understood to date.

To address the role of IP in AD, we investigated the impact of IP inhibition on cognitive function in AD mouse models and observed that YU102, a selective inhibitor of IP catalytic subunit LMP2, is highly effective in improving cognitive behavior of AD mice without affecting Aβ deposits or tau polymerization, strongly warranting further investigation of LMP2 inhibition in clinical settings as a new strategy for AD therapy. Considering the success of YU102 in improving the treatment of AD, we believe that any effort to identify AD drug candidates will extend from the exciting preliminary results obtained using YU102 to clinical trials. Thus, further medicinal chemistry efforts by our group have been yielding a library of structurally unique and diversified compounds. Our current compound, YU102, is quite promising in terms of the potency in inhibiting LMP2 and acceptable target selectivity. Thus, our optimization effort will focus on improving not just the potency and specificity, but also pharmaceutical properties. We now aim to develop most promising YU102 analogs (acyclic and macrocyclic) based on the potency, target selectivity and chemical stability. In addition, further optimization of YU102 will be necessary to BBB permeability. As well, in vivo efficacy and PK properties will move into the next phases of AD drug development.

REFERENCES

1. De Duve, C., et al., Tissue fractionation studies. 6. Intracellular distribution patterns of enzymes in rat-liver tissue. Biochem J, 1955. **60**(4): p. 604-17.
2. Goldknopf IL, Bumi H. Isopeptide linkage between nonhistone and histone 2A polypeptides of chromosomal conjugate-protein A24. Proc Natl Acad Sci USA. 1977. **74**: p. 864–868.
3. Ciehanover A, Hod Y, Hershko A. A heat-stable polypeptide component of an ATP-dependent proteolytic system from reticulocytes. Biochem Biophys Res Commun. 1978. **81**: p.1100–1105.
4. Hershko A, Ciechanover A, Rose IA. Resolution of the ATP-dependent proteolytic system from reticulocytes: a component that interacts with ATP. Proc Natl Acad Sci USA. 1979. **76**: p.3107– 3110.
5. Hershko A, Ciechanover A, Heller H, Haas AL, Rose IA. Proposed role of ATP in protein breakdown: conjugation of protein with multiple chains of the polypeptide of ATP-dependent proteolysis. Proc Natl Acad Sci USA. 1980. **77**: p.1783–1786.
6. Nobelprize.org. Press Release: The Nobel Prize in Chemistry 2004.
7. Adams, J., Development of the proteasome inhibitor PS-341. Oncologist, 2002. **7**(1): p.9-16.
8. Nandi, D., et al., The ubiquitin-proteasome system. J Biosci, 2006. **31**(1): p. 137 -155.
9. Finley, D., Recognition and processing of ubiquitin-protein conjugates by the proteasome. Annu Rev Biochem, 2009. **78**: p. 477-513.
10. Hershko, A. and A. Ciechanover, The ubiquitin system. Annu Rev Biochem, 1998. **67**: p. 425-79.
11. Huang, X. and V.M. Dixit, Drugging the undruggables: exploring the ubiquitin system for drug development. Cell Res, 2016. **26**(4): p. 484-98.
12. Orlowski M. The multicatalytic proteinase complex, a major extralysosomal proteolytic system. Biochemistry. 1990. **29**(45):10289-10297.
13. He, M., et al., The emerging role of deubiquitinating enzymes in genomic integrity, diseases, and therapeutics. Cell Biosci, 2016. **6**:p. 62.

14. Alonso, V. and P.A. Friedman, Minireview: ubiquitination-regulated G protein-coupled receptor signaling and trafficking. Mol Endocrinol, 2013. **27**(4): p. 558-572.

15. Braun, B.C., et al., The base of the proteasome regulatory particle exhibits chaperone-like activity. Nature Cell Biology, 1999. **1**(4): p. 221-226.

16. Liu, C.-w., et al., Conformational Remodeling of Proteasomal Substrates by PA700, the 19S regulatory Complex of the 26 S Proteasome. Journal of Biological Chemistry, 2002. **277**(30): p. 26815-26820.

17. Verma, R., et al., Role of Rpn11 Metalloprotease in Deubiquitination and Degradation by the 26S Proteasome. Science, 2002. **298**(5593): p. 611-615.

18. Yao, T. and R.E. Cohen, A cryptic protease couples deubiquitination and degradation by the proteasome. Nature, 2002. **419**(6905): p. 403.

19. Śledź, P., et al., Structure of the 26S proteasome with ATP-γS bound provides insights into the mechanism of nucleotide-dependent substrate translocation. Proceedings of the National Academy of Sciences, 2013. **110**(18): p. 7264-7269.

20. Dick, T.P., et al., Contribution of proteasomal beta-subunits to the cleavage of peptide substrates analyzed with yeast mutants. J Biol Chem, 1998. **273**(40): p. 25637-25646.

21. Kruger, E., P.M. Kloetzel, and C. Enenkel, 20S proteasome biogenesis. Biochimie, 2001.**83**(3-4): p. 289-293.

22. Frentzel, S., et al., 20 S proteasomes are assembled via distinct precursor complexes processing of LMP2 and LMP7 proproteins takes place in 13–16 preproteasome complexes. Journal of Molecular Biology, 1994. **236**(4): p. 975-981

23. Chen, P. and M. Hochstrasser, Autocatalytic Subunit Processing Couples Active Site Formation in the 20S Proteasome to Completion of Assembly. Cell, 1996. **86**(6): p. 961-972.

24. Schmidtke, G., et al., Analysis of mammalian 20S proteasome biogenesis: the maturation of beta-subunits is an ordered two-step mechanism involving autocatalysis. The EMBO Journal, 1996. **15**(24): p. 6887-6898.

25. Schmidtke, G., M. Schmidt, and P.M. Kloetzel, Maturation of mammalian 20 S proteasome: purification and characterization of 13 S and 16 S proteasome

precursor complexes. Journal of Molecular Biology, 1997. **268**(1): p. 95-106.

26. Ditzel, L., et al., Conformational constraints for protein self-cleavage in the proteasome. Journal of Molecular Biology, 1998. **279**(5): p. 1187-1191.

27. Kisselev, A.F., et al., The Sizes of Peptides Generated from Protein by Mammalian 26 and 20 S Proteasomes: IMPLICATIONS FOR UNDERSTANDING THE DEGRADATIVE MECHANISM AND ANTIGEN PRESENTATION. Journal of Biological Chemistry, 1999. **274**(6): p. 3363-3371.

28. Cascio, P., et al., 26S proteasomes and immunoproteasomes produce mainly Nextended versions of an antigenic peptide. EMBO Journal, 2001. **20**(10): p. 2357-2366.

29. Saric, T., C.I. Graef, and A.L. Goldberg, Pathway for Degradation of Peptides Generated by Proteasomes: A key role for thimet oligopeptidase and other metallopeptidases. Journal of Biological Chemistry, 2004. **279**(45): p. 46723-46732.

30. Groll, M.; Ditzel, L.; Lowe, J.; Stock, D.; Bochtler, M.; Bartunik, H. D.; Huber, R.: Structure of 20S proteasome from yeast at 2.4 A resolution. Nature 1997. **386**: p. 463-471.

31. Groll, M.; Heinemeyer, W.; Jager, S.; Ullrich, T.; Bochtler, M.; Wolf, D.H.; Huber, R.: The catalytic sites of 20S proteasomes and their role in subunit maturation: a mutational and crystallographic study. Proc. Natl. Acad. Sci. U.S.A. 1999. **96**: p. 10976–10983.

32. Heinemeyer, W.; Fischer, M.; Krimmer, T.; Stachon, U.; Wolf, D.H.: The active sites of the eukaryotic 20 S proteasome and their involvement in subunit precursor processing. J.Biol. Chem. 1997. **272**: p. 25200– 25209.

33. Dick, T.P., et al., Contribution of proteasomal beta-subunits to the cleavage of peptide substrates analyzed with yeast mutants. J Biol Chem, 1998. **273**(40): p. 25637-25646.

34. Huber, E.M., et al., Systematic Analyses of Substrate Preferences of 20S Proteasomes Using Peptidic Epoxyketone Inhibitors. J Am Chem Soc, 2015. **137**(24): p. 7835-7842.

35. Goldberg, A.L., Development of proteasome inhibitors as research tools and cancer drugs. J Cell Biol, 2012. **199**(4): p. 583-588.

36. Brown, M.G., J. Driscoll, and J.J. Monaco, Structural and serological similarity of

MHC-linked LMP and proteasome (multicatalytic proteinase) complexes. Nature, 1991. **353**(6342): p. 355-357.

37. Aki, M., et al., Interferon-gamma induces different subunit organizations and functional diversity of proteasomes. J Biochem (Tokyo), 1994. **115**(2): p. 257-269.

38. Ferrington, D.A. and D.S. Gregerson, Immunoproteasomes: structure, function, and antigen presentation. Prog Mol Biol Transl Sci, 2012. **109**: p. 75-112.

39. Murata, S., et al., Regulation of CD8+ T Cell Development by Thymus-Specific Proteasomes. Science, 2007. **316**(5829): p. 1349-1353.

40. Xing, Y., S.C. Jameson, and K.A. Hogquist, Thymoproteasome subunit-beta5T generates peptide-MHC complexes specialized for positive selection. Proc Natl Acad Sci U S A, 2013. **110**(17): p. 6979-6984.

41. Nitta, T., et al., Thymoproteasome shapes immunocompetent repertoire of CD8+ T cells. Immunity, 2010. **32**(1): p. 29-40.

42. Pickering, A.M., et al., The immunoproteasome, the 20S proteasome and the PA28alphabeta proteasome regulator are oxidative-stress-adaptive proteolytic complexes. Biochem J, 2010. **432**(3): p. 585-594.

43. Toes, R.E., et al., Discrete cleavage motifs of constitutive and immunoproteasomes revealed by quantitative analysis of cleavage products. J Exp Med, 2001. **194**(1): p. 1-12.

44. Dahlmann, B., Role of proteasomes in disease. BMC biochemistry, 2007. **8**(1), p.S3.

45. Seifert U, et al., Immunoproteasomes preserve protein homeostasis upon interferon-induced oxidative stress. Cell. 2010.**142**(4): p. 613-624

46. Ding Q, et al. LMP2 knock-out mice have reduced proteasome activities and increased levels of oxidatively damaged proteins. Antioxid Redox Signal. 2006. **8**:p. 130–135.

47. Ferrington. et el.Immunoproteasome responds to injury in the retina and brain. J Neurochem. 2008. **106**: p. 158–169.

48. Zu, L., et al., Evidence for a role of immunoproteasomes in regulating cardiac muscle mass in diabetic mice. J Mol Cell Cardiol, 2010. **49**(1): p. 5-15.

49. Cai, Z.P., et al., Ischemic preconditioning-induced cardioprotection is lost in mice

with immunoproteasome subunit low molecular mass polypeptide-2 deficiency. FASEB J., 2008. **22**(12): p. 4248-4257.

50. Martin, S., et al., Loss of an individual proteasome subunit alters motor function but not cognitive function or ambulation in mice. Neurosci Lett, 2004. **357**(1): p. 76-78.

51. Wagner LK, et al. Immunoproteasome deficiency alters microglial cytokine response and improves cognitive deficits in Alzheimer's disease-like APPPS1 mice. Acta neuropathologica communications. 2017. **5**(1): p.52.

52. Muchamuel, T. et al. Shwonek, P., Parlati, F., Demo, S. D., Bennett, M. K., Kirk, C. J., and Groettrup, M. A selective inhibitor of the immunoproteasome subunit LMP7 blocks cytokine production and attenuates progression of experimental arthritis, Nat Med 2009. **15**: p. 781-787.

53. Kalim, K. et al. Immunoproteasome subunit LMP7 deficiency and inhibition suppresses Th1 and Th17 but enhances regulatory T cell differentiation, J Immunol 2012. **189**: p. 4182-4193.

54. Sula Karreci, E. et al. Brief treatment with a highly selective immunoproteasome inhibitor promotes long-term cardiac allograft acceptance in mice, Proc Natl Acad Sci U S A 2016. **113**: p. E8425-E8432.

55. Althof, N. et al. The immunoproteasome-specific inhibitor ONX 0914 reverses susceptibility to acute viral myocarditis, EMBO Mol Med 2018. **10**: p. 200-218.

56. Johnson, H. W. B., Anderl, J. L., Bradley, E. K., Bui, J., Jones, J., Arastu-Kapur, S., Kelly, L. M., Lowe, E., Moebius, D. C., Muchamuel, T., Kirk, C., Wang, Z., and McMinn, D. Discovery of Highly Selective Inhibitors of the Immunoproteasome Low Molecular Mass Polypeptide 2 (LMP2) Subunit, ACS Med Chem Lett 2017. **8**: p. 413-417.

57. Basler, M., Dajee, M., Moll, C., Groettrup, M., and Kirk, C. J. Prevention of experimental colitis by a selective inhibitor of the immunoproteasome, J Immunol 2010. **185**: p. 634-641.

58. Hayashi, T., and Faustman, D. NOD mice are defective in proteasome production and activation of NF- kappaB, Mol Cell Biol 1999. **19**: p. 8646-8659.

59. Hayashi, T., and Faustman, D. Essential role of human leukocyte antigen-encoded proteasome subunits in NF-kappaB activation and prevention of tumor necrosis factor-alpha- induced apoptosis, J Biol Chem 2000. **275**: p. 5238-5247.

60. Hensley, S. E., et al. Unexpected role for the immunoproteasome subunit LMP2 in antiviral humoral and innate immune responses, J Immunol 2010. **184**: p. 4115-4122.

61. Vinitsky, A., et al., Inhibition of the chymotrypsin-like activity of the pituitary multicatalytic proteinase complex. Biochemistry, 1992. **31**(39): p. 9421-9428.

62. Adams, J., et al., Potent and selective inhibitors of the proteasome: Dipeptidyl boronic acids. Bioorganic & Medicinal Chemistry Letters, 1998. **8**(4): p. 333-338.

63. Fenteany, G., et al., Inhibition of proteasome activities and subunit-specific amino terminal threonine modification by lactacystin. Science, 1995. **268**(5211): p. 726-731.

64. Ostrowska, H., et al., Lactacystin, a Specific Inhibitor of the Proteasome, Inhibits Human Platelet Lysosomal Cathepsin A-like Enzyme. Biochemical and Biophysical Research Communications, 1997. **234**(3): p. 729-732.

65. Granot, Z., et al., Turnover of Mitochondrial Steroidogenic Acute Regulatory (StAR) Protein by Lon Protease: The Unexpected Effect of Proteasome Inhibitors. Molecular Endocrinology, 2007. **21**(9): p. 2164-2177.

66. NCT03345095, https://clinicaltrials.gov/ct2/show/NCT03345095?cond=NCT03345095&rank=1

67. Di, K., et al., Marizomib activity as a single agent in malignant gliomas: ability to cross the blood-brain barrier. Neuro Oncol, 2016. **18**(6): p. 840-848.

68. Bogyo, M., et al., Covalent modification of the active site threonine of proteasomal β subunits and the Escherichia coli homolog HslV by a new class of inhibitors. Proceedings of the National Academy of Sciences of the United States of America, 1997. **94**(13): p. 6629-6634.

69. Nazif, T. and M. Bogyo, Global analysis of proteasomal substrate specificity using positional-scanning libraries of covalent inhibitors. Proc Natl Acad Sci U S A, 2001. **98**(6): p. 2967-2972.

70. Verdoes, M., et al., A fluorescent broad-spectrum proteasome inhibitor for labeling proteasomes in vitro and in vivo. Chem Biol, 2006. **13**(11): p. 1217-1226.

71. Bogyo, M., et al., Substrate binding and sequence preference of the proteasome revealed by active-site-directed affinity probes. Chemistry & Biology, 1998. **5**(6): p. 307-320.

72. Meng, L., et al., Eponemycin Exerts Its Antitumor Effect through the Inhibition of Proteasome Function. Cancer Research, 1999. **59**(12): p. 2798-2801.

73. Meng, L., et al., Epoxomicin, a potent and selective proteasome inhibitor, exhibits in vivo antiinflammatory activity. Proceedings of the National Academy of Sciences of the United States of America, 1999. **96**(18): p. 10403-10408.

74. Groll, M., et al., Crystal Structure of Epoxomicin:20S Proteasome Reveals a Molecular Basis for Selectivity of a',b'-Epoxyketone Proteasome Inhibitors. J. Am. Chem. Soc., 2000. **122**(6): p. 1237-1238.

75. Schrader, J., et al., The inhibition mechanism of human 20S proteasomes enables next generation inhibitor design. Science, 2016. **353**(6299): p. 594-598.

76. Herndon, T.M., et al., U.s. Food and Drug Administration approval: carfilzomib for the treatment of multiple myeloma. Clin Cancer Res, 2013. **19**(17): p. 4559-4563.

77. Basler, M., et al., Inhibition of the immunoproteasome ameliorates experimental autoimmune encephalomyelitis. EMBO Molecular Medicine, 2014. **6**(2): p. 226-238.

78. Ichikawa, H.T., et al., Beneficial effect of novel proteasome inhibitors in murine lupus via dual inhibition of type I interferon and autoantibody-secreting cells. Arthritis & Rheumatism, 2012. **64**(2): p. 493-503.

79. Parlati, F., et al., Carfilzomib can induce tumor cell death through selective inhibition of the chymotrypsin-like activity of the proteasome. Blood, 2009. **114**(16): p. 3439-3447.

80. Basler, M., et al., The immunoproteasome: a novel drug target for autoimmune diseases. Clin Exp Rheumatol, 2015. **33**(4 Suppl 92): p. S74-79.

81. Singh, A.V., et al., PR-924, a selective inhibitor of the immunoproteasome subunit LMP-7, blocks multiple myeloma cell growth both in vitro and in vivo. British Journal of Haematology, 2011. **152**(2): p. 155-163.

82. Ho, Y.K., et al., LMP2-specific inhibitors: chemical genetic tools for proteasome biology. Chem Biol, 2007. **14**(4): p. 419-430.

83. Wehenkel, M., et al., A selective inhibitor of the immunoproteasome subunit LMP2 induces apoptosis in PC-3 cells and suppresses tumour growth in nude mice. British Journal of Cancer, 2012. **107**(1): p. 53-62.

84. de Bruin, G., et al., Structure-based design of beta1i or beta5i specific inhibitors of human immunoproteasomes. J Med Chem, 2014. **57**(14): p. 6197-6209.

85. Adams, J., et al., Proteasome Inhibitors: A Novel Class of Potent and Effective Antitumor Agents. Cancer Research, 1999. **59**(11): p. 2615-2622.

86. Demo, S.D., et al., Antitumor Activity of PR-171, a Novel Irreversible Inhibitor of the Proteasome. Cancer Research, 2007. **67**(13): p. 6383-6391.

87. Altun, M., et al., Effects of PS-341 on the Activity and Composition of Proteasomes in Multiple Myeloma Cells. Cancer Research, 2005. **65**(17): p. 7896-7901.

88. Kisselev, A.F., A. Callard, and A.L. Goldberg, Importance of the Different Proteolytic Sites of the Proteasome and the Efficacy of Inhibitors Varies with the Protein Substrate. Journal of Biological Chemistry, 2006. **281**(13): p. 8582-8590.

89. Berkers, C.R., et al., Activity probe for in vivo profiling of the specificity of proteasome inhibitor bortezomib. Nature Methods, 2005. **2**(5): p. 357-362.

90. Kraus, M., et al., Activity patterns of proteasome subunits reflect bortezomib sensitivity of hematologic malignancies and are variable in primary human leukemia cells. Leukemia, 2006. **21**(1): p. 84-92.

91. Adams, J., Development of the Proteasome Inhibitor PS-341. Oncologist, 2002. **7**(1): p. 9-16.

92. Richardson, P.G., et al., Bortezomib or high-dose dexamethasone for relapsed multiple myeloma. N Engl J Med, 2005. **352**(24): p. 2487-2498.

93. Cavo, M., et al., Bortezomib-thalidomide-dexamethasone is superior to thalidomidedexamethasone as consolidation therapy after autologous hematopoietic stem cell transplantation in patients with newly diagnosed multiple myeloma. Blood, 2012. **120**(1): p. 9-19.

94. Palumbo, A., et al., Bortezomib, doxorubicin and dexamethasone in advanced multiple myeloma. Ann Oncol, 2008. **19**(6): p. 1160-1165.

95. Kane, R.C., et al., Velcade: U.S. FDA approval for the treatment of multiple myeloma progressing on prior therapy. Oncologist, 2003. **8**(6): p. 508-513.

96. Robak, T., et al., Bortezomib-based therapy for newly diagnosed mantle-cell lymphoma.N Engl J Med, 2015. **372**(10): p. 944-953.

97. de la Rubia, J. and M. Roig, Bortezomib for previously untreated multiple myeloma. Expert Rev Hematol, 2011. **4**(4): p. 381-398.

98. Kuhn, D.J., et al., Potent activity of carfilzomib, a novel, irreversible inhibitor of the ubiquitin-proteasome pathway, against preclinical models of multiple myeloma. Blood, 2007. **110**(9): p. 3281–3290

99. Arastu-Kapur, S., et al., Nonproteasomal Targets of the Proteasome Inhibitors Bortezomib and Carfilzomib: a Link to Clinical Adverse Events. Clinical Cancer Research, 2011. 17(9): p. 2734-2743.

100. O'Connor, O.A., et al., A Phase 1 Dose Escalation Study of the Safety and Pharmacokinetics of the Novel Proteasome Inhibitor Carfilzomib (PR-171) in Patients with Hematologic Malignancies. Clinical Cancer Research, 2009. **15**(22): p. 7085-7091.

101. Alsina, M., et al., A Phase I Single-Agent Study of Twice-Weekly Consecutive- Day Dosing of the Proteasome Inhibitor Carfilzomib in Patients with Relapsed or Refractory Multiple Myeloma or Lymphoma. Clinical Cancer Research, 2012.

18(17): p. 4830-4840.

102. Papadopoulos, K.P., et al., A phase I/II study of carfilzomib 2–10-min infusion in patients with advanced solid tumors. Cancer Chemotherapy and Pharmacology, 2013. **72**(4): p. 861-868.

103. Vij, R., et al., An open-label, single-arm, phase 2 (PX-171-004) study of single-agent carfilzomib in bortezomib-naive patients with relapsed and/or refractory multiple myeloma. Blood 2012. **119**(24): p 5661-5670.

104. diCapua Siegel, D.S., et al., Results of PX-171-003-A1, An Open-Label, Single-Arm, Phase 2 (Ph 2) Study of Carfilzomib (CFZ) In Patients (pts) with Relapsed and Refractory Multiple Myeloma (MM). Blood, 2010. **116**(21): p. 985-985.

105. Stewart, A.K., et al., Carfilzomib, lenalidomide, and dexamethasone for relapsed multiple myeloma. N Engl J Med, 2015. **372**(2): p. 142-152.

106. Dimopoulos, M.A., et al., Carfilzomib and dexamethasone versus bortezomib and dexamethasone for patients with relapsed or refractory multiple myeloma (ENDEAVOR): a randomised, phase 3, open-label, multicentre study. Lancet Oncol,2016. **17**(1): p. 27-38.

107. Kupperman, E., et al., Evaluation of the Proteasome Inhibitor MLN9708 in Preclinical Models of Human Cancer. Cancer Research, 2010. **70**(5): p. 1970-1980.

108. Chauhan, D., et al., In Vitro and In Vivo Selective Antitumor Activity of a Novel Orally Bioavailable Proteasome Inhibitor MLN9708 against Multiple Myeloma Cells. Clinical Cancer Research, 2011. **17**(16): p. 5311-5321.

109. Moreau, P.M., et al., Ixazomib, an Investigational Oral Proteasome Inhibitor (PI), in Combination with Lenalidomide and Dexamethasone (IRd), Significantly Extends Progression-Free Survival (PFS) for Patients (Pts) with Relapsed and/or Refractory Multiple Myeloma (RRMM): The Phase 3 Tourmaline-MM1 Study (NCT01564537). Blood, 2015. **126**(23): p. 727.

110. Moreau, P., et al., Oral Ixazomib, Lenalidomide, and Dexamethasone for Multiple Myeloma. N Engl J Med, 2016. **374**(17): p. 1621-1634.

111. Kumar, S.K., et al., Safety and tolerability of ixazomib, an oral proteasome inhibitor, in combination with lenalidomide and dexamethasone in patients with previously untreated multiple myeloma: an open-label phase 1/2 study. Lancet Oncol, 2014.**15**(13): p. 1503-1512.

112. Muz, B., et al., Spotlight on ixazomib: potential in the treatment of multiple myeloma. Drug Design, Development and Therapy, 2016. **10**: p. 217-226.

113. Manochakian, R.; Miller, K. C.; Chanan-Khan, A. A. Clinical impact of bortezomib in frontline regimens for patients with multiple myeloma. Oncologist 2007. **12**(8): p. 978-990.

114. Herndon, T. M, et al., U.s. Food and Drug Administration approval: carfilzomib for the treatment of multiple myeloma. Clin Cancer Res 2013. **19**(17): p. 4559-4563.

115. Chen, D, et al. Bortezomib as the first proteasome inhibitor anticancer drug: current status and future perspectives. Curr Cancer Drug Targets 2011. **11**(3): p. 239-253.

116. Lu, S., et al., Overexpression of the PSMB5 gene contributes to bortezomib resistance in T-lymphoblastic lymphoma/leukemia cells derived from Jurkat line. Exp Hematol, 2008. **36**(10): p. 1278-1284.

117. Oerlemans, R., et al., Molecular basis of bortezomib resistance: proteasome subunit beta5 (PSMB5) gene mutation and overexpression of PSMB5 protein. Blood, 2008. **112**(6): p. 2489-2499.

118. Chapman, M.A., et al., Initial genome sequencing and analysis of multiple myeloma. Nature, 2011. **471**(7339): p. 467-472.

119. Lichter, D.I., et al., Sequence analysis of beta-subunit genes of the 20S proteasome in patients with relapsed multiple myeloma treated with bortezomib or dexamethasone. Blood, 2012. **120**(23): p. 4513-4516.

120. Barrio, S., et al., Parallel Parallel evolution of multiple PSMB5 mutations in a myeloma patient treated with bortezomib. Blood, 2016. **128**(22): p. 3282-3282.

121. Iwakoshi NN et al., Plasma cell differentiation and the unfolded protein response intersect at the transcription factor XBP-1. Nat Immunol. 2003. **4**(4): p. 321–329.

122. Reimold AM, Iwakoshi NN, Manis J, Vallabhajosyula P, Szomolanyi-Tsuda E, Gravallese EM, et al. Plasma cell differentiation requires the transcription factor XBP-1. Nature. 2001. **412**(6844): p. 300-307.

123. Lee, A.H., et al., Proteasome inhibitors disrupt the unfolded protein response in myeloma cells. Proc Natl Acad Sci U S A, 2003. **100**(17): p. 9946-9951.

124. Ling, S.C., et al., Response of myeloma to the proteasome inhibitor bortezomib is correlated with the unfolded protein response regulator XBP-1. Haematologica, 2012. **97**(1): p. 64-72.

125. Nikesitch, N., et al., Predicting the response of multiple myeloma to the proteasome inhibitor Bortezomib by evaluation of the unfolded protein response. Blood Cancer J,2016. **6**: p. e432.

126. Leung-Hagesteijn, C., et al., Xbp1s-negative tumor B cells and pre-plasmablasts mediate therapeutic proteasome inhibitor resistance in multiple myeloma. Cancer Cell, 2013. **24**(3): p. 289-304.

127. Gambella, M., et al., High XBP1 expression is a marker of better outcome in

multiple myeloma patients treated with bortezomib. Haematologica, 2014. **99**(2): p. e14-16.

128. Zhou, S.F., Structure, function and regulation of P-glycoprotein and its clinical relevance in drug disposition. Xenobiotica, 2008. **38**(7-8): p. 802-832.

129. Bellamy, W.T., P-glycoproteins and multidrug resistance. Annu Rev Pharmacol Toxicol, 1996. **36**: p. 161-183.

130. Bao, L., et al., Increased expression of P-glycoprotein is associated with doxorubicin chemoresistance in the metastatic 4T1 breast cancer model. Am J Pathol, 2011. **178**(2): p. 838-852.

131. Enokida, H., et al., Reversal of P-glycoprotein-mediated paclitaxel resistance by new synthetic isoprenoids in human bladder cancer cell line. Jpn J Cancer Res, 2002. **93**(9): p. 1037-1046.

132. Verbrugge, S.E., et al., Inactivating PSMB5 mutations and P-glycoprotein (multidrug resistance-associated protein/ATP-binding cassette B1) mediate resistance to proteasome inhibitors: ex vivo efficacy of (immuno)proteasome inhibitors in mononuclear blood cells from patients with rheumatoid arthritis. J Pharmacol Exp Ther, 2012. **341**(1): p. 174-182.

133. Ao, L., et al., Development of Peptide-based reversing agents for p-glycoprotein -mediated resistance to carfilzomib. Mol Pharm, 2012. **9**(8): p. 2197-2205.

134. Soriano, G.P., et al., Proteasome inhibitor-adapted myeloma cells are largely independent from proteasome activity and show complex proteomic changes, in particular in redox and energy metabolism. Leukemia, 2006. **30**(11): p.2198.

135. Besse, A., et al., Carfilzomib resistance due to ABCB1/MDR1 overexpression is overcome by nelfinavir and lopinavir in multiple myeloma. Leukemia, 2018. **32**(2): p.391.

136. Alzheimer's Association, 2016 Alzheimer's disease facts and figures. Alzheimer's & Dementia, 2016. **12**(4): p.459-509.

137. Alzheimer A. Über einen eigenartigen schweren Erkrankungsprozeβ der Hirnrincle. Neurol Central. 1906. **25**: p. 1134.

138. Möller, H.J. and Graeber, M.B., The case described by Alois Alzheimer in 1911. European archives of psychiatry and clinical neuroscience, 1998. **248**(3): p.111-122.

139. Kay, D.W., Beamish, P. & Roth, M., Old age mental disorders in Newcastle Upon Tyne. Part I A study of prevalence, Br J Psychiatry, 1964.**110**: p. 146.

140. Blessed, G., Tomlinson, B.E. & Roth, M., The association between quantitative measures of dementia and of senile changes in the cerebral matter of elderly subjects, Brit J Psychiat, 1968. **114**: p. 797-811.

141. Heston L.L. Mastri A.R. Anderson V.E. White J. Dementia of the Alzheimer type. Clinical genetics, natural history, and associated conditions.Arch. Gen. Psychiatry. 1981. **38**: p. 1085-1090.

142. Tanzi, R., Kovacs, D., Kim, T., Moir, K., Guenette, S. & Wasco, W., The gene defects responsible for familial Alzheimer's disease, Neurobiol Dis, 1996. **3** (3): p. 159-168.

143. Braak H, Braak E. Staging of Alzheimer's disease-related neurofibrillary changes. Neurobiology of aging. 1995.**16**(3): p.271-278.

144. Braak H, Braak E. Frequency of stages of Alzheimer-related lesions in different age categories. Neurobiol Aging 1997. **18**: p. 351–357.

145. Mills J, Reiner PB. Regulation of amyloid precursor protein cleavage. Journal of neurochemistry. 1999.**72**(2): p.443-460.

146. Blennow K, Zetterberg H. The application of cerebrospinal fluid biomarkers in early diagnosis of Alzheimer disease. Med Clin North Am 2013. **97**: p.369-376.

147. Pei JJ, Khatoon S, An WL, Nordlinder M, Tanak T, Braak H, et al. Role of protein kisase B in Alzheimer's neurofibrillary pathology. Acta Neuropathol 2003.**105**: p.381-392.

148. Hamdane M, Delobel P, Sambo AV, Smet C, Begard S, Violleau A, et al. Neurofibrillary degeneration of the Alzheimertype: an alternate pathway to neuronal apoptosis. Biochem Pharmacol 2003. **66**: p.1619-1625.

149. Lee HG, Perry G, Moreira PI, Garrett MR, Liu Q, Zho X, et al. Tau phosphorylation in Alzheimer's disease: pathogen or protector? Trends Mol Med 2005. **11**: p.164-69.

150. Martorana, A., Esposito, Z. and Koch, G., Beyond the cholinergic hypothesis: do current drugs work in Alzheimer's disease?. CNS neuroscience & therapeutics, 2010. **16**(4): p.235-245.

151. Davies P, Maloney AJF. Selective loss of central cholinergic neurones in Alzheimer's disease. Lancet 1976. **2**: p.1403

152. Bartus RT, Dean III RL, Beer B, Lippa AS. The cholinergic hypothesis of geriatric memory dysfunction. Science 1982. **217**: p.408–17.

153. Geerts H. Ispronicline (targacept). Curr Opin Investig Drugs 2006.**7**: p.60–69.

154. Hardy J., Allsop D. Amyloid deposition as the central event in the aetiology of Alzheimer's disease. Trends Pharmacol. Sci. 1996. **12**: p.383–388.

155. Hardy J., Selkoe D. J.The Amyloid hypothesis of Alzheimer's Disease: progress and problems on the road to therapeutics. Science 2002. **297**: p. 353–356.

156. Hardy J. A., Higgins G. A. Alzheimer's disease: the amyloid cascade hypothesis. Science 1992. **256**: p.184–185.

157. Kang J., Lemaire H. G., Unterbeck A., Salbaum J. M., Masters C. L., Grzeschik K. H., et al. The precursor of Alzheimer's disease amyloid A4 protein resembles a cell-surface receptor. Nature, 1987. **325**: p.733–736.

158. Selkoe DJ, Hardy J. The amyloid hypothesis of Alzheimer's disease at 25 years. EMBO Mol Med. 2016.**8**(6): p.595-608.

159. Selkoe, D.J., Clearing the brain's amyloid cobwebs. Neuron, 2001. **32**(2): p.177-180.

160. R. Deane, S. D. Yan, R. K. Submamaryan et al., RAGE mediates amyloid-β peptide transport across the blood-brain barrier and accumulation in brain," Nature Medicine, 2003. **9**(7): p. 907–913.

161. R. Deane, R. D. Bell, A. Sagare, and B. V. Zlokovic, "Clearance of amyloid-β peptide across the blood-brain barrier: Implication for therapies in Alzheimer's disease," CNS and Neurological Disorders, 2009. **8**(1): p. 16–30.

162. Honig, L. S. et al. Trial of Solanezumab for Mild Dementia Due to Alzheimer's Disease. N Engl J Med 2018. **378**: p.321-330.

163. Salloway, S. et al. Two Phase 3 Trials of Bapineuzumab in Mild-to-Moderate Alzheimer's Disease. N Engl J Med 2014. **370**: p.322-333.

164. Rygiel, K. Novel strategies for Alzheimer's disease treatment: An overview of anti-amyloid beta monoclonal antibodies. Indian J Pharmacol. 2016. **48**(6): p.629-636.

165. Van Dyck, C.H. Anti-Amyloid-β Monoclonal Antibodies for Alzheimer's Disease: Pitfalls and Promise. Biol Psychiatry. 2018. **83**(4): p.311-319.

166. Kosik, K.S, Joachim, C.L, and Selkoe, D.J. Microtubule-associated protein tau (tau) is a major antigenic component of paired helical filaments in Alzheimer disease. Proc Natl Acad Sci USA. 1986. **83**(11): p.4044-4048.

167. Braak, H. & Braak, E. Neuropathological stageing of Alzheimer-related changes. Acta Neuropathol. 1991. **82**(4): p.239-259.

168. Di, J., Cohen, L.S., Corbo, C.P., Phillips, G.R., El Idrissi, A. and Alonso, A.D., Abnormal tau induces cognitive impairment through two different mechanisms: synaptic dysfunction and neuronal loss. Scientific reports, 2016. **6**: p.20833.

169. Jesus R. de Paula, V., Guimaraes, F.B., Diniz, B.S., Forlenza, O.V. Neurobiological pathways to Alzheimer's disease: Amyloid-beta, TAU protein, or both? Dement Neuropsychol. 2009. **3**(3): p.188–194.

170. Jack Jr, C.R. and Holtzman, D.M., 2013. Biomarker modeling of Alzheimer's disease. Neuron, **80**(6): p.1347-1358.

171. Cummings, J. et al. Alzheimer's disease drug development pipeline: 2018. Alz & Dem: Transl Res & Clin Interventions. 2018. **4**: p.195-214.

172. Lovestone S, et al., A phase II trial of tideglusib in Alzheimer's disease. J Alzheimers Dis. 2015. **45**(1): p.75-88.

173. Mcgeer P, Mcgeer E, Rogers J, Sibley J. Anti-inflammatory drugs and Alzheimer disease. The Lancet. 1990. **335**(8696): p.1037.

174. Rich JB, Rasmusson DX, Folstein MF, Carson KA, Kawas C, Brandt J. Nonsteroidal anti-inflammatory drugs in Alzheimer's disease. Neurology. 1995. **45**(1): p.51-55.

175. Soscia S.J., et al., The Alzheimer's disease-associated amyloid betaprotein is an antimicrobial peptide, PLoS One, 2010. **5**(3): p. e9505.

176. Kontush A., et al., Amyloid-beta: acute-phase apolipoprotein with metalbinding activity", J Alzheimers Dis, 2005. **8**(2): p. 129.

177. Guo Z., et al., Head injury and the risk of AD in the MIRAGE study, Neurology, 2000. **54**(6): p. 1316.

178. Streit WJ, Kincaid-Colton CA. The brain's immune system. Sci Am. 1995. **273**(5): p.54-55, 58-61.

179. Benoit M, Desnues B, Mege JL. Macrophage polarization in bacterial infections. Journal of immunology. 2008. **181**(6): p.3733-3739.

180. Brown GC. Mechanisms of inflammatory neurodegeneration: iNOS and NADPH oxidase. Biochem Soc Trans. 2007.**35**(Pt 5): p.1119-1121.

181. Varnum MM, Ikezu T. The classification of microglial activation phenotypes on neurodegeneration and regeneration in Alzheimer's disease brain. Arch Immunol Ther Exp (Warsz). 2012. **60**(4): p. 251-266.

182. Ghoshal, A., et al., Proinflammatory mediators released byactivated microglia induces neuronal death in Japanese encephalitis, Glia, 2007. **55**(5): p. 483

183. Zotova, E., Nicoll, J.A., Kalaria, R., Holmes, C. and Boche, D., Inflammation in Alzheimer's disease: relevance to pathogenesis and therapy. Alzheimers Res Ther, 2010. **2**(1): p.1.

184. Frackowiak J, et al., Ultrastructure of the microglia that phagocytose amyloid and the microglia that produce beta-amyloid fibrils. Acta Neuropathol. 1992. **84**(3): p. 225-233.

185. Wisniewski HM, Barcikowska M, Kida E. Phagocytosis of beta/A4 amyloid fibrils of the neuritic neocortical plaques. Acta Neuropathol. 1991. **81**(5): p.588-590.

186. Herber DL, Roth LM, Wilson D, Wilson N, Mason JE, Morgan D, Gordon MN. Time-dependent reduction in Abeta levels after intracranial LPS administration in APP transgenic mice. Experimental neurology. 2004. **190**(1): p.245-253.

187. Chakrabarty, P., et al., Hippocampal expression of murine TNFα results in attenuation of amyloid deposition in vivo. Molecular neurodegeneration, 2011. **6**(1): p.16.

188. Chakrabarty, P., et al. Hippocampal expression of murine IL-4 results in exacerbation of amyloid deposition. Molecular neurodegeneration, 2012. **7**(1): p.36.

189. Chakrabarty P, et al., IL-10 alters immunoproteostasis in APP mice, increasing plaque burden and worsening cognitive behavior. Neuron. 2015. **85**(3): p. 519-533.

190. Wang, J., et al., Anti-inflammatory drugs and risk of Alzheimer's disease: an updated systematic review and meta-analysis, J Alzheimers Dis 2015. **44**: p. 385-396.

191. Schiavone, S. and Trabace, L., Small molecules: Therapeutic application in neuropsychiatric and neurodegenerative disorders. Molecules, 2018. **23**(2): p.411.

192. Bachstetter, A. D., et al., MW151 Inhibited IL-1beta Levels after Traumatic Brain Injury with No Effect on Microglia Physiological Responses, PLoS One 2016. **11**: p. e0149451.

193. Rogers, Sharon L et al. Donepezil Improves Cognition and Global Function in Alzheimer Disease: A 15-Week, Double-blind, Placebo-Controlled Study., Archives of Internal Medicine, 1998. **158**: p. 1021-1031.

194. Lanctot, Krista L., Ryan D. Rajaram, and Nathan Herrmann. Therapy for Alzheimer's Disease: How Effective Are Current Treatments?, Therapeutic Advances in Neurological Disorders, 2009. **2**: p.163-180.

195. Loy C and Schneider L. Galantamine for Alzheimer's disease and mild cognitive impairment., Cochrane Database of Systematic Reviews, 2006. (1)

196. Lippincott, Williams, and Wilkins. Alzheimer Disease Drugs. Nursing Drug Handbook Philadelphia: Wolters Kluwer Health, 2010. p 546-551.

197. Parsons, C.G., Danysz, W. and Quack, G., Memantine is a clinically well tolerated N-methyl-D-aspartate (NMDA) receptor antagonist—a review of preclinical data. Neuropharmacology, 1999. **38**(6): p.735-767.

198. Reisberg, Barry et al. Memantine in Moderate-to-Severe Alzheimer's Disease., New England Journal of Medicine, 2003. **348**: p.1333-1341.

199. Yiannopoulou, K. G. & Papageorgiou, S. G., Current and future treatments for Alzheimer's disease. Ther Adv Neurol Disord, 2013. **6**: p.19–33.

200. Gilman, S. et al. , Clinical effects of Aβ immunization (AN1792) in patients with AD in an interrupted trial., Neurology, 2005. **64**: p.1553–1562.

201. Bard F, Cannon C, Barbour R, et al. Peripherally administered antibodies against amyloid β-peptide enter the central nervous system and reduce pathology in a mouse model of Alzheimer disease., Nat Med., 2000. **6**: p.916–919.

202. Bard F, Barbour R, Cannon C, et al., Epitope and isotype specificities of antibodies to β-amyloid peptide for protection against Alzheimer's disease-like neuropathology. Proc Natl Acad Sci., 2003. **100**: p.2023–2028.

203. Buttini M, Masliah E, Barbour R, et al. β-amyloid immunotherapy prevents synaptic degeneration in a mouse model of Alzheimer's disease. J Neurosci., 2005. **25**: p.9096–9101.

204. Shankar GM, Li S, Mehta TH, et al., Amyloid-β protein dimers isolated directly from Alzheimer's brains impair synaptic plasticity and memory., Nat Med., 2008. **14**: p.837–842.

205. Zago W, Buttini M, Comery TA, et al., Neutralization of soluble, synaptotoxic amyloid β species by antibodies is epitope specific., J Neurosci., 2012. **32**: p. 2696–2702.

206. Salloway R, et al., A phase 2 multiple ascending dose trial of bapineuzumab in mild to moderate Alzheimer disease., Neurology., 2009. **73**: p.2061–2070.

207. Rinne DJ, et al., PET assessment of change in fibrillar amyloid-beta load in patients with Alzheimer's disease treated with bapineuzumab: a phase 2, double-blind, placebo-controlled, ascending-dose study., Lancet Neurol., 2010. **9**: p.363–372.

208. Pfizer Pharmaceutical. Pfizer Announces Co-Primary Clinical Endpoints Not Met In Second Phase 3 Bapineuzumab Study In Mild-To-Moderate Alzheimer's Disease Patients Who Do Not Carry The Apoe4 Genotype. 5–6 (2012), NCT00574132, https://clinicaltrials.gov/ct2/show/NCT00574132

209. Eli Lilly. Lilly Announces Top-Line Results of Solanezumab Phase 3 Clinical Trial. 2015–2017 (2017).

210. Ben Halima S., Mishra S., Raja K. M. P., Willem M., Baici A., Simons K., et al., Specific inhibition of β-secretase processing of the alzheimer disease amyloid precursor protein., Cell Rep., 2016. **14**: p.2127–2141.

211. Vassar R., BACE1 inhibition as a therapeutic strategy for Alzheimer's disease., J. Sport Health Sci., 2016. **5**: p. 388–390.

212. Yan R., Stepping closer to treating Alzheimer's disease patients with BACE1 inhibitor drugs., Transl. Neurodegener., 2016. **5**: p.1–11.

213. Mullard A., BACE inhibitor bust in Alzheimer trial. Nat. Rev. Drug Discov., 2017. **16**: p.5.

214. Merck S., Merck Announces Discontinuation of APECS Study Evaluating Verubecestat (MK-8931) for the Treatment of People with Prodromal Alzheimer's Disease.(2018): http://investors.merck.com/news/press-release-details/2018/Merck-Announces-Discontinuation-of-APECS-Study-Evaluating-Verubecestat-MK-8931-for-the-Treatment-of-People-with-Prodromal-Alzheimers-Disease/default.aspx

215. Hu X., Das B., Hou H., He W., Yan R., BACE1 deletion in the adult mouse reverses preformed amyloid deposition and improves cognitive functions. J. Exp. Med., 2018. **215**: p.927-940.

216. U.S. Food & Drug Administration. Orphan Drug Designations and Approvals: recombinant humanized anti-tau antibody. http://www.accessdata.fda.gov/scripts/opdlisting/oopd/detailedIndex.cfm?cfgridkey=460914

217. European Medicines Agency. Humanised recombinant IgG4 anti-human tau antibody for the treatment of progressive supranuclear palsy. http://www.ema.europa.eu/docs/en_GB/document_library/Orphan_designation/2016/05/WC500207488.pdf. Accessed January 2017.

218. West T, et al., Safety, tolerability and pharmacokinetics of ABBV-8E12, a humanized anti-tau monoclonal antibody, in a phase 1, single ascending dose, placebo-controlled study in subjects with Progressive Supranuclear Palsy., J Prev Alz Dis. 2016. **3**(1): p.285.

219. NCT02880956, https://clinicaltrials.gov/ct2/show/NCT02880956

220. NCT03352557, https://clinicaltrials.gov/ct2/show/NCT03352557

221. Yan SD, et al., RAGE and amyloid-beta peptide neurotoxicity in Alzheimer's disease. Nature 1996. **382**(6593): p.685–691.

222. Schmidt AM, et al., The role of RAGE in amyloid-beta peptide-mediated pathology in Alzheimer's disease., Curr Opin Investig Drugs., 2009. **10**(7): p. 672-680.

223. Yan SD, Chen X, Walker DG, Schmidt AM, Arancio O, Lue LF. RAGE: a potential target for Abeta-mediated cellular perturbation in Alzheimer's disease., Curr Mol Med., 2007. **7**(8): p.735-742.

224. Yan SD, Bierhaus A, Nawroth PP, Stern DM., RAGE and Alzheimer's disease: a progression factor for amyloid-beta-induced cellular perturbation?, J Alzheimers Dis., 2009. **16**(4): p.833-843.

225. Li XH, Lv BL, Xie JZ et al., AGEs induce Alzheimer's-like tau pathology and memory deficit via RAGE-mediated GSK-3 activation., Neurobiology of Aging, 2012. **33**: p.1400-1421.

226. NCT02080364, https://clinicaltrials.gov/ct2/show/NCT02080364

227. https://www.alzforum.org/news/conference-coverage/truly-new-deja-vu-five-hopefuls-lights-go-out-after-phase-2

228. NCT02817906,https://clinicaltrials.gov/ct2/show/NCT02817906?term=ITI

229. http://ir.intracellulartherapies.com/news-releases/news-release-details/intra-cellular-therapies-announces-update-iti-007-201-clinical

230. Ding, Q., Dimayuga, E., and Keller, J. N., Proteasome regulation of oxidative stress in aging and age-related diseases of the CNS., Antioxid. Redox Signal., 2006. **8**: p.163–172.

231. Oddo, S., The ubiquitin-proteasome system in Alzheimer's disease., J. Cell. Mol. Med., 2008. **12**: p.363–373.

232. Riederer, B. M., Leuba, G., Vernay, A., and Riederer, I. M. The role of the ubiquitin proteasome system in Alzheimer's disease. Exp. Biol. Med., 2011. **236**: p.268–276.

233. García Gil, M. L., Morán, M. A., and Gómez-Ramos, P., Ubiquitinated granular structures and initial neurofibrillary changes in the human brain., J. Neurol. Sci., 2001. **192**: p.27–34.

234. Upadhya, S. C., and Hegde, A. N., Role of the ubiquitin proteasome system in Alzheimer's disease., BMC Biochem., 2007. **8**(Suppl. 1): S12.

235. Bedford, L., Paine, S., Rezvani, N., Mee, M., Lowe, J., and Mayer, R. J., The UPS and autophagy in chronic neurodegenerative disease: six of one and half a dozen of the other-or not?, Autophagy, 2009. **5**: p.224–227.

236. Chu,C.T.,et al., Ubiquitin immunochemistry as a diagnostic aid for community pathologists evaluating patients who have dementia. Mod.Pathol., 2000. **13**: p. 420–426.

237. Keller,J.N.,Hanni,K.B.,andMarkesbery,W.R., Impaired proteasome function in Alzheimer's Disease., J. Neurochem., 2000. **75**: p.436–439.

238. Tseng,B.P., et al., Abeta inhibits the proteasome and enhances amyloid and tau accumulation. Neurobiol.Aging, 2008. **29**: p.1607–1618.

239. Zhao,X., Yang, J, Amyloid-beta peptide is a substrate of the human 20S proteasome., ACS Chem.Neurosci., 2010. **1**: p.655–660.

240. Orre, M., et al., Reactive glia show increased immunoproteasome activity in Alzheimer's disease, Brain, 2013. **136**: p.1415-1431.

241. Moritz, K. E., et al., The role of the immunoproteasome in interferon-gamma-mediated microglial activation, Sci Rep, 2017. **7**: p.9365.

242. Mishto, M.et al., The immunoproteasome beta5i subunit is a key contributor to ictogenesis in a rat model of chronic epilepsy, Brain Behav Immun, 2015. **49**: p.188-196.

243. Aso, E., et al., Amyloid generation and dysfunctional immunoproteasome activation with disease progression in animal model of familial Alzheimer's disease, Brain Pathol, 2012. **22**: p.636-653.

244. Mishto, M., et al., Immunoproteasome and LMP2 polymorphism in aged and Alzheimer's disease brains, Neurobiol Aging, 2006. **27**: p.54-66.

245. Chauhan D, Tian Z, Nicholson B, et al., A Small Molecule Inhibitor of Ubiquitin-Specific Protease-7 Induces Apoptosis in Multiple Myeloma Cells and Overcomes Bortezomib Resistance. Cancer Cell., 2012. **22**(3): p.345-358.

246. Tian Z, D'Arcy P, Wang X, et al., A novel small molecule inhibitor of deubiquitylating enzyme USP14 and UCHL5 induces apoptosis in multiple myeloma and overcomes bortezomib resistance., Blood., 2014. **123**(5): p.706-716.

247. Kraus J, Kraus M, Liu N, et al., The novel β2-selective proteasome inhibitor LU-102 decreases phosphorylation of I kappa B and induces highly synergistic cytotoxicity in combination with ibrutinib in multiple myeloma cells., Cancer Chemother Pharmacol., 2015. **76**(2): p.1-14.

248. Sarlus, H., and Heneka, M. T., Microglia in Alzheimer's disease, J Clin Invest, 2017. **127**: p.3240-3249.

249. Regen, F., et al., Neuroinflammation and Alzheimer's Disease: Implications for Microglial Activation, Curr Alzheimer Res, 2017. **14**: p.1140-1148.

250. Rankovic, Z., CNS drug design: balancing physicochemical properties for optimal brain exposure, J Med Chem, 2015. **58**: p.2584-2608.

251. Wang, X., Zhao, Z., Luo, Y., Chen, G. & Li, Z., Gel-based proteomics analysis of the heterogeneity of 20S proteasomes from four human pancreatic cancer cell lines., Proteomics Clin Appl, 2011. **5**: p.484-492.

252. Guillaume, B. et al., Two abundant proteasome subtypes that uniquely process some antigens presented by HLA class I molecules., Proc Natl Acad Sci U S A, 2010. **107**: p.18599-18604.

253. Dahlmann, B., Ruppert, T., Kuehn, L., Merforth, S. & Kloetzel, P. M., Different proteasome subtypes in a single tissue exhibit different enzymatic properties., J Mol Biol, 2000. **303**: p.643-653.

254. Kloss, A., et al., Multiple cardiac proteasome subtypes differ in their susceptibility to proteasome inhibitors., Cardiovasc Res, 2010. **85**: p.367-375.

255. Vigneron, N. & Van den Eynde, B. J., Proteasome subtypes and the processing of tumor antigens: increasing antigenic diversity., Curr Opin Immunol, 2012. **24**: p.84-91.

256. Zheng J, Dasgupta A, Bizzozero OA., Changes in 20S subunit composition are largely responsible for altered proteasomal activities in experimental autoimmune encephalomyelitis. J Neurochem., 2012. **121**(3): p.486-94.

257. Carmony K, Lee W, Kim KB., High-Resolution Snapshots of Proteasome Inhibitors in Action Revise Inhibition Paradigms and Inspire Next-Generation Inhibitor Design., Chembiochem., 2016. **17**(22): p.2115-2117.

258. Kisselev AF, van der Linden WA, Overkleeft HS., Proteasome inhibitors: an expanding army attacking a unique target., Chem Biol., 2012. **19**(1): p.99-115.

259. Mushtaq A, Kapoor V, Latif A, Iftikhar A, Zahid U, McBride A, et al., Efficacy and toxicity profile of carfilzomib based regimens for treatment of multiple myeloma: A systematic review., Crit Rev Oncol Hematol., 2018. **125**: p.1-11.

260. Siegel DS, Martin T, Wang M, Vij R, Jakubowiak AJ, Lonial S, et al. A phase 2 study of single-agent carfilzomib (PX-171-003-A1) in patients with relapsed and refractory multiple myeloma., Blood, 2012. **120**(14): p.2817-2825.

261. Dimopoulos MA, Stewart AK, Masszi T, Spicka I, Oriol A, Hajek R, et al., Carfilzomib, lenalidomide, and dexamethasone in patients with relapsed multiple myeloma categorised by age: secondary analysis from the phase 3 ASPIRE study., Br J Haematol., 2017. **177**(3): p.404-413.

262. Goldschmidt, H., et al., Carfilzomib–dexamethasone versus subcutaneous or intravenous bortezomib in relapsed or refractory multiple myeloma: secondary analysis of the phase 3 ENDEAVOR study. Leukemia & lymphoma, 2018. **59**(6): p.1364-1374.

263. Dimopoulos MA, Goldschmidt H, Niesvizky R, Joshua D, Chng WJ, Oriol A, et al. Carfilzomib or bortezomib in relapsed or refractory multiple myeloma (ENDEAVOR): an interim overall survival analysis of an open-label, randomised, phase 3 trial. Lancet Oncol. 2017. **18**(10): p.1327-1337.

264. Hajek R, Masszi T, Petrucci MT, Palumbo A, Rosinol L, Nagler A, et al., A randomized phase III study of carfilzomib vs low-dose corticosteroids with optional cyclophosphamide in relapsed and refractory multiple myeloma (FOCUS)., Leukemia., 2017. **31**(1): p.107-114.

265. Berenson JR, Cartmell A, Bessudo A, Lyons RM, Harb W, Tzachanis D, et al. CHAMPION-1: a phase 1/2 study of once-weekly carfilzomib and dexamethasone for relapsed or refractory multiple myeloma., Blood., 2016. **127**(26): p.3360-3368.

266. Shah C, Bishnoi R, Wang Y, Zou F, Bejjanki H, Master S, et al. Efficacy and safety of carfilzomib in relapsed and/or refractory multiple myeloma: systematic review and meta-analysis of 14 trials., Oncotarget., 2018. **9**(34): p.23704-23717.

267. Lendvai N, Hilden P, Devlin S, Landau H, Hassoun H, Lesokhin AM, et al. A phase 2 single-center study of carfilzomib 56 mg/m2 with or without low-dose dexamethasone in relapsed multiple myeloma., Blood, 2014. **124**(6): p.899-906.

268. Avet-Loiseau H, Fonseca R, Siegel D, Dimopoulos MA, Spicka I, Masszi T, et al., Carfilzomib significantly improves the progression-free survival of high-risk patients in multiple myeloma., Blood., 2016. **128**(9): p.1174-1180.

269. Shah JJ, Stadtmauer EA, Abonour R, Cohen AD, Bensinger WI, Gasparetto C, et al. Carfilzomib, pomalidomide, and dexamethasone for relapsed or refractory myeloma., Blood, 2015. **126**(20): p.2284-2290.

270. Dahlqvist J, Torma H, Badhai J, Dahl N. siRNA silencing of proteasome maturation protein (POMP) activates the unfolded protein response and constitutes a model for KLICK genodermatosis. PLoS One., 2012. **7**(1): p. e29471.

271. Murata S, Yashiroda H, Tanaka K., Molecular mechanisms of proteasome assembly., Nat Rev Mol Cell Biol., 2009; **10**(2): p.104-115.

272. Wu YX, Yang JH, Saitsu H. Bortezomib-resistance is associated with increased levels of proteasome subunits and apoptosis-avoidance., Oncotarget., 2016.,

7(47): p. 77622-77634.

273. Carmony KC, Kim KB., Activity-based imaging probes of the proteasome., Cell Biochem Biophys., 2013. **67**(1): p.91-101.

274. Park JE, Wu Y, Carmony KC, Miller Z, Sharma LK, Lee DM, et al., A FRET-based approach for identification of proteasome catalytic subunit composition, Mol Biosyst, 2014. **10**(2): p.196-200.

275. Lonial, S.; Durie, B.; Palumbo, A.; San-Miguel, J., Monoclonal antibodies in the treatment of multiple myeloma: current status and future perspectives, Leukemia, 2016. **30**: p. 526-535.

276. Sanchez, L.; Wang, Y.; Siegel, D. S.; Wang, M. L., Daratumumab: a first-in-class CD38 monoclonal antibody for the treatment of multiple myeloma., J Hematol Oncol, 2016. **9**: p. 51.

277. San-Miguel, J. F., et al. Overall survival of patients with relapsed multiple myeloma treated with panobinostat or placebo plus bortezomib and dexamethasone (the PANORAMA 1 trial): a randomised, placebo-controlled, phase 3 trial., Lancet Haematol, 2016. **3**: p. e506-e515.

278. Anderson, D. J. et al., Targeting the AAA ATPase p97 as an approach to treat cancer through disruption of protein homeostasis., Cancer Cell., 2015. **28**: p.653-665.

279. Harshbarger, W.; Miller, C.; Diedrich, C.; Sacchettini, J. Crystal structure of the human 20S proteasome in complex with carfilzomib., Structure., 2015. **23**: p. 418-424.

280. Adams, G. M.; Crotchett, B.; Slaughter, C. A.; DeMartino, G. N.; Gogol, E. P. Formation of proteasome PA700 complexes directly correlates with activation of peptidase activity. Biochemistry, 1998. **37**: p. 12927-12932.

281. Micale, N.; Scarbaci, K.; Troiano, V.; Ettari, R.; Grasso, S.; Zappala, M. Peptide-based proteasome inhibitors in anticancer drug design, Med Res Rev, 2014. **34**: p. 1001-1069.

282. Ao, L.; Reichel, D.; Hu, D.; Jeong, H.; Kim, K. B.; Bae, Y.; Lee, W., Polymer micelle formulations of proteasome inhibitor carfilzomib for improved metabolic stability and anticancer efficacy in human multiple myeloma and lung cancer cell lines., J Pharmacol Exp Ther, 2015. **355**: p.168-173.

283. Ho, A.; Cyrus, K.; Kim, K. B. Towards immunoproteasome-specific inhibitors: an improved synthesis of dihydroeponemycin. Eur. J. Org. Chem. 2005. 4829-4834.

284. Lei, B.; Abdul Hameed, M. D.; Hamza, A.; Wehenkel, M.; Muzyka, J. L.; Yao, X. J.; Kim, K. B.; Zhan, C. G. Molecular basis of the selectivity of the immunoproteasome catalytic subunit LMP2-specific inhibitor revealed by molecular modeling and dynamics simulations., J Phys Chem B, 2010. **114**: p. 12333-12339.

285. Papadopoulos, K. P.; Burris, H. A., 3rd; Gordon, M.; Lee, P.; Sausville, E. A.; Rosen, P. J.; Patnaik, A.; Cutler, R. E., Jr.; Wang, Z.; Lee, S.; Jones, S. F.; Infante, J. R., A phase I/II study of carfilzomib 2-10-min infusion in patients with advanced solid tumors., Cancer Chemother Pharmacol, 2013. **72**: p.861-868.

286. Wang, Z.; Yang, J.; Kirk, C.; Fang, Y.; Alsina, M.; Badros, A.; Papadopoulos, K.; Wong, A.; Woo, T.; Bomba, D.; Li, J.; Infante, J. R., Clinical pharmacokinetics, metabolism, and drug-drug interaction of carfilzomib., Drug Metab Dispos, 2013. **41**: 230-237.

287. Wang, Z.; Fang, Y.; Teague, J.; Wong, H.; Morisseau, C.; Hammock, B. D.; Rock, D. A.; Wang, Z. In vitro metabolism of oprozomib, an oral proteasome inhibitor: role of epoxide hydrolases and cytochrome P450s, Drug Metab Dispos, 2017. **45**: p.712-720.

288. Saenz-Mendez, P.; Katz, A.; Perez-Kempner, M. L.; Ventura, O. N.; Vazquez, M., Structural insights into human microsomal epoxide hydrolase by combined homology modeling, molecular dynamics simulations, and molecular docking calculations., Proteins, 2017. **85**: p.720-730.

289. Shen, H. C.; Hammock, B. D., Discovery of inhibitors of soluble epoxide hydrolase: a target with multiple potential therapeutic indications., J Med Chem, 2012. **55**: p.1789-1808.

290. Hosagrahara, V. P.; Rettie, A. E.; Hassett, C.; Omiecinski, C. J., Functional analysis of human microsomal epoxide hydrolase genetic variants., Chem Biol Interact, 2004. **150**: p.149-159.

291. Rafii, M. S., Targeting tau protein in Alzheimer's disease., Lancet, 2016. **388**: p. 2842-2844.

292. Schmidt, M. and Finley, D., Regulation of proteasome activity in health and disease. Biochimica et Biophysica Acta (BBA)-Molecular Cell Research, 2014. **1843**(1): p.13-25.

293. Kincaid, E. Z., Che, J. W., York, I., Escobar, H., Reyes-Vargas, E., Delgado, J. C., Welsh, R. M., Karow, M. L., Murphy, A. J., Valenzuela, D. M., Yancopoulos, G. D., and Rock, K. L. Mice completely lacking immunoproteasomes show major changes in antigen presentation, Nat Immunol 2011. **13**: p. 129-135.

294. Bitzer, A., Basler, M., Krappmann, D., and Groettrup, M., Immunoproteasome subunit deficiency has no influence on the canonical pathway of NF-kappaB activation, Mol Immunol, 2017. **83**: p.147-153.

295. Jang, E. R., Lee, N. R., Han, S., Wu, Y., Sharma, L. K., Carmony, K. C., Marks, J., Lee, D. M., Ban, J. O., Wehenkel, M., Hong, J. T., Kim, K. B., and Lee, W., Revisiting the role of the immunoproteasome in the activation of the canonical NF-kappaB pathway, Mol Biosyst, 2012. **8**: p.2295-2302.

296. Vorhees, C. V. & Williams, M. T. Morris water maze: procedures for assessing spatial and related forms of learning and memory., Nat Protoc 2006. **1**: p.848-858.

297. Zhan, X., Stamova, B. & Sharp, F. R. Lipopolysaccharide Associates with Amyloid Plaques, Neurons and Oligodendrocytes in Alzheimer's Disease Brain: A Review., Front Aging Neurosci, 2018. **10**: p 42.

298. Lee, J. W. et al., Neuro-inflammation induced by lipopolysaccharide causes cognitive impairment through enhancement of beta-amyloid generation., J Neuroinflammation, 2008. **5**: p. 37.

299. Panza, F., et al., Tau-centric targets and drugs in clinical development for the treatment of Alzheimer's disease. BioMed research international, 2016.

300. Lesne, S. et al., A specific amyloid-beta protein assembly in the brain impairs memory., Nature, 2006. **440**: p.352-357.

301. Kawarabayashi, T. et al., Age-dependent changes in brain, CSF, and plasma amyloid (beta) protein in the Tg2576 transgenic mouse model of Alzheimer's disease., J Neurosci, 2001. **21**: p.372-381.

302. Castillo-Carranza, D. L. et al., Tau immunotherapy modulates both pathological tau and upstream amyloid pathology in an Alzheimer's disease mouse model., J Neurosci, 2015. **35**: p.4857-4868.

303. Maia, L. F. et al., Changes in amyloid-beta and Tau in the cerebrospinal fluid of transgenic mice overexpressing amyloid precursor protein., Sci Transl Med, 2013. **5**: p.194re192.

304. Kawarabayashi, T. et al., Dimeric amyloid beta protein rapidly accumulates in lipid rafts followed by apolipoprotein E and phosphorylated tau accumulation in the Tg2576 mouse model of Alzheimer's disease., J Neurosci, 2004. **24**: p. 3801-3809.

305. Hansen, D. V., Hanson, J. E. & Sheng, M. Microglia in Alzheimer's disease. J Cell Biol 2018. **217**: p. 459-472.

306. Bronzuoli, M. R., Iacomino, A., Steardo, L. & Scuderi, C., Targeting neuroinflammation in Alzheimer's disease., J Inflamm Res, 2016. **9**: p. 199-208.

307. Abbott, A., Is 'friendly fire' in the brain provoking Alzheimer's disease?, Nature, 2018. **556**: p. 426-428.

308. Hoogland, I. C., Houbolt, C., van Westerloo, D. J., van Gool, W. A. & van de Beek, D., Systemic inflammation and microglial activation: systematic review of animal experiments. J Neuroinflammation 2015. **12**: p.114

309. Fekete, C. et al. Chronic Amyloid beta Oligomer Infusion Evokes Sustained Inflammation and Microglial Changes in the Rat Hippocampus via NLRP3. Neuroscience, 2018.

310. Zhao, Y. et al., TREM2 Is a Receptor for beta-Amyloid that Mediates Microglial Function., Neuron, 2018. **97**: p.1023-1031.

311. Sheng, W. et al., Pro-inflammatory cytokines and lipopolysaccharide induce changes in cell morphology, and upregulation of ERK1/2, iNOS and sPLA(2)-IIA expression in astrocytes and microglia., J Neuroinflammation, **8**: p.121.

312. Xiang, Z. et al. Cyclooxygenase-2 promotes amyloid plaque deposition in a mouse model of Alzheimer's disease neuropathology. *Gene Expr* 2002. **10**: p. 271-278.

313. Pasinetti, G. M. & Aisen, P. S. Cyclooxygenase-2 expression is increased in frontal cortex of Alzheimer's disease brain., Neuroscience 1998. **87**: p.319-324.

314. Ho, L. et al., Neuronal cyclooxygenase 2 expression in the hippocampal formation as a function of the clinical progression of Alzheimer disease., Arch Neurol, 2001. **58**: p. 487-492.

315. De Strooper, B. & Karran, E., The Cellular Phase of Alzheimer's Disease. Cell, 2016. **164**: p. 603-615.

316. Navarro, V. et al., Microglia in Alzheimer's Disease: Activated, Dysfunctional or Degenerative., Front Aging Neurosci 2018. **10**: p.140.

317. Henn, A. et al., The suitability of BV2 cells as alternative model system for primary microglia cultures or for animal experiments examining brain inflammation., ALTEX 2009. **26**: p.83-94.

318. Ambati, J. & Fowler, B. J., Mechanisms of age-related macular degeneration., Neuron, 2012. **75**: p.26-39.

319. Dong, Z. Z. et al. Amyloid beta deposition related retinal pigment epithelium cell impairment and subretinal microglia activation in aged APPswePS1 transgenic mice., Int J Ophthalmol, 2018. **11**: p. 747-755.

320. Perez, S. E., Lumayag, S., Kovacs, B., Mufson, E. J. & Xu, S., Beta-amyloid deposition and functional impairment in the retina of the APPswe/PS1DeltaE9 transgenic mouse model of Alzheimer's disease., Invest Ophthalmol Vis Sci 2009. **50**: p.793-800.

321. Liu, B. et al., Amyloid-peptide vaccinations reduce {beta}-amyloid plaques but exacerbate vascular deposition and inflammation in the retina of Alzheimer's transgenic mice., Am J Pathol, 2009. **175**: p. 2099-2110.

322. Ding, J. D. et al., Anti-amyloid therapy protects against retinal pigmented epithelium damage and vision loss in a model of age-related macular degeneration., *Proc Natl Acad Sci U S A*, 2011. **108**: p. E279-287.

323. Ablonczy, Z. et al., Human retinal pigment epithelium cells as functional models for the RPE in vivo., Invest Ophthalmol Vis Sci, 2011. **52**: p.8614-8620.

324. Maldonado, M. *et al.* Immunoproteasome deficiency modifies the alternative pathway of NFkappaB signaling. PLoS One 2013. **8**: p. e56187.

325. von Brzezinski, L. et al., Low Neurotoxicity of ONX-0914 Supports the Idea of Specific Immunoproteasome Inhibition as a Side-Effect-Limiting, Therapeutic Strategy., Eur J Microbiol Immunol (Bp)., 2017. **7**: p.234-245.

326. Lynn, S.A., et al., The complexities underlying age-related macular degeneration: could amyloid beta play an important role?, Neural Regen Res 2017. **12**: p.538-548.

327. Williams, M. A., Silvestri, V., Craig, D., Passmore, A. P. & Silvestri, G., The prevalence of age-related macular degeneration in Alzheimer's disease., J Alzheimers Dis 2014. **42**: p.909-914.

328. Koronyo, Y., Salumbides, B. C., Black, K. L. & Koronyo-Hamaoui, M., Alzheimer's disease in the retina: imaging retinal abeta plaques for early diagnosis and therapy assessment., Neurodegener Dis 2012. **10**: p. 285-293.

329. Hoh Kam, J., Lenassi, E. & Jeffery, G. Viewing ageing eyes: diverse sites of amyloid Beta accumulation in the ageing mouse retina and the up-regulation of macrophages. PLoS One 2010. **5**: p.e13127.

330. Ratnayaka, J. A., Serpell, L. C. & Lotery, A. J. Dementia of the eye: the role of amyloid beta in retinal degeneration. Eye (Lond) 2015. **29**: p.1013-1026.

331. Gonzalez, D. M. & Medici, D., Signaling mechanisms of the epithelial-mesenchymal transition., Sci Signal, 2014.**7**: p. re8.

332. Zhou, H. J. et al., Design and synthesis of an orally bioavailable and selective peptide epoxyketone proteasome inhibitor (PR-047). J Med Chem, 2009. **52**: p. 3028-3038.

333. Min Jae Lee, Zach Miller, Jieun Park, Deepak Bhattarai, Wooin Lee, and Kyung Bo Kim. H727 cells are inherently resistant to the proteasome inhibitor carfilzomib, yet require proteasome activity for cell survival and growth. Scientific Reports 2019; **9**: p. 4089.

334. Min Jae Lee *, Deepak Bhattarai * Jisu Yoo, Zach Miller, Ji Eun Park, Sukyeong Lee, Wooin Lee, James J. Driscoll, and Kyung Bo Kim. Development of novel epoxyketone-based proteasome inhibitors as a strategy to overcome cancer resistance to carfilzomib and bortezomib. The Journal of Medicinal Chemistry 2019; accepted in April 2019.

Min Jae Lee

EDUCATION

2008-2012   Bachelor of Science, Bioscience and Biotechnology

           Konkuk University, Seoul, South Korea

PUBLICATIONS

Reichel, Derek, **Min Jae Lee**, Wooin Lee, Kyung Bo Kim, and Younsoo Bae. Tethered polymer nanoassemblies for sustained carfilzomib release and prolonged suppression of proteasome activity. *Therapeutic delivery* 2016; **7**: 665-681.

Min Jae Lee, Zach Miller, Jieun Park, Deepak Bhattarai, Wooin Lee, and Kyung Bo Kim. H727 cells are inherently resistant to the proteasome inhibitor carfilzomib, yet require proteasome activity for cell survival and growth. *Scientific Reports* 2019; **9**: p. 4089.

Min Jae Lee *, Deepak Bhattarai * Jisu Yoo, Zach Miller, Ji Eun Park, Sukyeong Lee, Wooin Lee, James J. Driscoll, and Kyung Bo Kim. Development of novel epoxyketone-based proteasome inhibitors as a strategy to overcome cancer resistance to carfilzomib and bortezomib. *The Journal of Medicinal Chemistry 2019*; accepted in April 2019.

ES Woodle, S Tremblay, P Brailey, A Girnita, B Aronow, N Dasgupta, F Ebstein, PM Kloetzel, **MJ Lee**, KB Kim, H Singh, and JJ Driscoll, Genomic and biochemical proteasomal adaptations in carfilzomib-resistant plasma cells that limit HLA-desensitization in transplantation. *The Journal of Clinical Investigation*, resubmitted.

Preye Agbana, **Min Jae Lee**, et al. Core stabilized Alginic Acid Hydrogels for Enhanced Entrapment and Sustained Release of Carfilzomib. *The Journal of Pharmaceutical Sciences*, submitted.

Deepak Bhattarai *, **Min Jae Lee***, Areum Baek, Jisu Yoo, Zachary Miller, Yu Mi Baek, In Jun Yeo, Jin Tae Hong, Sukyeong Lee, Wooin Lee, Dong-Eun Kim, and Kyung Bo Kim. Immunoproteasome Subunit LMP2 Inhibitors as Anti-Neuroinflammatory Agents. *Cell Chemical Biology,* submitted.

Injun Yeo*, **Min Jae Lee** *, et al. "A selective inhibitor of the immunoproteasome subunit LMP2 attenuates disease progression in mouse models of Alzheimer's disease. *In preparation.*

Deepak Bhattarai *, **Min Jae Lee** *, et al. Development of macrocyclic peptide epoxyketone targeting LMP2 as promising drug candidates. *In preparation.*

PRESENTATIONS

Min Jae Lee and Kyung Bo Kim, Proteasome subunit composition contributes to unusually poor sensitivity of H727 cancer cells to carfilzomib, The American Association of Cancer Research Annual Meeting 2016, New Orleans, LA, April 25, 2016

Min Jae Lee, James J. Driscoll, and Kyung Bo Kim, Cancer cells with de novo or acquired resistance to carfilzomib remain dependent on the proteasome for their survival and growth, Experimental Biology 2017, Chicago, IL, April 26, 2017